

**Studies on the Chemistry of Functionalized Cyclic Silicon Compounds
Based on an Unsaturated Silicon Three-membered Ring
Cyclotrisilene: Synthesis, Structure and Properties**

Yu Ohmori

Doctoral Program in Chemistry

Submitted to the Graduate School of
Pure and Applied Sciences
in Partial Fulfillment of the Requirements
for the Degree of Doctor of Philosophy in Science

at the
University of Tsukuba

General Introduction	...	002
Chapter 1	...	022
Reaction of Cyclotrisilene with Isocyanides: Synthesis, Structure and Properties of Small-Ring Silicon		
Compounds Having Imino Group		
Chapter 2	...	058
Reaction of Cyclotrisilene Isocyanide Adduct with Methanol: Synthesis Structure and Properties of		
<i>C</i> -amino and <i>C</i> -hydroxyl Silenes		
Chapter 3	...	096
Reaction of Cyclotrisilene with Azides: Synthesis, Structure, and Properties of		
Azatrisilabicyclo[1.1.0]butane and Amide-substituted Cyclotrisilene		
List of Publication	...	140
Acknowledgement	...	141

General Introduction

Organosilicon Chemistry¹

The history of organosilicon chemistry started with the first synthesis of Et₄Si in 1863 by Friedel and Crafts. They achieved the synthesis of Et₄Si via the reaction of Et₂Zn and SiCl₄ at high temperature. Because the introduction of organic group into chlorosilane by organozinc needed severe conditions, the available organosilicon compounds had been hugely limited. The major versatile synthetic route for organosilicon compounds using Grignard reagent was established by Kipping, known as the pioneer of the chemistry of silicones. Although his aim to obtain silicon analogue of ketone (>Si=O double bond compounds “sila-ketone”) was failed, his work provided the fundamental knowledge for the modern organosilicon chemistry. Interestingly, the resulting slimy oil that comes from the synthesis of >Si=O compounds named silicone², which was actually a mixture of cyclic polysiloxane and polysilicone, attracted the industrial chemists greatly. After his finding, the applied silicon science was widely spread with the development of direct-method (or Müller-Rochow method).³

Carbon and Silicon atom

	C	Si
Electron arrangement	(1s) ² (2s) ² (2p) ²	(1s) ² (2s) ⁶ (2p) ² (3s) ² (3p) ²
Ionization energy (kcal/mol)	260	188
Electron affinity (kcal/mol)	36.8	31.9
Electronegativity		
Allred-Rochow	2.50	1.74
Pauling	2.55	1.90
Atomic radii (pm)	77	118
van der Waals radii (pm)	170	210
Valence orbital energy (eV)		
s	-19.39	-14.84
p	-11.07	-7.57
Difference	8.32	7.27
$\Delta r = (r_p - r_s)$ (pm)	-0.2	20.3

Table 0-3. Selected parameters of carbon and silicon atom.^{1b, 5}

While carbon and silicon atom belong to the same Group 14, their atomic properties are very different (Table 0-3). Both the first ionization energy and electron affinity of silicon atom are smaller than that of carbon due to the higher energy level of valence 3p orbital compared with that of 2p orbital of carbon. Small electronegativity of silicon atom also emphasizes the positive electronic character. That is why silicon atom can form highly strong bonds with electronegative atoms such as fluorine and oxygen. For this reason, the relatively large bond dissociation energies in Si-F and Si-O bond are often applied in organic chemistry, involving widely used alcohol protection and deprotection.⁴

Single Bond

Reflecting the atomic nature of carbon and silicon, the bonding properties of parent ethane and disilane also show dramatic differences. Because silicon atom has spatially-spread valence 3p orbital, Si-Si single bond is longer than C-C bond (Figure 0-1). This elongation leads less overlapped valence orbital in disilane than in ethane. In molecular orbital theory, the energy splitting of bonding and antibonding orbital (or stabilizing and destabilizing energy, ΔE and $\Delta E'$) usually depends on orbital overlap integration and energy levels of component orbitals. As a result, the energy level of Si-Si bonding orbital becomes higher than that of ethane (-8.11 vs. -9.25 eV). Likewise, the antibonding orbital of Si-Si bond locates at lower level 0.544 eV than that of ethane at 2.83 eV. Therefore, Si-Si single bond has much potential toward reduction and oxidation compared with chemically, thermally, and electronically stable C-C bond.^{1d}

Indeed, hexamethyldisilane is easily oxidized by bromine or peracid with a Si-Si bond cleavage (Figure 0-2).

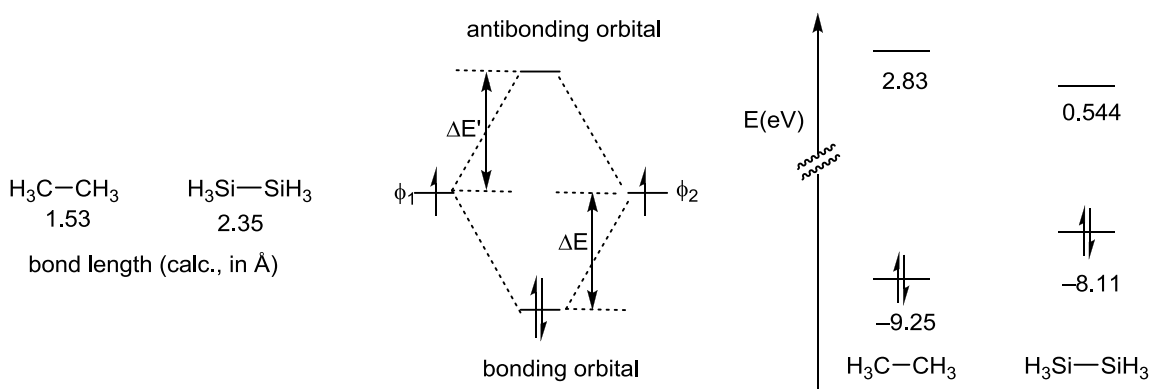


Figure 0-1. Bond length (\AA) and energy diagram of ethane and disilane calculated at B3LYP/6-31G(d) level.

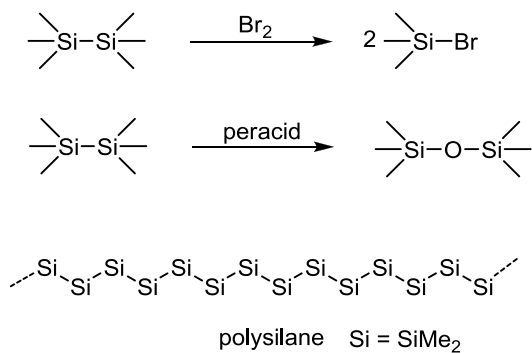


Figure 0-2. Oxidative Si-Si cleavage of hexamethyldisilane, and structure of polysilane.

Although the weakness of Si-Si single bond is emphasized here, it is noted that Si-Si single bond has comparable dissociation energy (ca. 74 kcal/mol) to C-C single bond (ca. 88 kcal/mol).⁶ Thus, stable oligo- and polysilanes are available. Because the small band gap of polysilanes formed by Si-Si σ catenation is suitable for electronic devices, its application to semiconductors and electrode active materials are energetically studied.⁷

Si=Si Double Bond

No one doubts the central position of carbon atom in organic chemistry. Among them, one of the most important elements giving functionality to the chemistry is multiple bonding. While the carbon chemistry holds a variety of unsaturated compounds, the information on their heavier silicon analogues could not be found in general text books.⁸ Indeed, *double bond rule*, which stated that the period 3 elements and lower do not form multiple bond, had been believed until the isolation of Si=Si⁹ and P=P¹⁰ double bond in 1981.

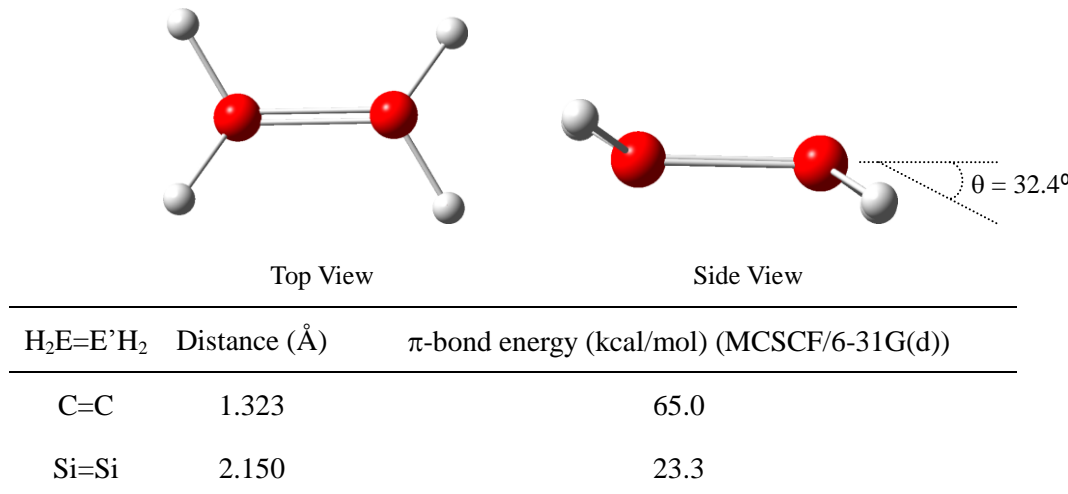


Figure 0-3. Optimized structure of $\text{H}_2\text{Si}=\text{SiH}_2$ at B3LYP/6-31G(d) and π bond energy for $\text{H}_2\text{E}=\text{EH}_2$.

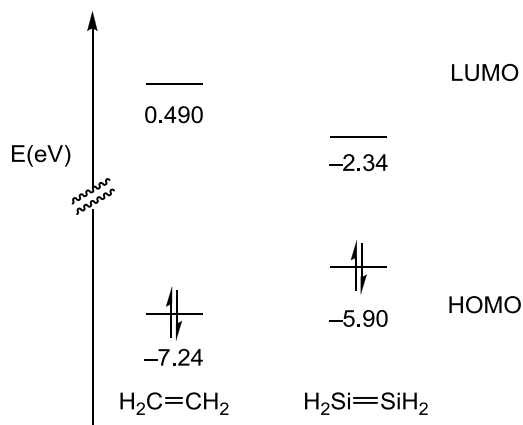


Figure 0-4. HOMO-LUMO energy level of ethylene and disilene calculated at B3LYP/6-31G(d) level.

Figure 0-3 shows the optimized structure of parent disilene and calculated parameters for $\text{H}_2\text{E}=\text{EH}_2$ ($\text{E} = \text{C}, \text{Si}$).¹¹ Calculated Si=Si bond length is much greater than C=C bond, as was seen in the single bonds. For this reason, π bonding interaction Si=Si bond becomes much weaker than that of C=C double bond. Indeed, the π bond energy of Si=Si double bond (23.3 kcal/mol) is ca. 1/3 compared with C=C double bond (65 kcal/mol). Likewise, the highest occupied and the lowest unoccupied molecular orbital (HOMO, LUMO), corresponding to π and π^* orbitals, give small HOMO-LUMO gap. Such electronic state of Si=Si bond provides high reactivity of disilenes that they easily react with

oxygen, moisture, and even themselves.¹² That is why no one had accomplished synthesis of Si=Si double bond compound for a long time.

As shown in the model picture of H₂Si=SiH₂ in Figure 0-3, one must notice its abnormal *trans*-bent structure (*trans*-bent angle = 32.4°). This feature can be realized by regarding a disilene as a dimer of divalent species (Figure 0-5). Parent carbene has triplet ground states with sp²-hybrid structure. Therefore carbenes can dimerize to form classical planar C=C double bond. However, ground singlet silylenes SiH₂ ($\Delta E_{ST} = 21.0$ kcal/mol) having lone pair and vacant p orbital cannot approach each other in classical planar fashion due to Pauli repulsion. Instead, singlet silylenes dimerize to the *trans*-bent fashion. This interaction called donor-acceptor model resulted in the characteristic *trans*-bent Si=Si double bond as shown in the model compound.

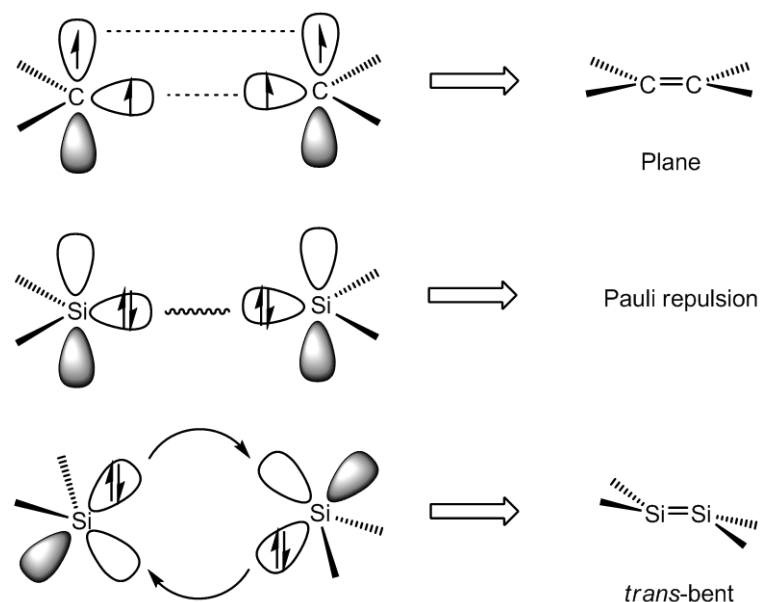


Figure 0-5. Molecular orbital model of C=C and Si=Si double bond.

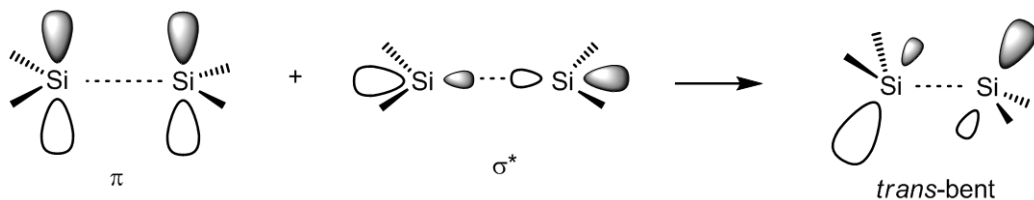


Figure 0-6. Mixing σ^* and π orbital in *trans*-bent structure.

The *trans*-bent structure can be also explained by π - σ^* orbital mixing (Figure 0-6).¹¹ When planar disilene transforms to *trans*-bent structure, the corresponding π -orbital also deforms to break the π -symmetry. This orbital transformation enables the mixing of *trans*-bent Si=Si π orbital and Si-Si σ^* -orbital. As a result, mixed π orbital of *trans*-bent disilene locates at energetically lower level than that of planar disilene, although π^* -orbital would be destabilized in some degree.

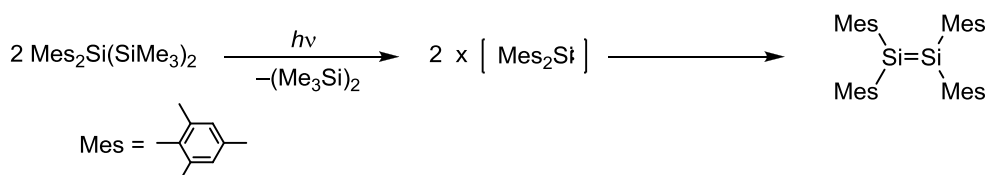
$$1/4E_{\sigma+\pi} < \Delta E_{ST} < 1/2E_{\sigma+\pi} \quad (1)$$

Computational studies on *trans*-bent structure and singlet-triplet energy splitting ΔE_{ST} were well performed.^{13, 14} Trinquier and Malreu predicted that when ΔE_{ST} satisfied equation (1), E=E double bond (E = C, Si, Ge, Sn) would have *trans*-bent structure. Apeloig et al. investigated the relationships between *trans*-bent angle of disilene H₂Si=SiHR and electronegativity of substituent R.^{14a} According to the work, when the substituent is electropositive groups such as R = SiH₃, the Si=Si bond has short and planar structure. On the other hand, disilenes with electronegative group (especially R = F, OH, NH₂) showed significant *trans*-bent angles and Si=Si bond elongations.

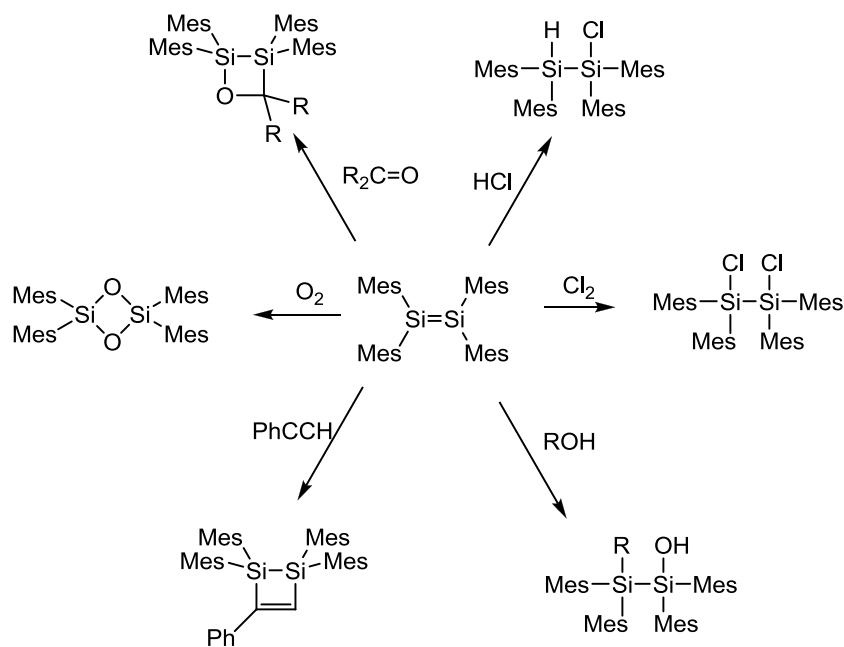
First Disilene – Tetramesityldisilene –

The first isolable disilene was synthesized by West in 1981 (Scheme 0-1).⁹ Photochemical reaction of 2,2-dimesitylhexamethyltrisilane gave tetramesityldisilene via dimerization of dimesitylsilylene. The bulky mesityl groups prevented the Si=Si bond from dimerization and polymerization. Such steric protection is called kinetic stabilization, which is now established as synthetic method for reactive species including a number of silicon unsaturated compounds.

Scheme 0-1



Scheme 0-2



As mentioned in the section *Double Bond*, Si=Si double bond has HOMO at high energy level and LUMO at low energy level. Therefore, disilene showed great reactivity toward small molecules at ambient conditions (Scheme 0-2).⁸ For example, 1,2-alcohol addition to Si=Si double bond is known as a simple trap method for disilene today.¹⁵ Other typical reactivity of disilene is [2 + 2] cycloaddition, which is thermally forbidden in carbon chemistry and accomplished by photochemical or catalytic methods. Disilenes react with unsaturated small molecules such as ketone, alkene, and alkyne, giving [2 + 2] cycloadducts under mild conditions via considerable polar or radical intermediate.¹⁶

Silicon unsaturated compounds

Since the first isolation of the disilene in 1981, a number of silicon unsaturated compounds involving triple bond,¹⁷ hetero multiple bond,¹⁸ allene derivative,¹⁹ cyclic compounds,²⁰ aromatic series,²¹ and conjugated and functionalized disilenes^{22,23} have been synthesized by kinetic stabilization (Figure 0-7). The synthetic routes toward a variety of silicon multiple bonds are also well established (e.g. photochemical generation of silylene, reduction of dihalosilane and dihalodisilane). In the next section, the chemistry of 3-membered cyclic disilenes, named cyclotrisilene,²⁴ related to this doctor's thesis, will be described.

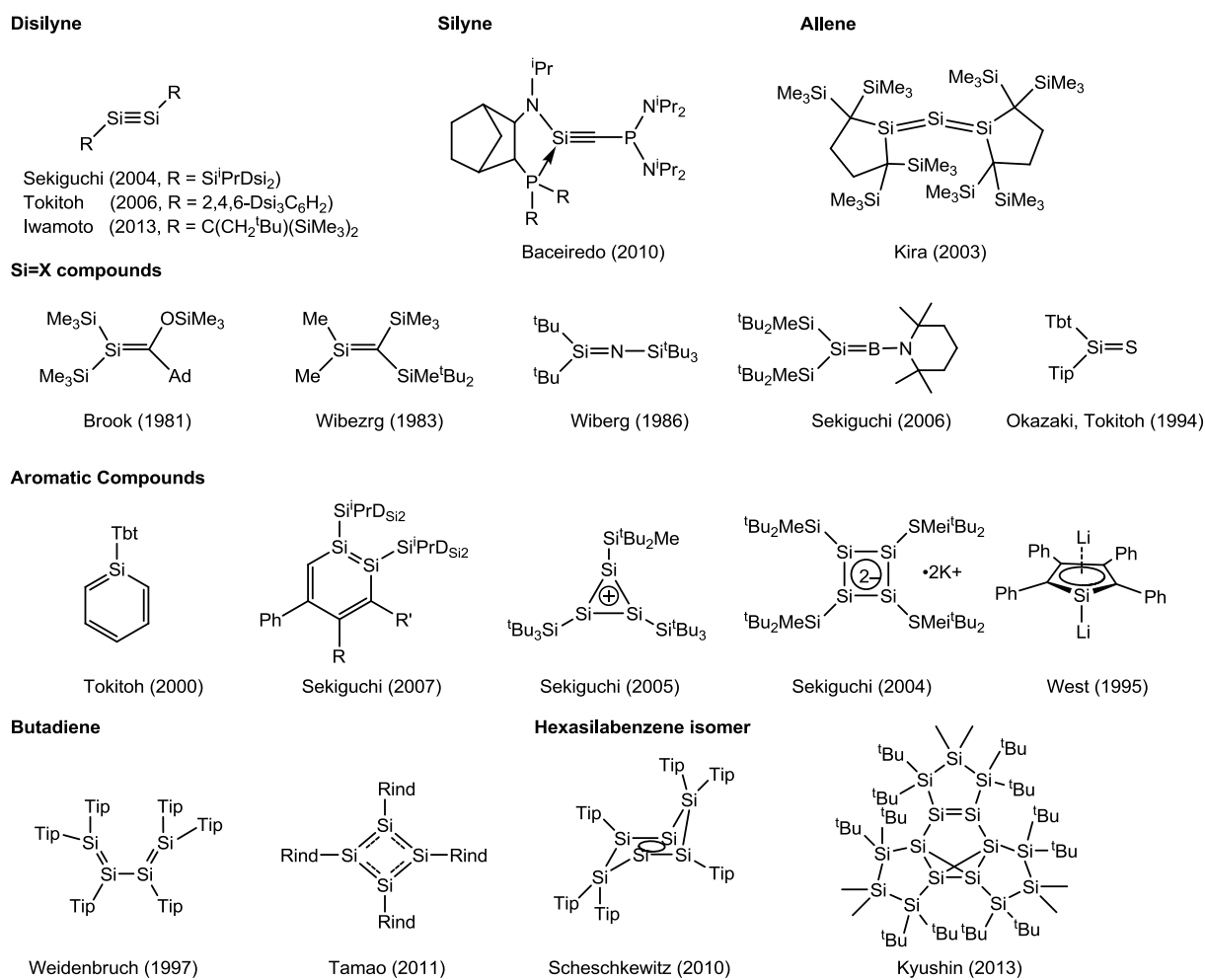


Figure 0-7. Examples of isolable silicon unsaturated compounds.

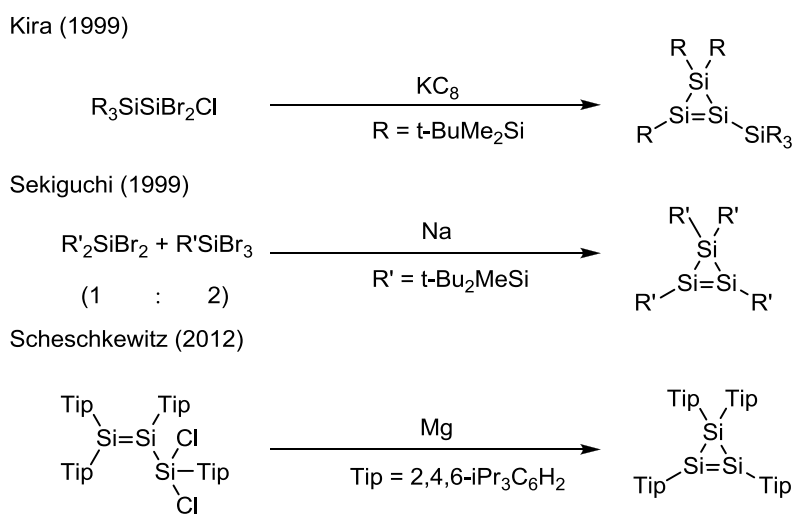
Cyclotrisilene

Cyclotrisilene, which is a persila analogue of cyclopropene, has attracted chemists because of the reactive Si=Si double bond incorporated in the highly strained skeletal. Theoretically, the strain energy (SE) of parent cyclotrisilene was estimated to be 34.5 kcal/mol and was comparable with trisilacyclop propane (35.5 kcal/mol), whereas the SE of carbon cyclopropene was much greater than that of cyclopropane (55.5 kcal/mol vs. 25.5 kcal/mol, Figure 0-8).²⁵

Scheme 0-3

M	$\begin{array}{c} M \\ \backslash \\ M-M \\ / \end{array}$	$\begin{array}{c} M \\ \backslash \\ M=M \\ / \end{array}$	
C	25.5	55.5	20.0
Si	35.5	34.5	-1.0

Figure 0-8. Strain energy of three-membered rings (M = C or Si).

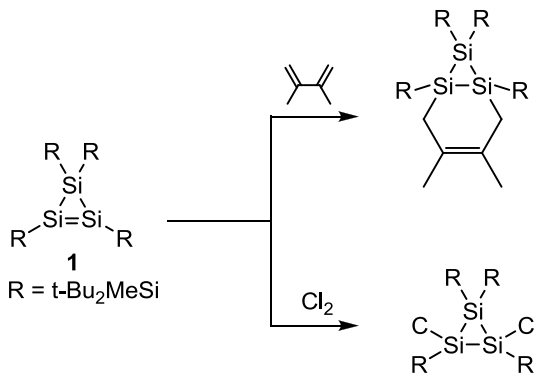


Scheme 0-3 shows cyclotrisilenes reported previously. Kira's group reported the first stable cyclotrisilene by the reduction of dibromochlorosilane with potassium graphite.²⁶ While molecular structure of the cyclotrisilene was not described in this paper, the spectroscopic characterization as well as trapping reaction using CCl_4 supported the generation of the first cyclotrisilene. The X-ray crystallographic analysis of cyclotrisilene was accomplished by Sekiguchi et al. in the same year 1999.²⁷ The reductive coupling of 1 : 2 mixture of di- and tribromosilanes by using sodium afforded the symmetrical tetrakis(di-*tert*-butylmethylsilyl)cyclotrisilene, which was fully characterized by structural and spectroscopic method. Peraryl substituted cyclotrisilene was recently synthesized by Scheschkewitz's group.²⁸ The reduction of dichlorosilyldisilene by magnesium led the generation of transient silylene^{II} species, which underwent cyclization to give cyclotrisilene.

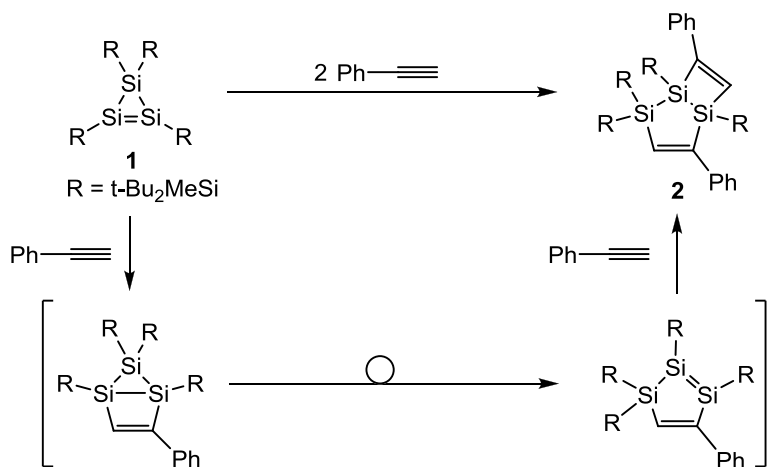
Basic Reactivity of Cyclotrisilene

Because cyclotrisilene has a highly reactive Si=Si double bond as well as a strained 3-membered ring, it showed unique reactivity toward small molecules compared with acyclic disilenes. As seen in tetramesityldisilene, tetrakis(di-*tert*-butylmethylsilyl)cyclotrisilene **1** reacts with diene to afford [2 + 4]cycloadduct (Scheme 0-4). Chlorine gas is also capable to chlorinate Si=Si double bond. However, cyclotrisilene **1** can react with two equivalent amounts of phenylacetylene, giving bicyclo[3.2.0]trisilaheptadiene derivative **2** (Scheme 0-5).²⁹ In this reaction, a characteristic isomerization from strained trisilabicyclo[2.1.0]pentene intermediate to trisilacyclopentadiene derivative led a new Si=Si double bond. The following second [2 + 2] cycloaddition will give bicyclo[3.2.0]trisilaheptadiene derivative **2**. A combination of internal alkyne and less bulky cyclotrisilene **3** allowed the isolation of trisilacyclopentadiene derivative **4**, which could be a precursor of silicon version cyclopentadienyl ring (Scheme 0-6).³⁰

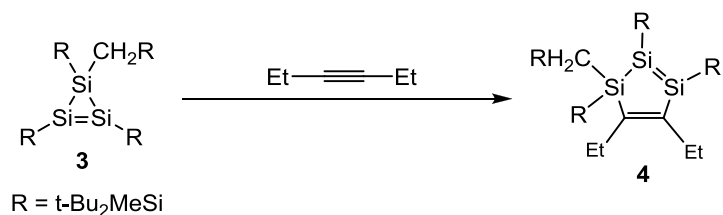
Scheme 0-4



Scheme 0-5



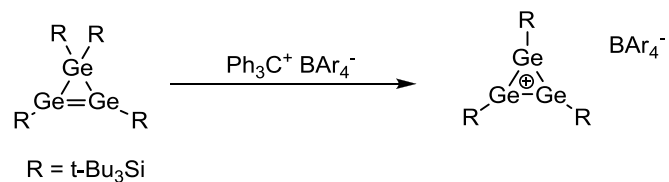
Scheme 0-6



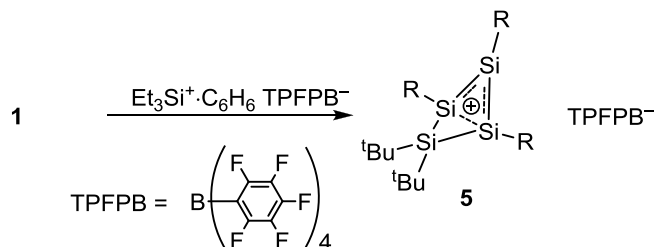
Aromatic and Homoaromatic Silicon Rings from Cyclotrisilene

Electron delocalization in ring system is one of the most intriguing phenomena in organic chemistry due to the aromatic or anti aromatic nature. From this point of view, Sekiguchi et al. succeeded in the isolation of trigermacyclopropenylum ion as a first pergerma aromatic ring compound, by the reaction of cyclotrigermene with triphenylmethylium borate (Scheme 0-7).³¹ Since cyclotrigermene was a good precursor for aromatic 3-membered cation ring, cyclotrisilene **1** also had potential toward aromatic compound by oxidative elimination of silyl group. For this reason, the reaction of **1** with several cationic species had been studied to synthesize 2π -trisilacycloprenylium ion.

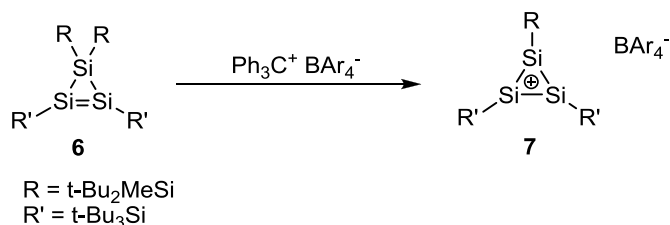
Scheme 0-7



Scheme 0-8



Scheme 0-9



The reaction of **1** with Et_3Si^+ cation led to a removal of methyl group instead of the desired silyl group, affording homoaromatic cyclotetrasilylium ion **5** (Scheme 0-8).³² Although the desired aromatic compound was not obtained, the cation **5** was shown to be the first example of non-classical 2π -electron delocalized silicon system. Following development of chemistry of **5** includes the first isolable silyl radical upon one-electron reduction.^{33, 34} Silicon 2π aromatic ring, cyclotrisilene **7**, was finally synthesized in 2005 via the reaction of bulky cyclotrisilene **6** and Ph_3C^+ cation (Scheme 0-9).^{21c} In the molecular structure of **7**, each skeletal Si-Si bond length was nearly equal in the range between the Si-Si single and double bond length. Moreover the ^{29}Si NMR signals of skeletal silicon atoms appeared at quite low-field, showing the 2π electron delocalization on the silicon 3-membered ring plane.

Bicyclo[1.1.0]butane Systems

Other important silicon rings related to cyclotrisilene **1** are heavy bicyclo[1.1.0]butanes.³⁵ As shown in Figure 0-9, theoretical calculation revealed that parent tetrasilabicyclo[1.1.0]butane is the most stable among Si_4H_6 isomers, while carbon analogue C_4H_6 favors ring-opening butadiene form rather than strained triangle frameworks. It is noted that Si_4H_6 isomers tend to form strained skeletons rather than acyclic multiple bonds. Such thermodynamic trend shown here is useful for understanding the chemistry of small cyclic silicon rings.

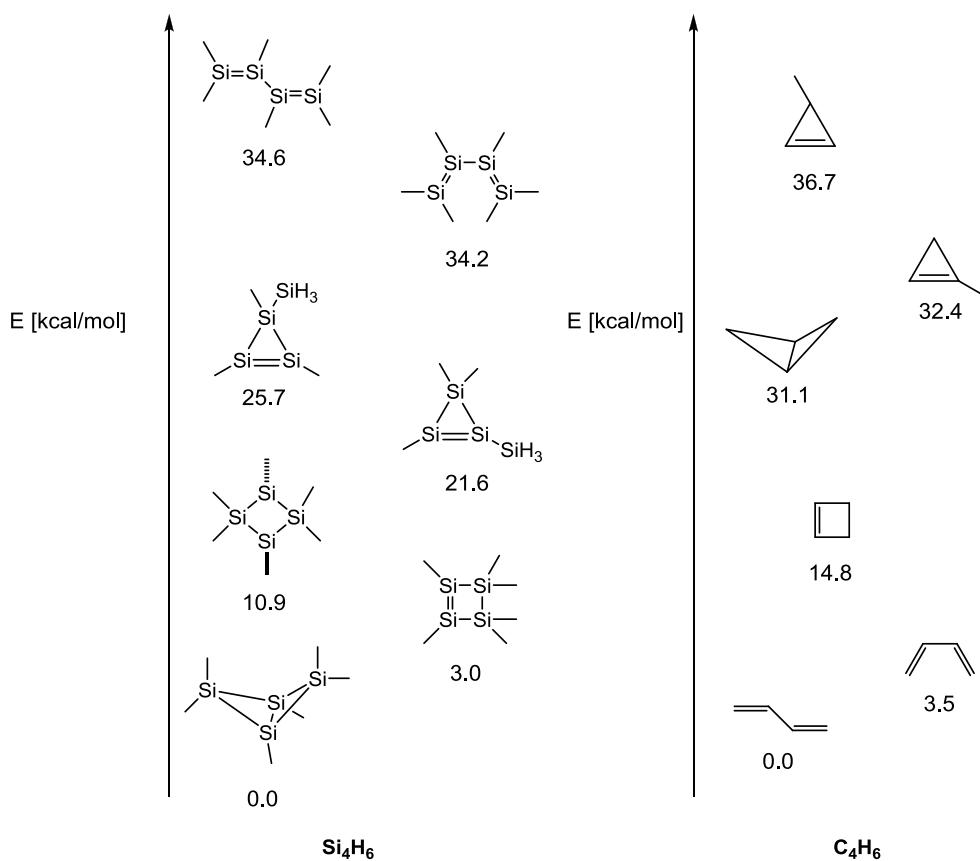
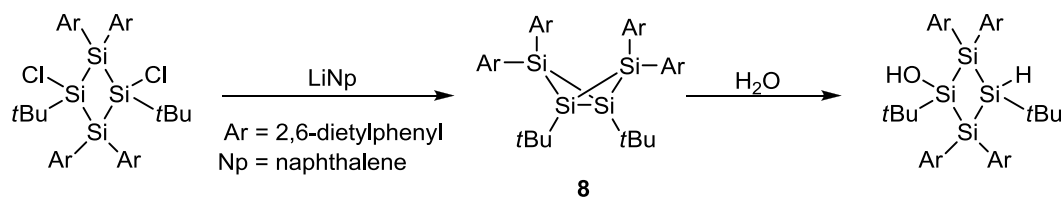


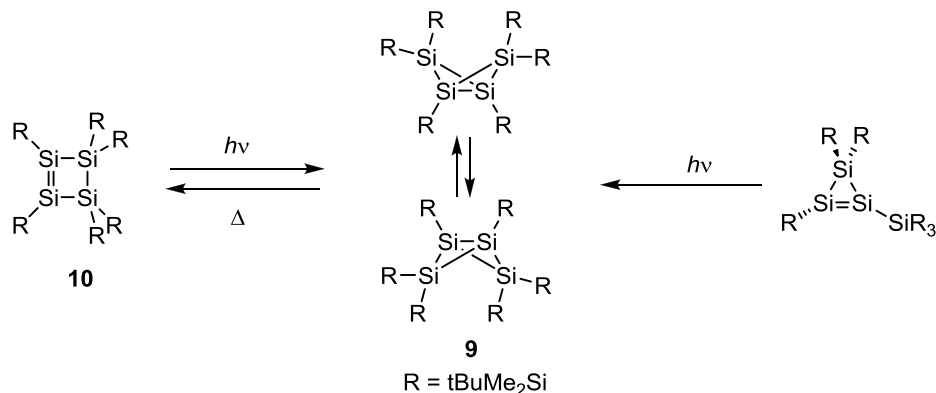
Figure 0-9. Relative energies of Si_4H_6 and C_4H_6 isomers.

The first bicyclo[1.1.0]tetrasilane **8** was prepared by Masamune, via reduction of cyclic 1,3-dichlorocyclotetrasilane (Scheme 0-10). Because of the highly strained structure, the bridge bond of bicyclo[1.1.0]tetrasilane can react toward O₂, Cl₂ and even H₂O.³⁶ Kira's group reported silyl substituted bicyclo[1.1.0]tetrasilane **9**, which showed reversible conversion toward tetrasilacyclobutene derivative **10** (Scheme 0-10).^{20a, 37} Interestingly, bicyclo[1.1.0]tetrasilane **9** showed the rapid ring flipping of four-membered skeleton depending on the temperature.

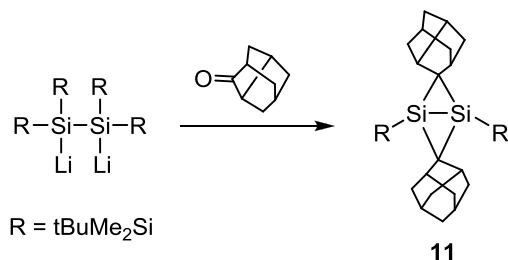
Scheme 0-10



Scheme 0-11



Scheme 0-12



Carbon and silicon hybrid bicyclo[1.1.0]butanes show great change in the molecular structural and even electronic properties. Disilabicyclo[1.1.0]butane C₂Si₂ **11** by Kira et al. showed a particular long Si-Si bridge bond (Scheme 0-12).³⁸ This type of bicyclo[1.1.0]butanes, named Long-Bond isomer (LB), is also located as energy minima of Si₄H₆ isomers (Figure 0-10).³⁹ Compared with the bridge Si-Si banana bond of Short-Bond isomer (SB), LB has inverted σ

bonding orbital and biradical character between central Si atoms. In contrast, Si_3C methylene bridged trisilabicyclo[1.1.0]butane **12** reported by Sekiguchi et al. has significant short bridge Si-Si bond (Scheme 0-13). Interestingly, thermal isomerization of **12** gave unsymmetrical cyclotrisilene **3**.⁴⁰

A few examples of silicon-heteroatom hybrid bicyclo[1.1.0]butanes were accomplished based on cyclotrisilene **1** as a key precursor. Simple, one-step conversions of cyclotrisilene **1** toward Si_3X trisilabicyclo[1.1.0]butane **13** ($\text{X} = \text{S, Se, Te}$) were reported recently (Scheme 0-14). Si_3X trisilabicyclo[1.1.0]butane **13** showed photochemical isomerization to functionalized cyclobutene derivatives.⁴¹

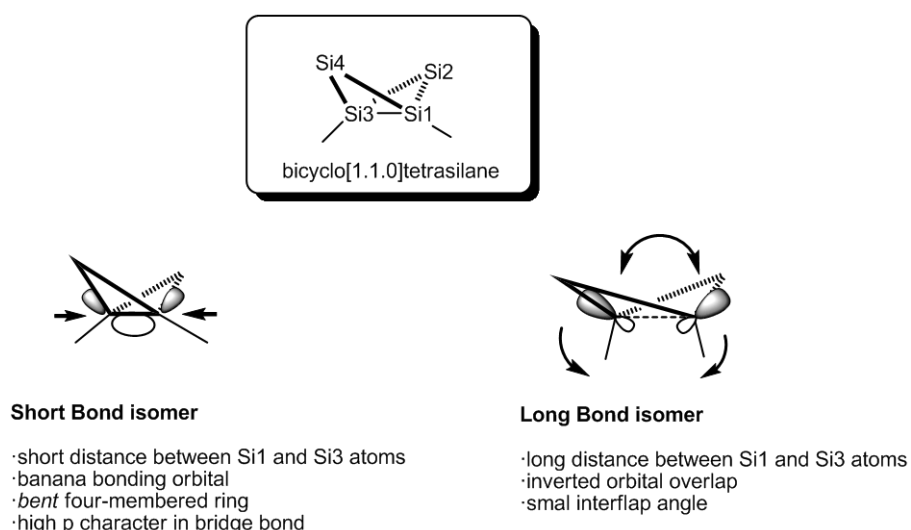
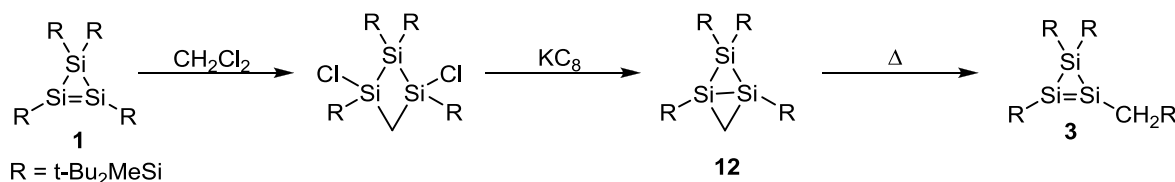
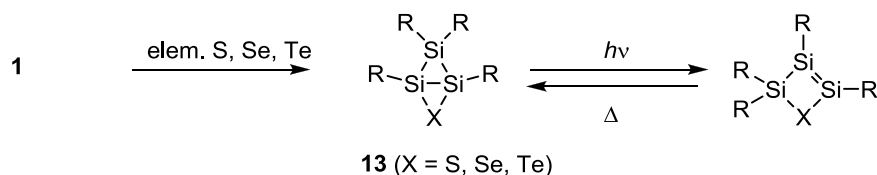


Figure 0-10. Molecular orbital drawing of bicyclo[1.1.0]tetrasilane short and long bond isomers.

Scheme 0-13



Scheme 0-14



Propose of the Present Studies

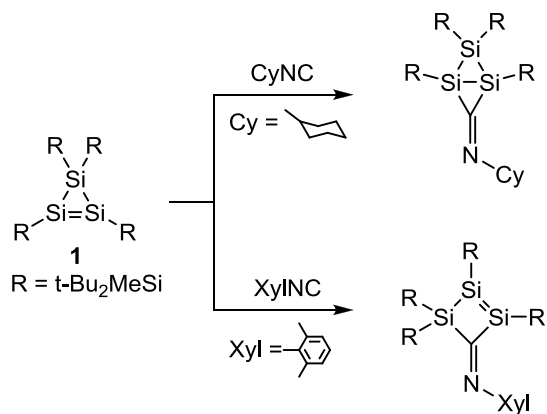
As mentioned, cyclotrisilene **1** has a potential for unique silicon unsaturated compounds involving silicon aromatic rings, functionalized trisilabicyclo[1.1.0]butanes and related isomers. Some of the functionalized small silicon rings could be difficult to be prepared without cyclotrisilene **1**, because of the synthetic difficulty.

Recently, functionalization toward silicon multiple bond is attractive chemistry in the view of isolable reactive species,⁴² tuning the electronic as well as structural states,⁴³ and development of new silicon reagents.⁴⁴ Especially, introduction of nitrogen and oxygen atoms into silicon unsaturated species are attractive challenges due to the inductive effect and interactions of lone-pair toward reactive silicon compounds. However, the presence of polar Si-N and Si-O bonds prevent isolation and even observation of such functionalized species by the nucleophilic attack under the reaction.

For this background, the author describes the new reactivity of key precursor cyclotrisilene **1** toward isonitriles, carbon monoxide, and azides in this doctor's thesis, in the hope of isolable novel silicon species. Synthesis, structure and properties of a variety of functionalized unsaturated small rings involving three Si atoms and N or O atom are described in detail.

In chapter 1, the reactivity of **1** toward alkyl and aryl isocyanides are described (Scheme 0-15). Structure and properties of resulting iminotrisilabicyclo[1.1.0]butane and iminotrisilacyclobutene derivatives are discussed.

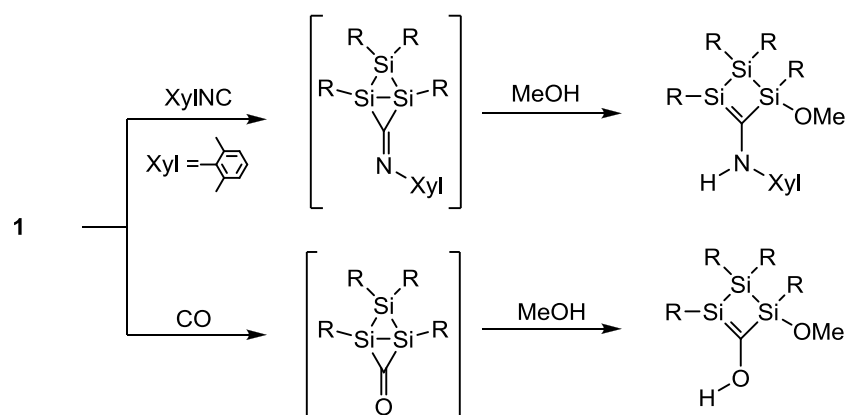
Scheme 0-15



In chapter 2, synthesis, structure and properties of cyclic *C*-aminosilene (sila-enamine) are described (Scheme 0-15).

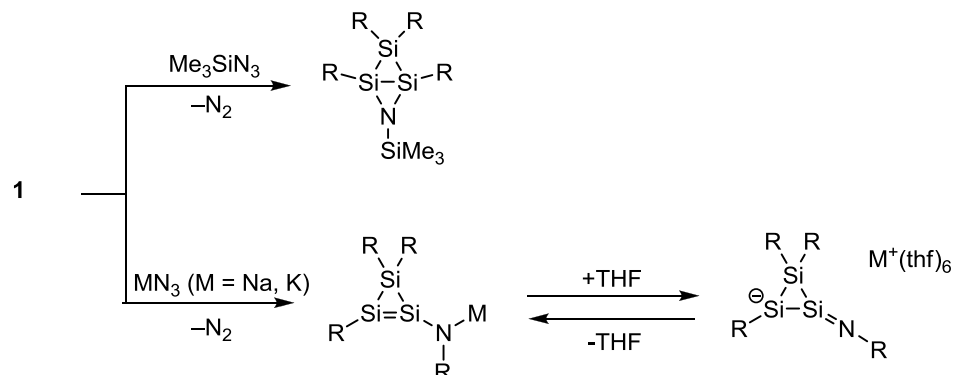
The first example of carbonylation of cyclotrisilene **1**, giving *C*-hydroxylsilene (sila-enol), are also described.

Scheme 0-15



In chapter 3, the reactivity of **1** toward azide is described (Scheme 0-16). Structure and properties of resulting azatrisilabicyclo[1.1.0]butane derivative and amide-substituted cyclotrisilene are discussed.

Scheme 0-16



References

- 1) Reviews on the organosilicon chemistry: (a) C. A. Burkhard, E. G. Rochow, H. S. Booth, J. Hartt, *Chem. Rev.* **1947**, *41*, 97; (b) *The Chemistry of Organic Silicon Compounds Vol. 3*, (Ed. by Z. Rappoport, Y. Apeloig) John Wiley & Sons, Ltd, Chichester, 2001; (c) V. Ya. Lee, A. Sekiguchi, *Organometallic Compounds of Low-Coordinate Si, Ge, Sn and Pb*, John Wiley & Sons, Ltd, Chichester, 2010; (d) *Gendai Keiso Kagaku (Modern Organosilicon Chemistry)*, (Ed. by K. Tamao, M. Kira) Kagaku Dojin, Ltd, Japan, 2013.
- 2) F. S. Kipping, *J. Chem. Soc.* **1912**, *101*, 2106.
- 3) E. G. Rochow, *The Chemistry of the Silicones*, John Wiley and Sons, Ltd, New York, 1946.
- 4) (a) E. J. Corey, A. Venkatewarlu, *J. Am. Chem. Soc.* **1972**, *94*, 6190; (b) T. D. Nelson, R. D. Crouch, *Synthesis* **1996**, *9*, 1031.
- 5) (a) W. Kutzelnigg, *Angew. Chem., Int. Ed.* **1984**, *23*, 272; (b) M. Driess, H. Grützmacher, *Angew. Chem., Int. Ed.* **1996**, *35*, 828.
- 6) R. Walsh, *Acc. Chem. Res.* **1981**, *14*, 246.
- 7) (a) R. D. Miller, J. Michl, *Chem. Rev.* **1989**, *89*, 1359. H. Maruyama, H. Nakano, M., Ogawa, M. Nakamoto, T. Ohta, A. Sekiguchi, *Sci. Rep.* **2015**, *5*, 13219; (c) Y. Kumai, S. Shirai, E. Sudo, J. Seki, H. Okamoto, Y. Sugiyama, H. Nakano, *J. Power Sources* **2011**, *196*, 1503; (d) G. Zhang, J. Ma, Y. Jiang, *J. Phys. Chem. B.* **2005**, *109*, 13499.
- 8) Reviews on disilenes: (a) G. Raabe, J. Michl, *Chem. Rev.* **1985**, *85*, 419; (b) R. West, *Angew. Chem., Int. Ed.* **1987**, *26*, 1201; (c) J. Barrau, J. Escudie, J. Satge, *Chem. Rev.* **1990**, *90*, 283; (d) T. Tsumuraya, S. A. Batcheller, S. Masamune, *Angew. Chem., Int. Ed.* **1991**, *30*, 902; (e) R. Okazaki, R. West, *Adv. Organomet. Chem.* **1996**, *39*, 231; (f) M. Kira, T. Iwamoto, *Adv. Organomet. Chem.* **2006**, *54*, 73; (g) T. L. Morking, T. R. Owens, W. J. Leigh, in *The Chemistry of Organic Silicon Compounds Vol. 3*, (Ed. by Z. Rappoport, Y. Apeloig) John Wiley & Sons, Ltd, Chichester, 2001, chap 17.
- 9) R. West, M. J. Fink, J. Michl, *Science* **1981**, *214*, 1343.
- 10) M. Yoshifuji, I. Shima, N. Inamoto, K. Hirotsu, T. Higuchi, *J. Am. Chem. Soc.* **1981**, *103*, 4587.
- 11) M. W. Schmidt, P. N. Truong, M. S. Gordon. *J. Am. Chem. Soc.* **1987**, *109*, 5217.
- 12) Reactivity of transient disilene and disilyne: (a) F. S. Kipping, J. E. Sands, *J. Chem. Soc. Trans.* **1921**, *119*, 830; (b) F. S. Kipping, J. E. Sands, *J. Chem. Soc. Trans.* **1921**, *119*, 848; (c) F. S. Kipping, J. E. Sands, *J. Chem. Soc.* **1927**, 2719; (d) D. N. Roark, G. J. D. Peddle, *J. Am. Chem. Soc.* **1972**, *94*, 5837; (e) A. Sekiguchi, S. S. Zigler, R. West, J. Michl, *J. Am. Chem. Soc.* **1986**, *108*, 4241.
- 13) (a) G. Trinquier, *J. Am. Chem. Soc.* **1990**, *112*, 2130; (b) J. -P. Malrieu, G. Trinquier, *J. Am. Chem. Soc.* **1989**, *111*,

- 14) For substituent effect on silicon multiple bond, see (a) M. Karni, Y. Apeloig, *J. Am. Chem. Soc.* **1990**, *112*, 8589; (b) P. P. Power, *Chem. Rev.* **1999**, *99*, 3463; (c) M. Takahashi, K. Sakamoto, *Organometallics* **2002**, *21*, 4212; (d) M. Bendikov, S. R. Quadt, O. Rabin, Y. Apeloig, *Organometallics* **2002**, *21*, 3930; (e) K. Kobayashi, S. Nagase, *Organometallics* **1997**, *16*, 2489.
- 15) Y. Apeloig, M. Nakash, *J. Am. Chem. Soc.* **1996**, *118*, 9798.
- 16) D. J. D. Young, R. West, *Chem. Lett.* **1986**, *6*, 883.
- 17) (a) A. Sekiguchi, R. Kinjo, M. Ichinohe, *Science* **2004**, *305*, 1755; (b) A. Sekiguchi, M. Ichinohe, R. Kinjo, *Bull. Chem. Soc. Japan* **2006**, *79*, 825; (c) T. Sasamori, K. Hironaka, Y. Sugiyama, N. Takagi, S. Nagase, Y. Hosoi, Y. Furukawa, N. Tokitoh, *J. Am. Chem. Soc.* **2008**, *130*, 13856; (d) S. Ishida, R. Sugawara, Y. Misawa, T. Iwamoto, *Angew. Chem., Int. Ed.* **2013**, *52*, 12869. (e) D. Gau, T. Kato, N. Saffon-Merceron, A. D. C  zar, F. P. Coss  , A. Baceiredo, *Angew. Chem.* **2010**, *122*, 6735.
- 18) (a) A. G. Brook, F. Abdesaken, B. Gutekunst, G. Gutekunst, R. K. Kallury, *J. Chem. Soc., Chem. Commun.* **1981**, 191; (b) N. Nakata, A. Sekiguchi, *J. Am. Chem. Soc.* **2006**, *128*, 422; (c) N. Wiberg, K. Churz, G. Reber, G. M  ller, *J. Chem. Soc., Chem. Commun.* **1986**, 591; (d) E. Niecke, E. Klein, M. Nieger, *Angew. Chem., Int. Ed.* **1989**, *28*, 7511, (e) H. Suzuki, N. Tokitoh, R. Okazaki, *J. Am. Chem. Soc.* **1994**, *116*, 11578; (f) N. Tokitoh, T. Sadahiro, K. Hatano, T. Sasaki, N. Takeda, R. Okazaki, *Chem. Lett.* **2002**, *34*; (g) T. Iwamoto, K. Sato, S. Ishida, C. Kabuto, M. Kira, *J. Am. Chem. Soc.* **2006**, *128*, 16914.
- 19) (a) S. Ishida, T. Iwamoto, C. Kabuto, M. Kira, *Nature* **2003**, *421*, 725; (b) H. Tanaka, S. Inoue, M. Ichinohe, M. Driess, and A. Sekiguchi, *Organometallics* **2011**, *30*, 3475.
- 20) (a) M. Kira, T. Iwamoto, C. Kabuto, *J. Am. Chem. Soc.* **1996**, *118*, 10303; (b) M. Kira, *J. Organomet. Chem.* **2004**, *689*, 4475.
- 21) (a) K. Wakita, N. Tokitoh, R. Okazaki, *Angew. Chem., Int. Ed.* **2000**, *39*, 634; (b) R. Kinjo, M. Ichinohe, A. Sekiguchi, N. Takagi, M. Sumimoto, S. Nagase, *J. Am. Chem. Soc.* **2007**, *129*, 7766; (c) M. Ichinohe, M. Igarashi, K. Sanuki, A. Sekiguchi, *J. Am. Chem. Soc.* **2005**, *127*, 9978; (d) K. Takanashi, V. Ya, Lee, T. Matsuno, M. Ichinohe, A. Sekiguchi, *J. Am. Chem. Soc.* **2005**, *127*, 5768; (e) R. West, H. Sohn, U. Bankwitz, J. Calabrese, Y. Apeloig, T. Mueller, *J. Am. Chem. Soc.* **1995**, *117*, 11608. (f) K. Suzuki, T. Matsuo, D. Hashizume, H. Fueno, K. Tanaka, K. Tamao, *Science* **2011**, *331*, 1306; (g) K. Abersfelder, A. J. P. White, H. S. Rzepa-, D. Scheschkeowitz, *Science* **2010**, *327*, 564; (h) A. Tsurusaki, C. Iizuka, K. Otsuka, S. Kyushin, *J. Am. Chem. Soc.* **2013**, *135*, 16340.
- 22) (a) M. Weidenbruch, S. Willms, W. Saak, G. Henkel, *Angew. Chem., Int. Ed.* **1997**, *36*, 2503; (b) K. Uchiyama, S.

- Nagendran, S. Ishida, T. Iwamoto, M. Kira, *J. Am. Chem. Soc.* **2007**, *129*, 10638; (c) I. Bejan, D. Scheschkewitz, *Angew. Chem., Int. Ed.* **2007**, *46*, 5783.
- 23) (a) K. Takeuchi, M. Ikoshi, M. Ichinohe, A. Sekiguchi, *J. Am. Chem. Soc.* **2010**, *132*, 930. (b) K. Takeuchi, M. Ichinohe, A. Sekiguchi, *Organometallics* **2011**, *30*, 2044; (c) K. Takeuchi, M. Ikoshi, M. Ichinohe, A. Sekiguchi, *J. Organomet. Chem.* **2011**, *696*, 1156.
- 24) A. Sekiguchi, V. Ya. Lee, *Chem. Rev.* **2003**, *103*, 1429.
- 25) Y. Naruse, J. Ma, S. Inagaki, *Tetrahedron Lett.* **2001**, *42*, 6553.
- 26) (a) T. Iwamoto, C. Kabuto, M. Kira, *J. Am. Chem. Soc.* **1999**, *121*, 886; (b) T. Iwamoto, M. Tamura, C. Kabuto, M. Kira, *Organometallics* **2003**, *22*, 2342.
- 27) M. Ichinohe, T. Matsuno, A. Sekiguchi, *Angew. Chem., Int. Ed.* **1999**, *38*, 2194.
- 28) K. Leszczyńska, D. –C. K. Abersfelder, A. Mix, B. Neumann, H. Stammier, M. Cowley, P. Jutzi, D. Scheschkewitz, *Angew. Chem.* **2012**, *51*, 6785.
- 29) M. Ichinohe, T. Matsuno, A. Sekiguchi, *Chem. Commun.* **2001**, 183.
- 30) H. Yasuda, V. Ya. Lee, and A. Sekiguchi, *J. Am. Chem. Soc.* **2009**, *131*, 9902.
- 31) A. Sekiguchi, M. Tsukamoto, M. Ichinohe, *Science* **1997**, *275*, 60.
- 32) A. Sekiguchi, T. Matsuno, M. Ichinohe, *J. Am. Chem. Soc.* **2000**, *122*, 11250.
- 33) (a) A. Sekiguchi, T. Matsuno, M. Ichinohe, *J. Am. Chem. Soc.* **2001**, *123*, 12436; (b) T. Matsuno, M. Ichinohe, A. Sekiguchi, *Angew. Chem. Int. Ed.* **2002**, *41*, 1575.
- 34) Chemistry of silyl radicals, see (a) A. Sekiguchi, T. Fukawa, M. Nakamoto, V. Ya. Lee, M. Ichinohe, *J. Am. Chem. Soc.* **2002**, *124*, 9865; (b) V. Ya. Lee, A. Sekiguchi, *Acc. Chem. Res.* **2007**, *40*, 410; (c) T. Nozawa, M. Nagata, M. Ichinohe, A. Sekiguchi, *J. Am. Chem. Soc.* **2011**, *133*, 5773; (d) K. Taira, M. Ichinohe, A. Sekiguchi, *Chem. Eur. J.* **2014**, *20*, 9342; (e) H. Maruyama, H. Nakano, M. Nakamoto, A. Sekiguchi, *Angew. Chem., Int. Ed.* **2014**, *53*, 1324.
- 35) Reviews on bicyclo[1.1.0]tetrasilane: (a) M. Karni, J. Kapp, P. v. R. Schleyer, Y. Apeloig in *The Chemistry of Organic Silicon Compounds Vol. 3*, (Ed. by Z. Rappoport, Y. Apeloig) John Wiley & Sons, Ltd, Chichester, 2001 chap. 1; (b) M. Rohmer, M. Bénard, *Chem. Soc. Rev.* **2001**, *30*, 340; (c) M. Kira, *Organometallics* **2014**, *33*, 644; (d) T. Müller in *Organosilicon Chemistry IV From Molecules to Materials*, (Ed. by N. Auner and J. Weis) Wiley-VCH Ltd, 2000, 110.
- 36) (a) S. Masamune, Y. Kabe, S. Collins, *J. Am. Chem. Soc.* **1985**, *107*, 5552; (b) R. Jones, D. Williams, Y. Kabe, S. Masamune, *Angew. Chem., Int. Ed.* **1986**, *25*, 173.

- 37) K. Ueba-Ohshima, T. Iwamoto, M. Kira, *Organometallics* **2008**, *27*, 320.
- 38) T. Iwamoto, D. Yin, C. Kabuto, M. Kira, *J. Am. Chem. Soc.* **2001**, *123*, 12730.
- 39) P. v. R. Schleyer, A. F. Sax, J. Kalcher, R. Janoschek, *Angew. Chem., Int. Ed. Engl.* **1987**, *26*, 364.
- 40) V. Ya. Lee, H. Yasuda, A. Sekiguchi, *J. Am. Chem. Soc.* **2007**, *129*, 2436.
- 41) (a) V. Ya. Lee, S. Miyazaki, H. Yasuda, and A. Sekiguchi, *J. Am. Chem. Soc.* **2008**, *130*, 2758; (b) V. Ya. Lee, O. A. Gapurenko, S. Miyazaki, A. Sekiguchi, R. M. Minyaev, V. I. Minkin, and H. Gornitzka, *Angew. Chem., Int. Ed.* **2015**, *127*, 14324.
- 42) For example Y. Apeloir, M. Karni, *J. Am. Chem. Soc.* **1984**, *106*, 6676.
- 43) (a) M. Takahashi, K. Sakamoto, *Organometallics* **2002**, *21*, 4212; (b) P. P. Power, *Chem. Rev.* **1999**, *99*, 3463; (c) K. Kobayashi, S. Nagase, *Organometallics* **1997**, *16*, 2489; (d) K. Takeuchi, M. Ikoshi, M. Ichinohe, A. Sekiguchi, *J. Am. Chem. Soc.* **2010**, *132*, 930.
- 44) T. Guliashvili, I. El-Sayed, A. Fischer, H. Ottosson, *Angew. Chem. Int. Ed.* **2003**, *42*, 1640.

Chapter 1

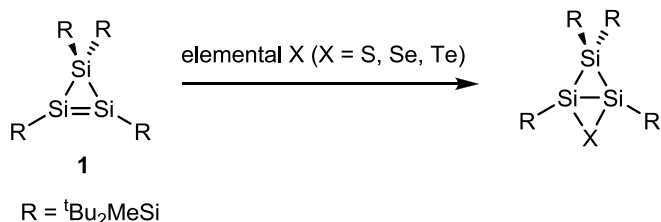
**Reaction of Cyclotrisilene with Isocyanides: Synthesis, Structure and Properties of
Small-Ring Silicon Compounds Having Imino Group**

1-1. Summary

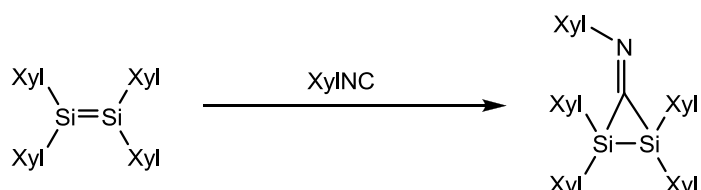
The reaction of tetrakis(di-*tert*-butylmethylsilyl)cyclotrisilene with cyclohexylisocyanide gave iminotrisilabicyclo[1.1.0]butane derivative as [1 + 2] cycloadduct, which also react with additional cyclohexylisocyanide at bridging Si-Si bond, affording diiminotrisilabicyclo[1.1.1]pentane derivative. On the other hand, the reaction of cyclotrisilene with xylylisocyanide (xylyl = 2, 6-dimethylophenyl) gave ring expanding iminotrisilacyclobutene derivative, which is formed by the thermal isomerization of iminotrisilabicyclo[1.1.0]butane intermediate.

1-2. Introduction

The chemistry of unsaturated silicon compounds has matured dramatically in the past few decades.¹ In particular, small, unsaturated silacycles² involving special ring systems (e.g. aromatic ring, homoaromatic ring) are energetically studied and still attractive target.³ Silicon analogues of bicyclo[1.1.0]butanes, which is the smallest and quite strained bicyclic, are one of such silicon splices due to not only the unusual structural property but also characteristic isomeric behaviour.⁴ Since the first synthesis of bicyclo[1.1.0]tetrasilane by Masamune,⁵ a variety of heavier bicyclo[1.1.0]butanes and its isomers have been isolated.⁶ Steric and electronic influence of constituent elements on the bicyclo[1.1.0]butane skeleton is critical, giving a variety of isomers such as bond stretching isomers, very short bond isomer, and unsaturated silacycles.⁷ However, functionalization of silicon analogue of bicyclo[1.1.0]butane skeleton is still poor because of the synthetic difficulty. Especially, study on the interaction of Si-Si banana bond in bicyclo[1.1.0]butane analogue toward double bond is little to our knowledge, while that on carbon chemistry is theoretically and experimentally investigated.⁸



Recently, our group reported the synthesis of chalcogen introduced Si_3X trisilabicyclo[1.1.0]butanes by the reaction of cyclotrisilene **1** with elemental X ($X = \text{S, Se, Te}$).⁹ Although the chalcogen atoms did not give significant change to the bicyclo[1.1.0]butane skeleton, notable photochemical conversion from trisilabicyclo[1.1.0]butane to trisilacyclobutene are observed. Importantly, this result suggests that the highly reactive cyclotrisilene **1** can be a good precursor for further functionalized trisilabicyclo[1.1.0]butanes and related isomers.

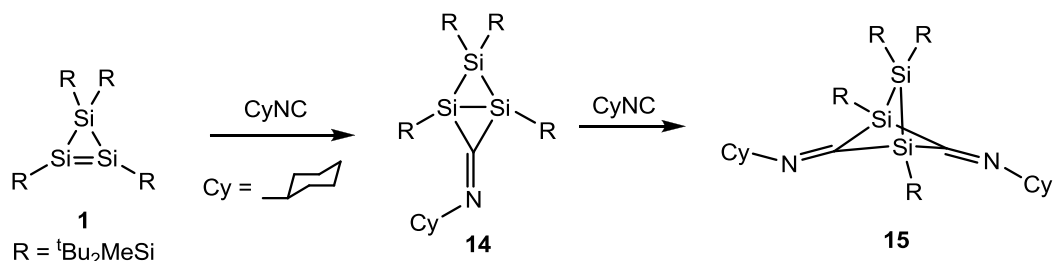


In this chapter, the author describes the reaction of cyclotrisilene **1** with isocyanides, which reacts with Si=Si double to give disilacyclopropanimine via [1 + 2]cycloaddition,¹⁰ in order to introduce imino group into Si_3X trisilabicyclo[1.1.0]butane. Investigation of the substituent effect on N atom of imine, using alkyl and arylisocyanide, is also described.

1-3. Result and Discussion

1-3-1. Formal cycloaddition reactions of isonitriles with cyclotrisilene

Scheme 1-3-1



Treatment of cyclotrisilenes **1** with one equivalent amount of cyclohexylisonitrile resulted in the formation of bicyclic compounds **14** as crystalline material in 58% yields from pentane (Scheme 1-3-1). The ^{29}Si NMR spectrum of **14** exhibits three signals of skeletal silicon atoms at $\delta = -93.9$, -105.4 and -127.9 ppm, indicating that inversion of imine nitrogen is not involved.¹¹ The two higher field resonances are assigned to the bridgehead silicon atoms, and the other one to bridging Si atom. These skeletal ^{29}Si chemical shifts at high field region is comparable to other Si_3X bicyclo[1.1.0]butanes (for example, -81.5 (bridging Si) -132.3 ppm (bridgehead Si) $\text{X} = \text{CH}_2$).^{6a} The imine ^{13}C resonances of **14** are found at low field $\delta = 198.2$ ppm, as is usual for cyclic bis(silyl)imines,¹⁰.

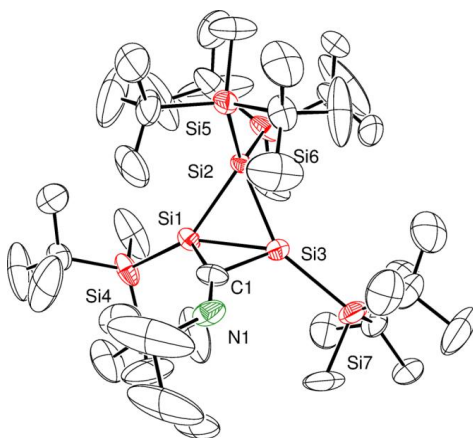


Figure 1-3-1. ORTEP drawing of cyclohexyliminotrisilabicyclo[1.0]butane **14**. Selected bond distances (\AA): $\text{Si1-Si2} = 2.3557(12)$, $\text{Si1-Si3} = 2.3608(13)$, $\text{Si2-Si3} = 2.3431(12)$, $\text{Si1-C1} = 1.898(4)$, $\text{Si3-C1} = 1.884(4)$, $\text{C1-N1} = 1.311(6)$. Selected bond angles (deg): $\text{Si1-Si2-Si3} = 60.32(4)$, $\text{Si1-Si3-Si2} = 60.10(4)$, $\text{Si3-Si1-Si2} = 59.58(4)$, $\text{C1-Si3-Si1} = 51.12(12)$, $\text{C1-Si1-Si3} = 51.63(12)$, $\text{Si1-C1-Si3} = 77.25(13)$.

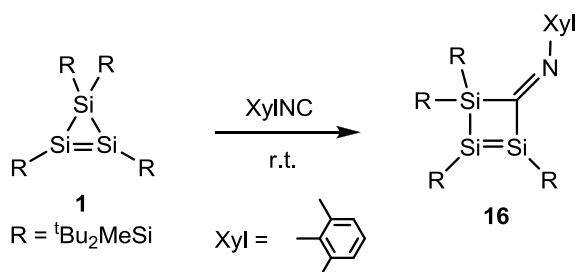
Single crystals of **14** were obtained by recrystallization from pentane. The folded bicylobutane-type structure exhibits a

bonding interaction between the two bridging atoms (Si1-Si3 2.3608(13) Å) comparable to bicyclo[1.1.0]tetrasilane derivative (2.373(3) Å) by Masamune (Figure. 1-3-1).⁵ The acutely folded angle of internal planes (119.52°) is close to that of methylene bridged trisilabicyclo[1.1.0]butane (115.5°). The two bonds between the bridging silicon atoms and the imine carbon have an essentially similar bond length (Si2-C1 = 1.898(4), Si3-C1 = 1.884(4) Å) within a normal Si-C single bond range. The imine C1-N1 double bond length is 1.311(6) Å, being in the typical C=N double bond region. Because the structural parameters of **14** are similar to those of typical bicyclo[1.1.0]butane silicon analogues, cyclohexylimino group would have small effect on the molecular structure of **14**.

When cyclotrisilene **1** was reacted with two equivalent amounts of cyclohexyl isocyanide, diiminotrisilabicyclo[1.1.1]pentane **15** was formed, presumably via the insertion of isocyanide into the strained Si–Si bridging-bond of **14** (Scheme 1). The skeletal silicon atoms in **15** have two resonances in the ²⁹Si NMR spectrum at δ = –19.4 and –108.1 ppm, reflecting the symmetrical molecular structure. A single resonance for the two imine carbon atoms was detected at δ = 194.2 ppm in the ¹³C NMR spectrum. An X-ray structural determination of a single crystal of **15** was sufficient to confirm the structure of the product, however the discussion of structural parameters is precluded by the significant disorder.

1-3-2. Iminotrisilacyclobutenes

Scheme 1-3-2



When the cyclotrisilene **1** was reacted with xylylisocyanide, different type reactivity was observed. Addition of xylylisocyanide to benzene solution of **1** at room temperature afforded a ring-expanded compound, iminotrisilacyclobutene derivative **16**, as dark red crystals in 48% yield (Scheme 1-3-2). Two low field resonances (δ = 173.9 and 165.1 ppm) in the ²⁹Si silicon NMR spectrum of **16** are characteristic for a silyl-substituted Si=Si double bond, although these values are somewhat downfield compared with non-conjugated four-membered disilenes (141.3–167.6 ppm). The imino carbon atom was observed at δ = 206.7 ppm in the ¹³C NMR spectrum, in the same region of those for **14** and **15**.

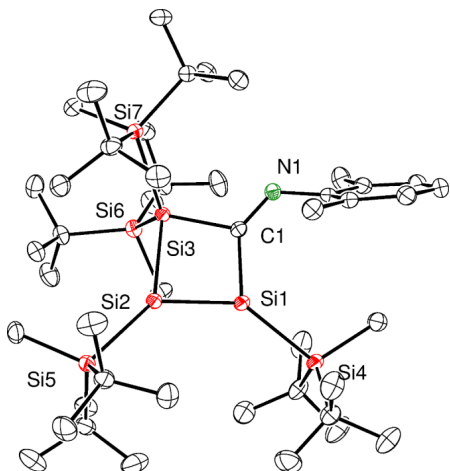


Figure 1-3-2. ORTEP drawing of **16**. Selected bond distances (\AA): Si1–Si2 = 2.1975(7), Si1–C1 = 1.9169(18), Si2–Si3 = 2.3835(7), Si3–C1 = 1.9567(18), N1–C1 = 1.286(2). Selected bond angles (deg): Si2–Si1–Si4 = 142.95(3), Si2–Si1–C1 = 88.91(6), Si4–Si1–C1 = 125.78(6), Si1–Si2–Si3 = 83.26(2), Si1–Si2–Si5 = 134.78(3), Si3–Si2–Si5 = 141.93(3), Si2–Si3–Si6 = 103.89(2), Si2–Si3–Si7 = 122.04(3), Si6–Si3–Si7 = 118.52(3), Si2–Si3–C1 = 82.81(5), Si6–Si3–C1 = 111.27(5), Si7–Si3–C1 = 112.83(5), C1–N1–C38 = 125.51(15), Si1–C1–Si3 = 103.72(8), Si1–C1–N1 = 135.10(14), Si3–C1–N1 = 120.66(13).

The molecular structures of **16** (Figure. 1-3-2) in the solid state were determined by single-crystal X-ray diffraction analysis. The four-membered ring of **16** is almost planar with the sum of the internal angles being close to 360° (358.7°). Dihedral angle of Si=Si and C=N double bonds shows 161.6° , and the values for the sum of angles at Si(1) [$\Sigma\text{Si}1$], $\Sigma\text{Si}2$, and $\Sigma\text{C}1$ are all close to 360° . Despite the conformation that enables the conjugation between Si=Si and C=N double bonds in **16**, the bond lengths of Si=Si ($2.1975(7)$ \AA) and C=N ($1.286(2)$ \AA) are very similar to that observed in other four-membered cyclic disilene (2.174 \AA)¹² and no conjugated imines C=N bond (1.279 \AA) respectively. Moreover, the skeletal Si1–C1 bond length of $1.9169(18)$ \AA is longer than that of typical Si-C single bond (1.863 \AA), indicating that there is no double bond character in Si1–C1 bond .

As seen in NMR spectroscopic and structural data, the UV-Vis absorption spectrum of **16** in hexane also showed no evidence for conjugation of π bonds (Figure 1-3-3). Thus a strong absorption band at 455 nm ($\varepsilon = 11000 \text{ L}\cdot\text{mol}^{-1}\cdot\text{cm}^{-1}$) appeared. This absorption band was assigned to the $\pi-\pi^*$ (Si=Si) electronic transition by TD-DFT calculations. The maximum wavelength of **16** is very close to that of other non-conjugated four-membered disilene (465 nm).¹² The absorption band of **16** has a shoulder around 500 nm, corresponding to the n (lone pair on nitrogen) to π^* (Si=Si) forbidden transition.

The possibility of Si=Si and C=N conjugation in **16** was also examined by DFT calculation of the model compound

16' (in which the Me^tBu₂Si groups of **16** are replaced by Me₃Si groups). The optimized structural parameters of **16'** are in good agreement with the X-ray crystallographic data of **16**. The molecular orbitals of **16'** show that the HOMO consists of the π -bonding interaction between the Si=Si π orbital and substitutional Si–SiMe₃ σ -orbital (Figure 1-3-4). The LUMO consists of the π^* orbital of the Si=Si bond slightly mixed with the π^* orbital of the C=N bond. The C=N π bonding orbital is mainly located in the HOMO-15. These computational results are consistent with both the spectroscopic and structural properties of **16**, which indicate a lack of interaction between the Si=Si and C=N double bonds. This is most likely attributable to the much higher energy of the Si=Si π -orbital level compared with that of the C=N double bond.

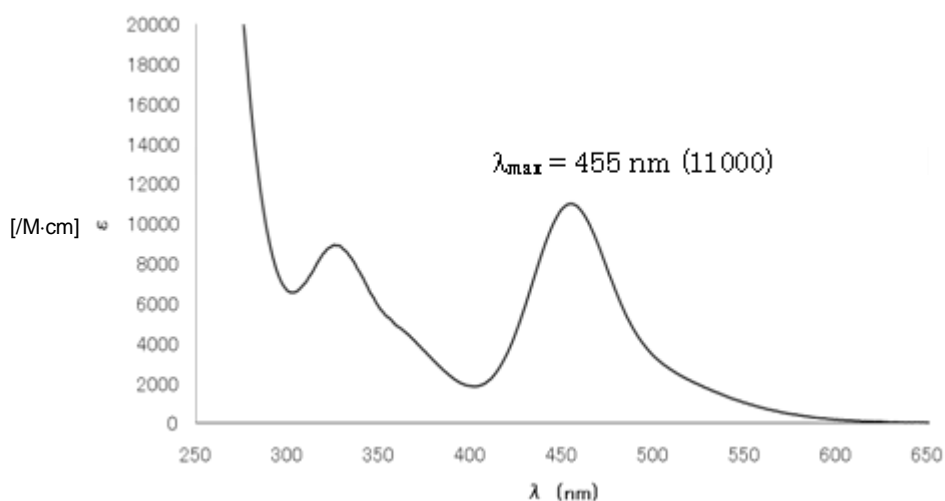


Figure 1-3-3. UV-Vis absorption spectrum of **16**.

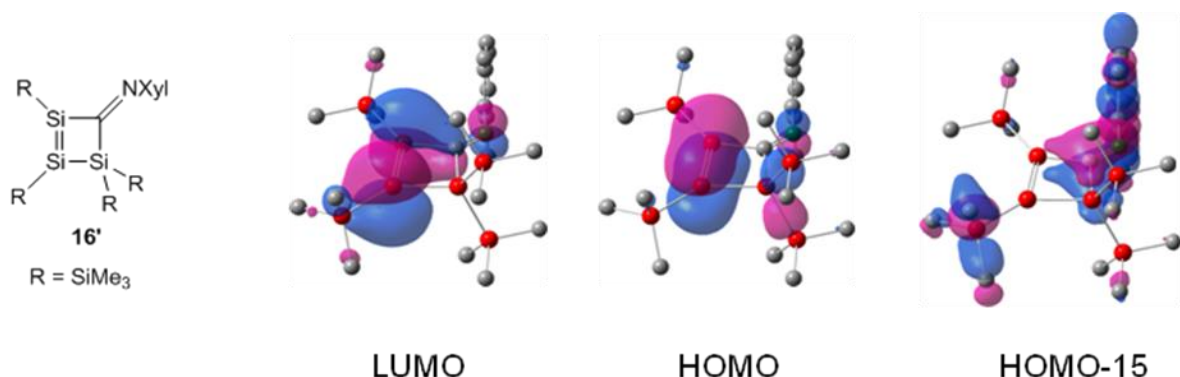
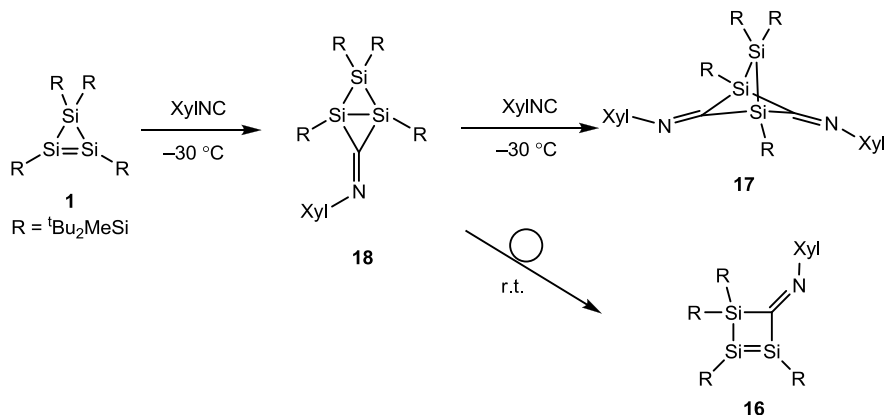


Figure 1-3-4. Molecular orbital of optimized model compound **16'**.

1-3-3. Mechanism for the formation of 16

Scheme 1-3-3



When cyclotrisilene **1** was treated with excess amount of isocyanide at $-30\text{ }^\circ\text{C}$, the sole product iminotrisilabicyclo[1.1.1]pentane **17** was isolated. This result indicates that xylyliminotrisilabicyclo[1.1.0]butane **18** is the common intermediate toward **16** and **17** (Scheme 1-3-3).

To investigate the factors controlling formation of iminobicyclobutane **14** vs. iminocyclobutene **16**, calculations on the model compounds, iminobicyclobutane **I** and iminocyclobutene **II** were performed (Figure 1-3-5). Both model iminotrisilabicyclo[1.1.0]butane structures **Ia** and **Ib** are found to be less stable than their cyclobutene isomers **II**. These results suggest that **14** is formed under kinetic control.

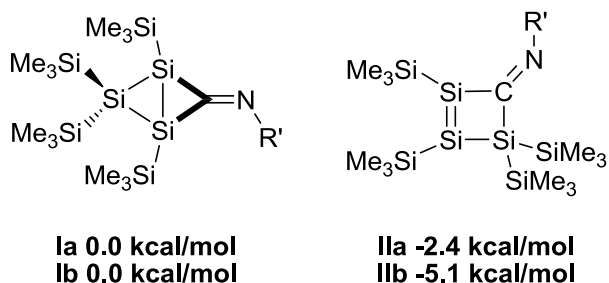


Figure 1-3-5. Relative energies of trimethylsilyl-substituted Si_3C bicyclo[1.1.0]butanes **I** and cyclobutenes **II** (optimized at the B3LYP/6-31G(d) level). **Ia**, **IIa**, R' = Cy, **Ib**, **IIb**: R' = xylyl.

Less thermal stability of **18** can be explained by the aryl group on imine. In particular, *ortho*-substituted aryl imine shows the rotation (or inversion) of lone pair on N atom, even at room temperature (for example the activation barrier of inversion process for $\text{XylN}=\text{C}(^i\text{Pr})\text{SiMe}_3$ is 14.8 kcal/mol, Chart 1-3-1, top).¹¹ Plausible linear transient state of the rotation process is considered to have radical or polar character with a cleavage of C-N π bond.¹³ Similarly, tetrasilabicyclo[1.1.0]butane framework is also known to proceed a ring inversion (Chart 1-3-1, bottom). Moreover, the

transition state of inversion process of bicyclo[1.1.0]butane is a planar biradical like state. Such planar conformation of the transition state would enable the electron delocalization from bicyclo[1.1.0]butane skeleton to C=N-Ar moiety like shown as **TS** in Chart 1-3-2. As a result, the interflip process of **18** including **TS** is induced by the electron delocalization with arylimino group. Following silyl group migration in **TS** would give product **16**. Such isomeric behaviour of **18** have been reported for tetrasilabicyclo[1.1.0]butane by Kira et al., which also showed thermal flipping and isomerization toward tetrasilacyclobutene derivative.¹⁴

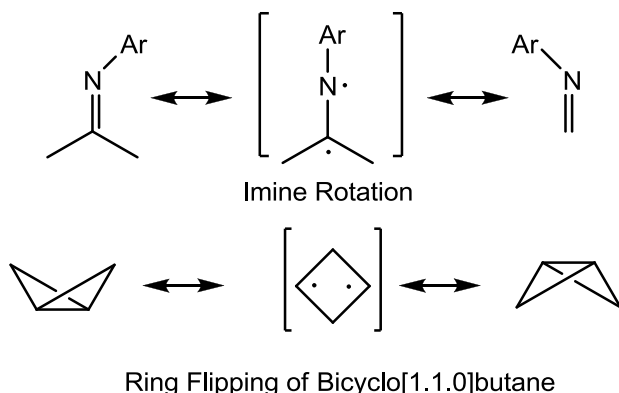


Chart 1-3-1. Inversion process of imine and interflipping process of bicyclo[1.1.0]butane.

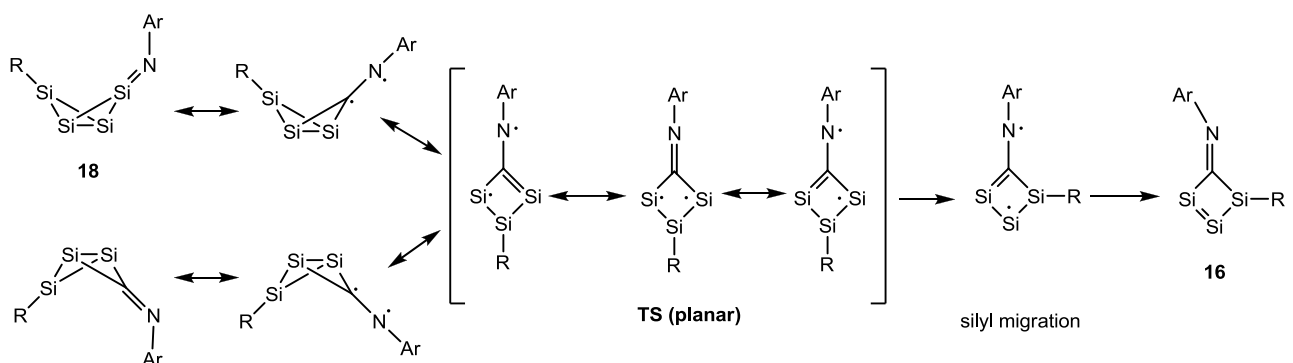


Chart 1-3-2. Multiple inversion process of iminotrisilabicyclo[1.1.0]butane **18** and silylmigration process toward **16** (Polar process is not shown here).

1-4. Conclusion

In conclusion, the reactions of the highly strained cyclotrisilene **1** with isocyanides initially result in the formation of cyclohexyliminotrisilabicyclo[1.1.0]butanes **14**, which can also react with a further equivalent of isocyanide to form diiminotrisilabicyclo[1.1.1]pentanes **15**. Thermally unstable xylyliminotrisilabicyclobutane **18** can rearrange to the iminotrisilacyclobutene **16**. Based on the spectroscopic and structural data of **16**, there is no indication of a significant interaction between the Si=Si and C=N double bonds despite the apparent coplanar conformations of the π -system.

1-5. Experimental Section

General Procedure. All experiments were performed using high-vacuum line techniques or in an argon atmosphere using MBRAUN MB 150B-G glove box. All solvents were dried and degassed over potassium mirror in vacuum prior to use. NMR spectra were recorded on Bruker AC-300FT NMR (¹H NMR at 300.1 MHz; ¹³C NMR at 75.5 MHz; ²⁹Si NMR at 59.6 MHz), AV-400FT NMR (¹H NMR at 400 MHz; ¹³C NMR at 100.6 MHz; ²⁹Si NMR at 79.5 MHz) spectrometers. High-resolution mass spectra were measured on Bruker Daltonics microTOF-TU mass spectrometer with APCI (atmospheric pressure chemical ionization method). UV-Vis spectra were recorded on Simadzu UV-3150 UV-Vis spectrophotometer. All computations were carried out using the Gaussian 03 and 98 suite of programs B3LYP level at 6-31G(d) basis set. Tetrakis[di-*tert*-butyl(methyl)silyl]cyclotrisilene **1** was prepared according to the published procedure.

Experimental	Procedure	and	Spectral	Data	of
1,2,2,3-tetrakis[di-<i>tert</i>-butyl(methyl)silyl]-4-cyclohexylimino-1,2,3-trisilabicyclo[1.1.0]butane 14.					

Cyclohexylisocyanide (3.5 μ l, 0.038 mmol) was added to a dry oxygen-free benzene solution (0.5 ml) of 1,2,3,3-tetrakis[di-*tert*-butyl(methyl)silyl]cyclotrisilene **1** (27 mg, 0.038 mmol) and stirred at room temperature for 10 minutes. The solution color changed yellow from orange of **1**. After evaporation of solvent and remaining isocyanide, the residue was recrystallized from pentane (0.5 ml) at -30 °C to give 1,2,2,3-tetrakis[di-*tert*-butyl(methyl)silyl]-4-cyclohexylimino-1,2,3-trisilabicyclo[1.1.0]butane **14** as yellow crystals (18 mg, 58% yield); decomposition point = 75.0-76.0 °C; ¹H NMR (C_6D_6 , δ) 0.34 (s, 3 H, SiMe), 0.42 (s, 3 H, SiMe), 0.43 (s, 3 H, SiMe), 0.47 (s, 3 H, SiMe), 1.17 (s, 9 H, Si'Bu), 1.20 (s, 9 H, Si'Bu), 1.21 (s, 9 H, Si'Bu), 1.21 (s, 9 H, Si'Bu), 1.25 (s, 9 H, Si'Bu), 1.28 (s, 9 H, Si'Bu), 1.29 (s, 9 H, Si'Bu), 1.32 (s, 9 H, Si'Bu), 1.45-1.98 (m, 10 H, Cy), 3.26 (m, 1 H, Cy); ¹³C NMR (C_6D_6 , δ) -4.6 (SiMe), -3.6 (SiMe), -2.7 (SiMe), -2.7 (SiMe), 21.1 (CMe₃), 21.3 (CMe₃), 21.8 (CMe₃), 22.5 (CMe₃), 22.6 (CMe₃), 22.7 (CMe₃), 23.0 (CMe₃), 23.0 (CMe₃), 24.7 (Cy), 25.1 (Cy), 26.4 (Cy), 29.8 (CMe₃), 29.9 (CMe₃), 30.1 (CMe₃), 30.3 (CMe₃), 30.4 (CMe₃), 30.7 (CMe₃), 31.3 (CMe₃), 31.3 (CMe₃), 34.0 (Cy), 35.0 (Cy), 75.6 (Cy), 198.2 (C=N); ²⁹Si NMR (C_6D_6 , δ) -127.9 (skeletal Si), -105.4 (skeletal Si), -93.9 (skeletal Si), 9.4 (Si'Bu₂Me), 21.6 (Si'Bu₂Me), 25.1 (Si'Bu₂Me), 28.7 (Si'Bu₂Me); Anal. Calcd for C₄₃H₉₅NSi₇: C, 62.77; H, 11.64; N, 1.70; Found: C, 62.85; H, 11.82; N, 1.61.

The single crystals of **14** for X-ray diffraction analysis were grown from a pentane solution. Diffraction data were collected at 120 K on a Bruker AXS APEX II CCD X-ray diffractometer (Mo-K α radiation, l = 0.71073 Å, 50 kV, 30 mA). The structure was solved by the direct method, using SIR-92 program, and refined by the full-matrix least-squares

method by SHELXL-97 program. Crystal data for **14** at 120 K: MF = C₄₃H₉₅NSi₇, MW = 822.83, monoclinic, space group P 2₁/n, *a* = 12.0962(7) Å, *b* = 21.7036(12) Å, *c* = 20.2182(11) Å, β = 92.8640(10)°, *V* = 5301.3(5) Å³, *Z* = 4, D_{calcd} = 1.031 g/cm³, The final *R* factor was 0.0874 (*R*_w = 0.2426 for all data) for 12068 reflections with *I* > 2σ(*I*), GOF = 1.031.

Experimental	Procedure	and	Spectral	Data	of
--------------	-----------	-----	----------	------	----

1,1,2,4-tetrakis[di-*tert*-butyl(methyl)silyl]-3,5-bis(cyclohexylimino)-1,2,4-trisilabicyclo[1.1.1]pentane 15.

Cyclohexylisocyanide (17.5 µl, 0.15 mmol) was added to a dry oxygen-free benzene solution (1.0 ml) of 1,2,3,3-tetrakis[di-*tert*-butyl(methyl)silyl]cyclotrisilene **1** (50 mg, 0.070 mmol) and stirred at room temperature for 1 day. The solution color changed yellow from orange of **1**. After evaporation of the solvent and remaining isocyanide, the residue was recrystallized from pentane (0.5 ml) at -30 °C to give 1,1,2,4-tetrakis[di-*tert*-butyl(methyl)silyl]-3,5-bis(cyclohexylimino)-1,2,4-trisilabicyclo[1.1.1]pentane **15** as yellow crystals (65 mg, 81% yield); decomposition point = 116.0-116.5 °C; ¹H NMR (C₆D₆, δ) 0.51 (s, 6 H, SiMe), 0.61 (s, 6 H, SiMe), 1.25 (s, 18 H, ¹Bu), 1.26 (s, 9 H, ¹Bu), 1.28 (s, 9 H, ¹Bu), 1.5-3.5 (m, 11 H, Cy); ¹³C NMR (C₆D₆, δ) -3.1 (SiMe), -0.4 (SiMe), 22.2 (CMe), 22.4 (CMe), 22.6 (CMe), 22.9 (CMe), 24.4 (Cy), 24.5 (Cy), 26.1 (Cy), 29.9 (CMe), 30.8 (CMe), 31.2 (CMe), 31.3 (CMe), 33.1 (Cy), 34.7 (Cy), 75.4 (Cy_{ipso}), 194.2 (skeletal C); ²⁹Si NMR (C₆D₆, δ) -108.1 (skeletal Si), -19.4 (skeletal Si), 16.7 (Si^tBu₂Me), 26.9 (Si^tBu₂Me); Anal. Calcd for C₅₀H₁₀₆N₂Si₇: C, 64.44; H, 11.64; N, 3.01. Found: C, 64.57; H, 11.26; N, 3.20.

The single crystals of **15** for X-ray diffraction analysis were grown from a pentane solution. Diffraction data were collected at 120 K on a Bruker AXS APEX II CCD X-ray diffractometer (Mo- *K*α radiation, *l* = 0.71073 Å, 50 kV, 30 mA). The structure was solved by the direct method, using SIR-92 program, and refined by the full-matrix least-squares method by SHELXL-97 program. Crystal data for **15** at 120 K: MF = C₅₀H₁₀₆N₂Si₇, MW = 932.00, monoclinic, space group P 2₁/n, *a* = 13.594(3) Å, *b* = 20.159(4) Å, *c* = 21.603(5) Å, β = 94.275(2)°, *V* = 5904(2) Å³, *Z* = 4, D_{calcd} = 1.049 g/cm³, The final *R* factor was 0.0937 (*R*_w = 0.2353 for all data) for 13406 reflections with *I* > 2σ(*I*), GOF = 0.968.

Experimental	Procedure	and	Spectral	Data	of
--------------	-----------	-----	----------	------	----

1,2,3,3-tetrakis[di-*tert*-butyl(methyl)silyl]-4-(2,6-dimethylphenyl)imino-1,2,3-trisilacyclobutene 16.

Dry oxygen-free C₆H₆ (3.0 ml) was added by vacuum transfer to mixture of 1,2,3,3-tetrakis[di-*tert*-butyl(methyl)silyl]cyclotrisilene **1** (300 mg, 0.42 mmol) and 2,6-xylylisocyanide (60 mg, 0.46 mmol) and stirred at room temperature for 6 h. The solution color changed dark red from orange of **1**. After evaporation,

the residue was recrystallized from hexane (2.0 ml) at -30°C to give 1,2,3,3-tetrakis[di-*tert*-butyl(methyl)silyl]-4-(2,6-dimethylphenyl)imino-1,2,3-trisilabutene **16** as dark red crystals (170 mg, 48% yield); mp = 175.0–176.0 $^{\circ}\text{C}$; ^1H NMR (C_6D_6 , δ) –0.44 (s, 3 H, Si*Me*), 0.44 (s, 3 H, Si*Me*), 0.53 (s, 6 H, Si*Me*), 1.02 (s, 18 H, Si*tBu*₂), 1.25 (s, 18 H, Si*tBu*₂), 1.30 (s, 18 H, Si*tBu*₂), 1.30 (s, 18 H, Si*tBu*₂), 2.43 (s, 6 H, Ar*Me*), 6.83 (t, *J* = 6.0 Hz, 1 H, Ar), 6.95 (d, *J* = 6.0 Hz, 2 H, Ar); ^{13}C NMR (C_6D_6 , δ) –6.5 (Si*Me*), –4.1 (Si*Me*), –1.6 (Si*Me*), 21.1 (Ar*Me*), 21.2 (C*Me*₃), 22.1 (C*Me*₃), 22.5 (C*Me*₃), 23.2 (C*Me*₃), 30.1 (C*Me*₃), 30.7 (C*Me*₃), 31.2 (C*Me*₃), 31.7 (C*Me*₃), 123.3 (Ar), 127.4 (Ar), 129.5 (Ar), 154.7 (Ar), 206.7 (C=N); ^{29}Si NMR (C_6D_6 , δ) 2.46 (skeletal sp³ Si), 12.3 (Si*tBu*₂Me), 19.7 (Si*tBu*₂Me), 25.9 (Si*tBu*₂Me), 165.1 (Si=Si), 173.9 (Si=Si); HRMS: *m/z* calcd for $\text{C}_{45}\text{H}_{93}\text{NSi}_7$ (M)⁺ 843.5687, found 843.5675; UV/Vis (hexane): λ_{max} / nm (ϵ): 455 (11000).

The single crystals of **16** for X-ray diffraction analysis were grown from a pentane solution. Diffraction data were collected at 120 K on a Bruker AXS APEX II CCD X-ray diffractometer (Mo- *K* α radiation, *l* = 0.71073 Å, 50 kV, 30 mA). The structure was solved by the direct method, using SIR-92 program, and refined by the full-matrix least-squares method by SHELXL-97 program. Crystal data for **16** at 120 K: MF = $\text{C}_{45}\text{H}_{93}\text{NSi}_7$, MW = 844.83, monoclinic, space group *P* 2₁/n, *a* = 20.0059(6) Å, *b* = 14.7795(5) Å, *c* = 20.1475(6) Å, β = 115.714(1) $^{\circ}$, *V* = 5367.2(3) Å³, *Z* = 4, D_{calcd} = 1.046 g/cm³, The final *R* factor was 0.0418 (*R*_w = 0.1122 for all data) for 12057 reflections with *I* > 2 σ (*I*), GOF = 0.980.

Experimental Procedure and Spectral Data of 1,1,2,4-tetrakis[di-*tert*-butyl(methyl)silyl]-3,5-bis(cyclohexylimino)-1,2,4-trisilabicyclo[1.1.1]pentane **17**.

Dry oxygen-free C_6H_6 (3.0 ml) was added to mixture of 1,2,3,3-tetrakis[di-*tert*-butyl(methyl)silyl]cyclotrisilene **1** (100 mg, 0.14 mmol) and XyLNC (36 mg, 0.28 mmol), and stirred at room temperature for 5 min. The solution color changed dark red from orange of **1**. Then, the solvent was changed from benzene to pentane and cooled at -30°C . After 24 h, the thermally unstable

1,1,2,4-tetrakis[di-*tert*-butyl(methyl)silyl]-3,5-bis(cyclohexylimino)-1,2,4-trisilabicyclo[1.1.1]pentane **17** was obtained as red crystals (53 mg, 39% yield); ^1H NMR (toluene-*d*₈, 250 K, δ) 0.44 (s, 6 H, Si*Me*), 0.46 (s, 6 H, Si*Me*), 1.17 (s, 18 H, *tBu*), 1.32 (s, 18 H, *tBu*), 2.47 (s, 6 H, Ae*Me*), 2.55 (s, 6 H, Ar*Me*), 6.94 (m, 6 H, Ar); ^{29}Si NMR (toluene-*d*₈, 250 K, δ) –120.3 (skeletal Si), –23.0 (skeletal Si), 23.7 (Si*tBu*₂Me), 25.2 (Si*tBu*₂Me)

The single crystals of **17** for X-ray diffraction analysis were grown from a pentane solution. Diffraction data were collected at 120 K on a Bruker AXS APEX II CCD X-ray diffractometer (Mo- *K* α radiation, *l* = 0.71073 Å, 50 kV, 30 mA). The structure was solved by the direct method, using SIR-92 program, and refined by the full-matrix least-squares method by SHELXL-97 program. Crystal data for **17** at 120 K: MF = $\text{C}_{59}\text{H}_{114}\text{N}_2\text{Si}_7$, MW = 1048.15, triclinic, space

group *P*-1, $a = 12.3120(6)$ Å, $b = 13.0946(6)$ Å, $c = 22.2223(10)$ Å, $\beta = 88.378(1)^\circ$, $V = 3212.0(3)$ Å³, $Z = 2$, $D_{\text{calcd}} = 1.084$ g/cm³, The final *R* factor was 0.0474 ($R_w = 0.1352$ for all data) for 14310 reflections with $I > 2\sigma(I)$, GOF = 1.026.

Preparation and Spectral Data of

1,2,2,3-tetrakis[di-*tert*-butyl(methyl)silyl]-4-(2,6)-xylylimino-1,2,3-trisilabicyclo[1.1.0]butane 18.

Dried C₆D₆ was transferred to xylylisocyanide (4.0 µl, 0.028 mmol) and 1,2,3,3-tetrakis[di-*tert*-butyl(methyl)silyl]cyclotrisilene **1** (20 mg, 0.028 mmol) in a NMR tube. The ¹H NMR in the sealed tube showed generation of 1,2,2,3-tetrakis[di-*tert*-butyl(methyl)silyl]-4-(2,6)-xylylimino-1,2,3-trisilabicyclo[1.1.0]butane **18**, which isomerizes to **16** in 5 hours at room temperature; ¹H NMR (C₆D₆, δ) 0.36 (s, 6 H, SiMe), 0.45 (s, 6 H, SiMe), 1.15 (s, 36 H, ¹Bu), 1.25 (s, 36 H, ¹Bu), 2.42 (s, 6 H, ArMe), 6.87 (t, 1 H, *J* = 6 Hz, *para*-H), 7.00 (d, 2 H, *J* = 6 Hz, *meta*-H).

Crystal data

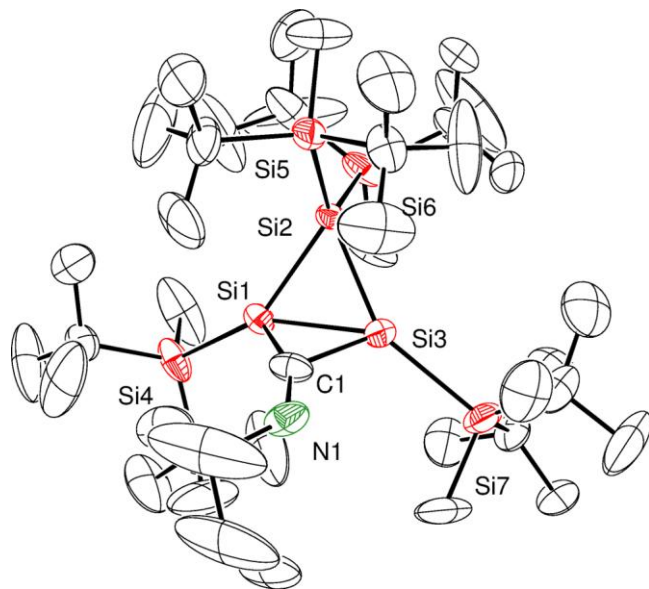


Figure 1-5-1. ORTEP drawing of Compound 14 (H atoms are omitted for clarity).

Table 1-5-1. Crystal data and structure refinement for compound **14**.

Identification code	(tBu2MeSi)4Si3CNCyh		
Empirical formula	C43 H95 N Si7		
Formula weight	822.83		
Temperature	120(1) K		
Wavelength	0.71073 Å		
Crystal system	Monoclinic		
Space group	P2(1)/n		
Unit cell dimensions	a = 12.0962(7) Å	α= 90 deg.	
	b = 21.7036(12) Å	β= 92.8640(10) deg.	
	c = 20.2182(11) Å	γ = 90 deg.	
Volume	5301.3(5) Å ³		
Z	4		
Density (calculated)	1.031 Mg/m ³		
Absorption coefficient	0.207 mm ⁻¹		
F(000)	1832		
Crystal size	0.40 x 0.35 x 0.13 mm ³		
Theta range for data collection	1.38 to 27.48°.		
Index ranges	-15≤h≤15, -28≤k≤28, -25≤l≤26		
Reflections collected	59439		
Independent reflections	12068 [R(int) = 0.0343]		
Completeness to theta = 27.48 deg	99.2 %		
Absorption correction	Empirical		
Max. and min. transmission	0.9744 and 0.9212		
Refinement method	Full-matrix least-squares on F ²		
Data / restraints / parameters	12068 / 273 / 608		
Goodness-of-fit on F ²	1.031		
Final R indices [I>2sigma(I)]	R1 = 0.0874, wR2 = 0.2239		
R indices (all data)	R1 = 0.1077, wR2 = 0.2426		
Largest diff. peak and hole	1.402 and -1.199 e. Å ⁻³		

Table 1-5-2. Atomic coordinates ($\times 10^4$) and equivalent isotropic displacement parameters ($\text{\AA}^2 \times 10^3$)for compound **14**. $U(\text{eq})$ is defined as one third of the trace of the orthogonalized U^{ij} tensor.

	x	y	z	$U(\text{eq})$
Si(1)	5568(1)	1319(1)	2024(1)	34(1)
Si(2)	7142(1)	713(1)	2294(1)	28(1)
Si(3)	5400(1)	384(1)	2609(1)	33(1)
Si(4)	4764(1)	1961(1)	1166(1)	50(1)
Si(5)	8513(1)	1020(1)	3135(1)	40(1)
Si(6)	7690(1)	224(1)	1304(1)	49(1)
Si(7)	4079(3)	-429(2)	2830(2)	48(1)
Si(57)	4422(3)	-534(3)	2798(2)	33(1)
N(1)	4438(5)	1331(3)	3378(3)	53(2)
N(51)	4649(7)	1652(4)	3218(4)	45(2)
C(1)	5035(3)	1195(2)	2874(2)	42(1)
C(2)	5328(7)	1786(3)	326(2)	110(3)
C(3)	3255(4)	1790(2)	1093(3)	76(2)
C(4)	3140(8)	1114(3)	845(7)	209(7)
C(5)	2724(4)	1828(5)	1707(4)	130(3)
C(6)	2595(6)	2187(3)	598(4)	113(3)
C(7)	5177(3)	2785(2)	1357(2)	48(1)
C(8)	4801(8)	3009(3)	2000(4)	138(4)
C(9)	4762(8)	3226(3)	819(4)	133(4)
C(10)	6433(5)	2838(3)	1426(5)	129(3)
C(11)	9936(3)	856(3)	2849(3)	83(2)
C(12)	8485(4)	1898(2)	3278(3)	79(2)
C(13)	7406(5)	2129(3)	3483(5)	131(4)
C(14)	8665(9)	2206(4)	2610(5)	173(5)
C(15)	9404(5)	2112(3)	3770(4)	108(3)
C(16)	8359(4)	545(2)	3919(2)	51(1)
C(17)	9331(5)	632(3)	4420(3)	91(2)
C(18)	8314(8)	-130(2)	3735(3)	126(3)
C(19)	7312(5)	715(4)	4265(3)	113(3)
C(20)	6344(4)	84(3)	820(2)	72(2)
C(21)	8617(5)	779(3)	798(2)	86(2)
C(22)	9834(5)	746(3)	955(3)	86(2)
C(23)	8423(6)	611(7)	64(3)	203(7)
C(24)	8309(10)	1444(4)	943(6)	252(9)
C(25)	8342(4)	-579(2)	1456(2)	52(1)
C(26)	9486(4)	-560(3)	1817(4)	103(2)
C(27)	8501(9)	-899(4)	801(3)	180(6)
C(28)	7634(5)	-943(2)	1885(4)	95(2)
C(29)	2823(8)	4(6)	3124(9)	114(5)
C(30)	4686(6)	-892(3)	3577(3)	65(2)
C(31)	4880(10)	-463(5)	4172(4)	89(3)
C(32)	5802(8)	-1183(5)	3435(5)	88(3)
C(33)	3894(9)	-1403(5)	3777(7)	127(6)
C(34)	3560(6)	-879(4)	2059(4)	51(2)
C(35)	2511(7)	-1249(4)	2167(6)	62(3)
C(36)	3279(9)	-409(5)	1514(6)	87(3)
C(37)	4456(7)	-1312(4)	1824(6)	83(3)
C(38)	3962(5)	1950(3)	3383(4)	59(2)
C(39)	2751(6)	1890(5)	3573(4)	66(2)
C(40)	2630(6)	1652(4)	4285(4)	81(3)
C(41)	3281(8)	2047(7)	4801(6)	172(10)
C(42)	4476(9)	2144(7)	4603(5)	218(15)

C(43)	4578(7)	2370(4)	3886(5)	92(4)
-------	---------	---------	---------	-------

Table 1-5-3. Bond lengths [\AA] and angles [deg] for compound **14**.

Si(1)-C(1)	1.884(4)	C(1)-Si(1)-Si(2)	91.09(11)
Si(1)-Si(2)	2.3557(12)	C(1)-Si(1)-Si(3)	51.63(12)
Si(1)-Si(3)	2.3608(13)	Si(2)-Si(1)-Si(3)	59.58(4)
Si(1)-Si(4)	2.3940(13)	C(1)-Si(1)-Si(4)	126.80(12)
Si(2)-Si(3)	2.3431(12)	Si(2)-Si(1)-Si(4)	141.90(6)
Si(2)-Si(6)	2.3883(13)	Si(3)-Si(1)-Si(4)	145.18(6)
Si(2)-Si(5)	2.4100(13)	Si(3)-Si(2)-Si(1)	60.32(4)
Si(3)-C(1)	1.898(4)	Si(3)-Si(2)-Si(6)	112.55(5)
Si(3)-Si(7)	2.437(5)	Si(1)-Si(2)-Si(6)	108.04(5)
Si(4)-C(3)	1.861(5)	Si(3)-Si(2)-Si(5)	119.29(5)
Si(4)-C(7)	1.892(4)	Si(1)-Si(2)-Si(5)	121.93(5)
Si(4)-C(2)	1.901(5)	Si(6)-Si(2)-Si(5)	120.28(5)
Si(5)-C(11)	1.878(5)	C(1)-Si(3)-Si(2)	91.13(12)
Si(5)-C(16)	1.909(4)	C(1)-Si(3)-Si(1)	51.12(12)
Si(5)-C(12)	1.927(5)	Si(2)-Si(3)-Si(1)	60.10(4)
Si(6)-C(20)	1.884(5)	Si(57)-Si(3)-Si(1)	149.70(13)
Si(6)-C(25)	1.930(4)	C(1)-Si(3)-Si(7)	117.10(15)
Si(6)-C(21)	1.967(6)	Si(2)-Si(3)-Si(7)	151.31(10)
Si(7)-C(29)	1.907(9)	Si(57)-Si(3)-Si(7)	11.36(12)
Si(7)-C(34)	1.919(6)	Si(1)-Si(3)-Si(7)	141.94(10)
Si(7)-C(30)	1.929(7)	C(3)-Si(4)-C(7)	116.9(2)
N(1)-C(1)	1.311(6)	C(3)-Si(4)-C(2)	106.5(3)
N(1)-C(38)	1.462(8)	C(7)-Si(4)-C(2)	105.6(3)
C(3)-C(5)	1.430(10)	C(3)-Si(4)-Si(1)	107.64(18)
C(3)-C(6)	1.517(7)	C(7)-Si(4)-Si(1)	107.97(12)
C(3)-C(4)	1.554(8)	C(2)-Si(4)-Si(1)	112.35(17)
C(7)-C(8)	1.481(7)	C(11)-Si(5)-C(16)	106.4(2)
C(7)-C(9)	1.517(6)	C(11)-Si(5)-C(12)	104.9(3)
C(7)-C(10)	1.523(7)	C(16)-Si(5)-C(12)	114.0(2)
C(12)-C(13)	1.477(9)	C(11)-Si(5)-Si(2)	109.80(18)
C(12)-C(15)	1.527(7)	C(16)-Si(5)-Si(2)	110.12(14)
C(12)-C(14)	1.532(11)	C(12)-Si(5)-Si(2)	111.26(15)
C(16)-C(18)	1.511(7)	C(20)-Si(6)-C(25)	105.8(2)
C(16)-C(19)	1.521(8)	C(20)-Si(6)-C(21)	109.2(3)
C(16)-C(17)	1.525(6)	C(25)-Si(6)-C(21)	113.39(19)
C(21)-C(22)	1.492(8)	C(20)-Si(6)-Si(2)	103.80(13)
C(21)-C(24)	1.524(10)	C(25)-Si(6)-Si(2)	113.36(13)
C(21)-C(23)	1.535(9)	C(21)-Si(6)-Si(2)	110.66(19)
C(25)-C(28)	1.477(7)	C(29)-Si(7)-C(34)	105.8(6)
C(25)-C(27)	1.516(6)	C(29)-Si(7)-C(30)	106.9(6)
C(25)-C(26)	1.533(7)	C(34)-Si(7)-C(30)	117.8(4)
C(30)-C(32)	1.530(7)	C(29)-Si(7)-Si(3)	103.9(4)
C(30)-C(31)	1.531(7)	C(34)-Si(7)-Si(3)	114.2(3)
C(30)-C(33)	1.533(6)	C(30)-Si(7)-Si(3)	107.1(2)
C(34)-C(35)	1.527(7)	C(1)-N(1)-C(38)	116.5(6)
C(34)-C(36)	1.528(7)	N(1)-C(1)-Si(1)	154.5(4)
C(34)-C(37)	1.528(7)	N(51)-C(1)-Si(3)	161.0(5)
C(38)-C(43)	1.530(6)	N(1)-C(1)-Si(3)	125.0(4)
C(38)-C(39)	1.538(6)	Si(1)-C(1)-Si(3)	77.25(13)
C(39)-C(40)	1.543(7)	C(5)-C(3)-C(6)	107.2(6)
C(40)-C(41)	1.537(7)	C(5)-C(3)-C(4)	107.3(8)
C(41)-C(42)	1.535(7)	C(6)-C(3)-C(4)	106.7(5)
C(42)-C(43)	1.540(8)	C(5)-C(3)-Si(4)	113.6(4)
		C(6)-C(3)-Si(4)	114.9(5)

C(4)-C(3)-Si(4)	106.6(5)	C(28)-C(25)-C(26)	105.8(5)
C(8)-C(7)-C(9)	108.5(6)	C(27)-C(25)-C(26)	106.1(5)
C(8)-C(7)-C(10)	104.1(6)	C(28)-C(25)-Si(6)	109.4(3)
C(9)-C(7)-C(10)	108.0(5)	C(27)-C(25)-Si(6)	110.1(4)
C(8)-C(7)-Si(4)	113.7(3)	C(26)-C(25)-Si(6)	113.7(3)
C(9)-C(7)-Si(4)	112.1(3)	C(32)-C(30)-C(31)	107.2(6)
C(10)-C(7)-Si(4)	110.0(4)	C(32)-C(30)-C(33)	108.7(7)
C(13)-C(12)-C(15)	109.8(6)	C(31)-C(30)-C(33)	107.8(7)
C(13)-C(12)-C(14)	105.4(6)	C(32)-C(30)-Si(7)	111.9(5)
C(15)-C(12)-C(14)	108.1(6)	C(31)-C(30)-Si(7)	109.6(6)
C(13)-C(12)-Si(5)	113.6(4)	C(33)-C(30)-Si(7)	111.4(6)
C(15)-C(12)-Si(5)	112.4(4)	C(35)-C(34)-C(36)	107.3(6)
C(14)-C(12)-Si(5)	107.2(5)	C(35)-C(34)-C(37)	109.2(6)
C(18)-C(16)-C(19)	109.1(6)	C(36)-C(34)-C(37)	108.8(7)
C(18)-C(16)-C(17)	107.5(5)	C(35)-C(34)-Si(7)	113.0(7)
C(19)-C(16)-C(17)	107.3(4)	C(36)-C(34)-Si(7)	107.3(6)
C(18)-C(16)-Si(5)	108.9(3)	C(37)-C(34)-Si(7)	110.9(6)
C(19)-C(16)-Si(5)	111.6(3)	N(1)-C(38)-C(43)	111.9(7)
C(17)-C(16)-Si(5)	112.3(4)	N(1)-C(38)-C(39)	107.7(6)
C(22)-C(21)-C(24)	104.6(8)	C(43)-C(38)-C(39)	108.8(5)
C(22)-C(21)-C(23)	107.2(4)	C(38)-C(39)-C(40)	113.4(6)
C(24)-C(21)-C(23)	112.6(8)	C(41)-C(40)-C(39)	112.2(7)
C(22)-C(21)-Si(6)	116.2(3)	C(42)-C(41)-C(40)	110.8(6)
C(24)-C(21)-Si(6)	109.2(3)	C(41)-C(42)-C(43)	114.3(8)
C(23)-C(21)-Si(6)	107.1(6)	C(38)-C(43)-C(42)	112.1(6)
C(28)-C(25)-C(27)	111.7(6)		

Symmetry transformations used to generate equivalent atoms:

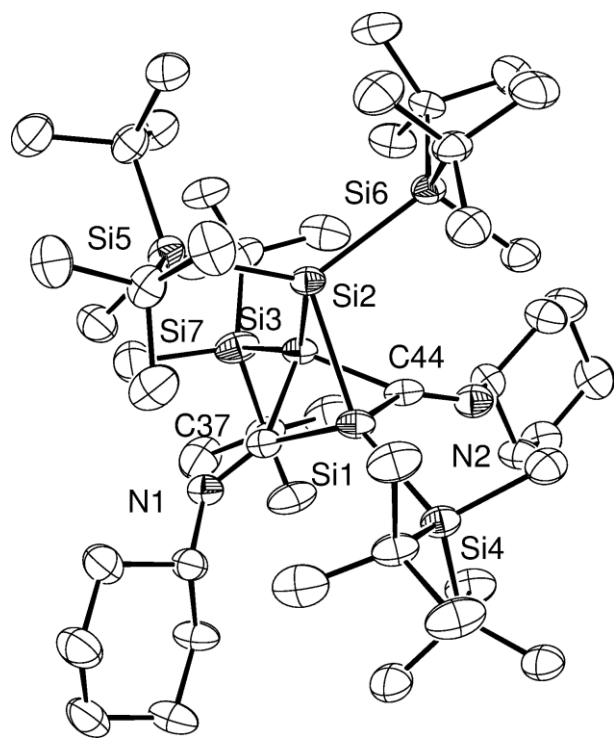


Figure 1-5-2. ORTEP drawing of Compound **15** (H atoms are omitted for clarity).

Table 1-5-4. Crystal data and structure refinement for compound **15**.

Identification code	(tBu ₂ MeSi)4Si ₃ + 2CNCy		
Empirical formula	C ₅₀ H ₁₀₆ N ₂ Si ₇		
Formula weight	932.00		
Temperature	120.0(1) K		
Wavelength	0.71073 Å		
Crystal system	Monoclinic		
Space group	P2(1)/n		
Unit cell dimensions	a = 13.594(3) Å	α= 90 deg.	
	b = 20.159(4) Å	β= 94.275(2) deg.	
	c = 21.603(5) Å	γ = 90 deg.	
Volume	5904(2) Å ³		
Z	4		
Density (calculated)	1.049 Mg/m ³		
Absorption coefficient	0.193 mm ⁻¹		
F(000)	2072		
Crystal size	0.22 x 0.08 x 0.06 mm ³		
Theta range for data collection	1.38 to 27.48°.		
Index ranges	-17<=h<=17, -26<=k<=25, -28<=l<=27		
Reflections collected	64320		
Independent reflections	13406 [R(int) = 0.2763]		
Completeness to theta = 27.48 deg	99.0 %		
Absorption correction	Empirical		
Max. and min. transmission	0.9883 and 0.9597		
Refinement method	Full-matrix least-squares on F ²		
Data / restraints / parameters	13406 / 0 / 533		
Goodness-of-fit on F ²	0.968		
Final R indices [I>2sigma(I)]	R1 = 0.0937, wR2 = 0.1713		
R indices (all data)	R1 = 0.2647, wR2 = 0.2353		
Extinction coefficient	0.0043(4)		
Largest diff. peak and hole	1.043 and -0.605 e. Å ⁻³		

Table 1-5-5. Atomic coordinates ($\times 10^4$) and equivalent isotropic displacement parameters ($\text{\AA}^2 \times 10^3$)for compound **15**. U(eq) is defined as one third of the trace of the orthogonalized U^{ij} tensor.

	x	y	z	U(eq)
Si(1)	5603(1)	7969(1)	1258(1)	29(1)
Si(2)	5623(1)	7704(1)	2362(1)	26(1)
Si(3)	4094(1)	7394(1)	1759(1)	28(1)
Si(4)	6452(1)	8651(1)	554(1)	32(1)
Si(5)	6512(1)	6705(1)	2705(1)	34(1)
Si(6)	5528(1)	8745(1)	2942(1)	30(1)
Si(7)	2683(1)	6666(1)	1758(1)	43(1)
N(1)	4930(3)	6584(2)	814(2)	31(1)
N(2)	3784(4)	8788(3)	1211(2)	36(1)
C(1)	6385(4)	9513(3)	879(3)	39(2)
C(2)	7808(4)	8412(3)	521(3)	37(2)
C(3)	8333(4)	8527(4)	1176(3)	48(2)
C(4)	8331(5)	8860(4)	66(3)	53(2)
C(5)	7969(5)	7683(4)	342(3)	53(2)
C(6)	5706(4)	8670(3)	-243(3)	35(2)
C(7)	5949(5)	9300(3)	-598(3)	42(2)
C(8)	5918(5)	8073(3)	-658(3)	50(2)
C(9)	4594(4)	8669(4)	-150(3)	49(2)
C(10)	5958(5)	5992(3)	2226(3)	44(2)
C(11)	7879(4)	6733(3)	2538(3)	37(2)
C(12)	8449(5)	7343(3)	2777(3)	51(2)
C(13)	8443(5)	6115(3)	2805(3)	48(2)
C(14)	7914(5)	6709(4)	1826(3)	52(2)
C(15)	6263(4)	6466(3)	3538(3)	37(2)
C(16)	5159(4)	6516(3)	3611(3)	49(2)
C(17)	6836(5)	6916(3)	4030(3)	49(2)
C(18)	6572(5)	5733(3)	3688(3)	50(2)
C(19)	5097(4)	9396(3)	2363(3)	39(2)
C(20)	6807(4)	9074(3)	3255(3)	35(2)
C(21)	6723(5)	9740(3)	3592(3)	50(2)
C(22)	7390(5)	8606(3)	3704(3)	52(2)
C(23)	7422(4)	9182(3)	2695(3)	43(2)
C(24)	4573(4)	8722(3)	3560(2)	31(1)
C(25)	3662(4)	8321(3)	3303(3)	46(2)
C(26)	4214(5)	9425(3)	3694(3)	52(2)
C(27)	4956(5)	8408(3)	4178(3)	50(2)
C(28)	3271(5)	5816(3)	1760(3)	53(2)
C(29)	1898(4)	6741(3)	982(3)	40(2)
C(30)	2512(5)	6993(4)	475(3)	55(2)
C(31)	1018(5)	7224(4)	1013(3)	66(2)
C(32)	1475(6)	6060(3)	790(3)	68(2)
C(33)	1984(5)	6712(3)	2474(3)	46(2)
C(34)	1574(5)	7428(4)	2571(3)	59(2)
C(35)	1137(5)	6198(4)	2447(3)	62(2)
C(36)	2689(5)	6536(3)	3037(3)	48(2)
C(37)	4945(4)	7119(3)	1129(2)	27(1)
C(38)	5589(4)	6484(3)	319(3)	34(2)
C(39)	6236(5)	5878(3)	447(3)	48(2)
C(40)	6878(5)	5727(4)	-88(3)	54(2)
C(41)	6241(5)	5620(3)	-691(3)	51(2)
C(42)	5586(5)	6216(4)	-831(3)	50(2)
C(43)	4958(4)	6382(3)	-298(3)	43(2)

C(44)	4242(4)	8252(3)	1364(2)	31(1)
C(45)	2714(4)	8841(3)	1278(3)	34(2)
C(46)	2252(4)	9017(3)	633(3)	42(2)
C(47)	1137(4)	9138(3)	632(3)	47(2)
C(48)	904(5)	9662(3)	1098(3)	52(2)
C(49)	1362(5)	9484(4)	1750(3)	54(2)
C(50)	2487(4)	9383(3)	1740(3)	45(2)

Table 1-5-6. Bond lengths [Å] and angles [deg] for compound **15**.

Si(1)-C(37)	1.944(6)	C(29)-C(31)	1.547(9)
Si(1)-C(44)	1.965(6)	C(33)-C(35)	1.547(8)
Si(1)-Si(4)	2.408(2)	C(33)-C(36)	1.533(8)
Si(1)-Si(2)	2.441(2)	C(33)-C(34)	1.567(9)
Si(1)-Si(3)	2.654(2)	C(38)-C(39)	1.518(8)
Si(2)-Si(5)	2.436(2)	C(38)-C(43)	1.543(7)
Si(2)-Si(3)	2.449(2)	C(39)-C(40)	1.530(8)
Si(2)-Si(6)	2.453(2)	C(40)-C(41)	1.526(9)
Si(3)-C(37)	1.931(6)	C(41)-C(42)	1.512(9)
Si(3)-C(44)	1.944(6)	C(42)-C(43)	1.522(8)
Si(3)-Si(7)	2.416(2)	C(45)-C(50)	1.527(8)
Si(4)-C(1)	1.880(6)	C(45)-C(46)	1.527(8)
Si(4)-C(2)	1.912(6)	C(46)-C(47)	1.535(8)
Si(4)-C(6)	1.933(6)	C(47)-C(48)	1.510(8)
Si(5)-C(15)	1.917(6)	C(48)-C(49)	1.539(9)
Si(5)-C(10)	1.894(6)	C(49)-C(50)	1.544(8)
Si(5)-C(11)	1.920(6)		
Si(6)-C(19)	1.876(6)	C(37)-Si(1)-C(44)	81.1(2)
Si(6)-C(24)	1.931(6)	C(37)-Si(1)-Si(4)	130.51(18)
Si(6)-C(20)	1.935(6)	C(44)-Si(1)-Si(4)	114.06(19)
Si(7)-C(33)	1.876(7)	C(37)-Si(1)-Si(2)	85.33(17)
Si(7)-C(28)	1.891(7)	C(44)-Si(1)-Si(2)	83.81(17)
Si(7)-C(29)	1.924(6)	Si(4)-Si(1)-Si(2)	140.45(9)
N(1)-C(37)	1.274(7)	C(37)-Si(1)-Si(3)	46.56(17)
N(1)-C(38)	1.461(7)	C(44)-Si(1)-Si(3)	46.91(18)
N(2)-C(44)	1.279(7)	Si(4)-Si(1)-Si(3)	158.08(9)
N(2)-C(45)	1.475(7)	Si(2)-Si(1)-Si(3)	57.28(6)
C(2)-C(4)	1.547(8)	Si(5)-Si(2)-Si(1)	116.58(8)
C(2)-C(5)	1.539(9)	Si(5)-Si(2)-Si(3)	109.46(9)
C(2)-C(3)	1.553(8)	Si(1)-Si(2)-Si(3)	65.74(6)
C(6)-C(8)	1.541(8)	Si(5)-Si(2)-Si(6)	126.59(8)
C(6)-C(7)	1.532(8)	Si(1)-Si(2)-Si(6)	108.31(8)
C(6)-C(9)	1.539(8)	Si(3)-Si(2)-Si(6)	114.51(8)
C(11)-C(12)	1.523(8)	C(37)-Si(3)-C(44)	82.0(2)
C(11)-C(13)	1.550(8)	C(37)-Si(3)-Si(7)	110.01(19)
C(11)-C(14)	1.544(8)	C(44)-Si(3)-Si(7)	130.36(19)
C(15)-C(16)	1.523(8)	C(37)-Si(3)-Si(2)	85.37(18)
C(15)-C(18)	1.563(8)	C(44)-Si(3)-Si(2)	84.01(18)
C(15)-C(17)	1.560(8)	Si(7)-Si(3)-Si(2)	142.88(9)
C(20)-C(23)	1.537(8)	C(37)-Si(3)-Si(1)	46.97(18)
C(20)-C(21)	1.535(8)	C(44)-Si(3)-Si(1)	47.57(18)
C(20)-C(22)	1.533(8)	Si(7)-Si(3)-Si(1)	154.51(9)
C(24)-C(27)	1.533(8)	Si(2)-Si(3)-Si(1)	56.98(6)
C(24)-C(26)	1.534(8)	C(1)-Si(4)-C(2)	108.7(3)
C(24)-C(25)	1.546(8)	C(1)-Si(4)-C(6)	106.1(3)
C(29)-C(30)	1.515(8)	C(2)-Si(4)-C(6)	114.6(3)
C(29)-C(32)	1.534(8)	C(1)-Si(4)-Si(1)	104.7(2)

C(2)-Si(4)-Si(1)	112.9(2)	C(23)-C(20)-C(21)	108.3(5)
C(6)-Si(4)-Si(1)	109.3(2)	C(23)-C(20)-C(22)	107.4(5)
C(15)-Si(5)-C(10)	103.4(3)	C(21)-C(20)-C(22)	106.9(5)
C(15)-Si(5)-C(11)	115.1(3)	C(23)-C(20)-Si(6)	107.5(4)
C(10)-Si(5)-C(11)	105.7(3)	C(21)-C(20)-Si(6)	111.7(4)
C(15)-Si(5)-Si(2)	112.0(2)	C(22)-C(20)-Si(6)	114.8(4)
C(10)-Si(5)-Si(2)	107.0(2)	C(27)-C(24)-C(26)	108.0(5)
C(11)-Si(5)-Si(2)	112.6(2)	C(27)-C(24)-C(25)	107.9(5)
C(19)-Si(6)-C(24)	106.6(3)	C(26)-C(24)-C(25)	107.1(5)
C(19)-Si(6)-C(20)	102.8(3)	C(27)-C(24)-Si(6)	114.1(4)
C(24)-Si(6)-C(20)	113.5(2)	C(26)-C(24)-Si(6)	110.4(4)
C(19)-Si(6)-Si(2)	106.5(2)	C(25)-C(24)-Si(6)	109.1(4)
C(24)-Si(6)-Si(2)	113.35(19)	C(30)-C(29)-C(32)	108.6(5)
C(20)-Si(6)-Si(2)	113.1(2)	C(30)-C(29)-C(31)	106.9(5)
C(33)-Si(7)-C(28)	106.4(3)	C(32)-C(29)-C(31)	107.4(6)
C(33)-Si(7)-C(29)	115.6(3)	C(30)-C(29)-Si(7)	110.9(4)
C(28)-Si(7)-C(29)	106.2(3)	C(32)-C(29)-Si(7)	109.8(4)
C(33)-Si(7)-Si(3)	114.9(2)	C(31)-C(29)-Si(7)	113.1(4)
C(28)-Si(7)-Si(3)	102.4(2)	C(35)-C(33)-C(36)	107.0(5)
C(29)-Si(7)-Si(3)	110.0(2)	C(35)-C(33)-C(34)	110.5(6)
C(37)-N(1)-C(38)	121.4(5)	C(36)-C(33)-C(34)	108.3(5)
C(44)-N(2)-C(45)	120.0(5)	C(35)-C(33)-Si(7)	111.0(5)
C(4)-C(2)-C(5)	108.5(5)	C(36)-C(33)-Si(7)	108.5(4)
C(4)-C(2)-C(3)	106.9(5)	C(34)-C(33)-Si(7)	111.3(4)
C(5)-C(2)-C(3)	107.9(5)	N(1)-C(37)-Si(3)	129.3(4)
C(4)-C(2)-Si(4)	111.5(4)	N(1)-C(37)-Si(1)	144.3(4)
C(5)-C(2)-Si(4)	113.9(4)	Si(3)-C(37)-Si(1)	86.5(2)
C(3)-C(2)-Si(4)	107.9(4)	N(1)-C(38)-C(39)	110.8(5)
C(8)-C(6)-C(7)	107.5(5)	N(1)-C(38)-C(43)	108.6(5)
C(8)-C(6)-C(9)	107.7(5)	C(39)-C(38)-C(43)	109.1(5)
C(7)-C(6)-C(9)	108.5(5)	C(38)-C(39)-C(40)	112.2(5)
C(8)-C(6)-Si(4)	113.2(4)	C(41)-C(40)-C(39)	110.7(6)
C(7)-C(6)-Si(4)	110.1(4)	C(42)-C(41)-C(40)	110.3(5)
C(9)-C(6)-Si(4)	109.8(4)	C(41)-C(42)-C(43)	112.2(6)
C(12)-C(11)-C(13)	107.4(5)	C(42)-C(43)-C(38)	112.0(5)
C(12)-C(11)-C(14)	108.0(5)	N(2)-C(44)-Si(3)	143.2(5)
C(13)-C(11)-C(14)	107.1(5)	N(2)-C(44)-Si(1)	131.3(5)
C(12)-C(11)-Si(5)	115.8(4)	Si(3)-C(44)-Si(1)	85.5(3)
C(13)-C(11)-Si(5)	111.4(4)	N(2)-C(45)-C(50)	111.3(5)
C(14)-C(11)-Si(5)	106.7(4)	N(2)-C(45)-C(46)	105.6(5)
C(16)-C(15)-C(18)	107.0(5)	C(50)-C(45)-C(46)	109.9(5)
C(16)-C(15)-C(17)	109.7(5)	C(47)-C(46)-C(45)	112.2(5)
C(18)-C(15)-C(17)	107.1(5)	C(48)-C(47)-C(46)	111.5(5)
C(16)-C(15)-Si(5)	108.9(4)	C(47)-C(48)-C(49)	110.8(6)
C(18)-C(15)-Si(5)	111.6(4)	C(50)-C(49)-C(48)	110.6(5)
C(17)-C(15)-Si(5)	112.3(4)	C(45)-C(50)-C(49)	110.6(5)

Symmetry transformations used to generate equivalent atoms:

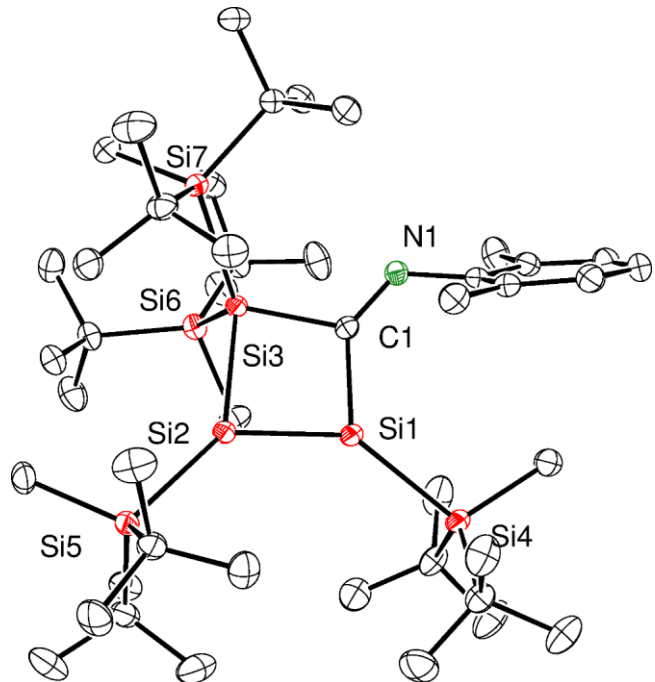


Figure 1-5-3. ORTEP drawing of Compound **16** (H atoms are omitted for clarity).

Table 1-5-7. Crystal data and structure refinement for compound **16**.

Identification code	(tBu ₂ MeSi)4Si ₃ CNXyl		
Empirical formula	C ₄₅ H ₉₃ N Si ₇		
Formula weight	844.83		
Temperature	120(1) K		
Wavelength	0.71073 Å		
Crystal system	Monoclinic		
Space group	P2(1)/n		
Unit cell dimensions	a = 20.0059(6) Å	α= 90 deg.	
	b = 14.7795(5) Å	β= 115.714(1) deg.	
	c = 20.1475(6) Å	γ = 90 deg.	
Volume	5367.2(3) Å ³		
Z	4		
Density (calculated)	1.046 Mg/m ³		
Absorption coefficient	0.206 mm ⁻¹		
F(000)	1872		
Crystal size	0.48 x 0.27 x 0.22 mm ³		
Theta range for data collection	1.20 to 27.48°.		
Index ranges	-25<=h<=25, -18<=k<=19, -19<=l<=26		
Reflections collected	29883		
Independent reflections	12057 [R(int) = 0.0252]		
Completeness to theta = 27.48 deg	97.9 %		
Absorption correction	Empirical		
Max. and min. transmission	0.9568 and 0.9072		
Refinement method	Full-matrix least-squares on F ²		
Data / restraints / parameters	12057 / 0 / 478		
Goodness-of-fit on F ²	0.980		
Final R indices [I>2sigma(I)]	R1 = 0.0418, wR2 = 0.1048		
R indices (all data)	R1 = 0.0532, wR2 = 0.1122		
Largest diff. peak and hole	1.758 and -0.595 e. Å ⁻³		

Table 1-5-8. Atomic coordinates ($\times 10^4$) and equivalent isotropic displacement parameters ($\text{\AA}^2 \times 10^3$)for compound **16**. U(eq) is defined as one third of the trace of the orthogonalized U^{ij} tensor.

	x	y	z	U(eq)
Si(1)	4600(1)	169(1)	6879(1)	18(1)
Si(2)	5538(1)	1039(1)	7564(1)	17(1)
Si(3)	4584(1)	1973(1)	7603(1)	15(1)
Si(4)	4264(1)	-1374(1)	6508(1)	19(1)
Si(5)	6856(1)	972(1)	7980(1)	19(1)
Si(6)	4638(1)	1676(1)	8813(1)	20(1)
Si(7)	4392(1)	3522(1)	7149(1)	17(1)
N(1)	3250(1)	1296(1)	6470(1)	18(1)
C(1)	3936(1)	1107(1)	6873(1)	16(1)
C(2)	3258(1)	-1416(1)	5846(1)	32(1)
C(3)	4376(1)	-1997(1)	7386(1)	27(1)
C(4)	3774(1)	-1631(2)	7600(1)	39(1)
C(5)	5136(1)	-1854(2)	8036(1)	33(1)
C(6)	4243(2)	-3021(1)	7246(1)	42(1)
C(7)	4788(1)	-1871(1)	5988(1)	25(1)
C(8)	5598(1)	-2103(2)	6488(1)	40(1)
C(9)	4391(1)	-2738(2)	5574(1)	38(1)
C(10)	4767(1)	-1181(2)	5407(1)	36(1)
C(11)	7319(1)	2000(1)	8545(1)	28(1)
C(12)	7248(1)	-58(1)	8617(1)	25(1)
C(13)	6908(1)	-96(2)	9168(1)	30(1)
C(14)	8099(1)	23(2)	9062(1)	39(1)
C(15)	7070(1)	-951(2)	8192(1)	38(1)
C(16)	7042(1)	981(1)	7120(1)	23(1)
C(17)	7869(1)	818(2)	7325(1)	35(1)
C(18)	6580(1)	278(2)	6545(1)	30(1)
C(19)	6832(1)	1915(2)	6762(1)	37(1)
C(20)	4819(1)	421(1)	8926(1)	29(1)
C(21)	5475(1)	2257(1)	9591(1)	23(1)
C(22)	5808(1)	1633(2)	10265(1)	35(1)
C(23)	6075(1)	2460(1)	9334(1)	25(1)
C(24)	5280(1)	3157(2)	9862(1)	33(1)
C(25)	3718(1)	1848(2)	8877(1)	26(1)
C(26)	3118(1)	1352(2)	8232(1)	36(1)
C(27)	3485(1)	2852(2)	8823(1)	36(1)
C(28)	3753(1)	1458(2)	9599(1)	34(1)
C(29)	4686(1)	4300(1)	7973(1)	26(1)
C(30)	5054(1)	3769(1)	6706(1)	23(1)
C(31)	5848(1)	3678(1)	7320(1)	29(1)
C(32)	4962(1)	3093(1)	6092(1)	29(1)
C(33)	4967(1)	4731(2)	6388(1)	37(1)
C(34)	3370(1)	3825(1)	6525(1)	21(1)
C(35)	3084(1)	3407(1)	5754(1)	26(1)
C(36)	3272(1)	4859(1)	6443(1)	31(1)
C(37)	2871(1)	3491(1)	6877(1)	26(1)
C(38)	2770(1)	815(1)	5829(1)	19(1)
C(39)	2878(1)	815(1)	5183(1)	21(1)
C(40)	2329(1)	435(1)	4544(1)	27(1)
C(41)	1700(1)	38(1)	4540(1)	30(1)
C(42)	1601(1)	44(1)	5179(1)	27(1)
C(43)	2118(1)	441(1)	5822(1)	23(1)
C(44)	3549(1)	1225(1)	5139(1)	25(1)

C(45)	1989(1)	474(2)	6502(1)	31(1)
-------	---------	--------	---------	-------

Table 1-5-9. Bond lengths [\AA] and angles [deg] for compound **16**.

Si(1)-C(1)	1.9169(18)	C(43)-C(45)	1.502(3)
Si(1)-Si(2)	2.1975(7)	C(1)-Si(1)-Si(2)	88.91(6)
Si(1)-Si(4)	2.4037(7)	C(1)-Si(1)-Si(4)	125.78(6)
Si(2)-Si(3)	2.3835(7)	Si(2)-Si(1)-Si(4)	142.95(3)
Si(2)-Si(5)	2.3973(7)	Si(1)-Si(2)-Si(3)	83.26(2)
Si(3)-C(1)	1.9567(18)	Si(1)-Si(2)-Si(5)	134.78(3)
Si(3)-Si(6)	2.4318(7)	Si(3)-Si(2)-Si(5)	141.93(3)
Si(3)-Si(7)	2.4336(7)	C(1)-Si(3)-Si(2)	82.81(5)
Si(4)-C(2)	1.873(2)	C(1)-Si(3)-Si(6)	111.27(5)
Si(4)-C(3)	1.920(2)	Si(2)-Si(3)-Si(6)	103.89(2)
Si(4)-C(7)	1.921(2)	C(1)-Si(3)-Si(7)	112.83(5)
Si(5)-C(11)	1.883(2)	Si(2)-Si(3)-Si(7)	122.04(3)
Si(5)-C(16)	1.923(2)	Si(6)-Si(3)-Si(7)	118.52(3)
Si(5)-C(12)	1.925(2)	C(2)-Si(4)-C(3)	107.44(10)
Si(6)-C(20)	1.886(2)	C(2)-Si(4)-C(7)	105.78(10)
Si(6)-C(25)	1.917(2)	C(3)-Si(4)-C(7)	116.59(9)
Si(6)-C(21)	1.9281(19)	C(2)-Si(4)-Si(1)	108.77(7)
Si(7)-C(29)	1.890(2)	C(3)-Si(4)-Si(1)	105.24(6)
Si(7)-C(30)	1.927(2)	C(7)-Si(4)-Si(1)	112.76(6)
Si(7)-C(34)	1.9314(19)	C(11)-Si(5)-C(16)	107.57(9)
N(1)-C(1)	1.286(2)	C(11)-Si(5)-C(12)	106.49(9)
N(1)-C(38)	1.421(2)	C(16)-Si(5)-C(12)	115.02(9)
C(3)-C(5)	1.531(3)	C(11)-Si(5)-Si(2)	110.87(6)
C(3)-C(6)	1.542(3)	C(16)-Si(5)-Si(2)	107.35(6)
C(3)-C(4)	1.541(3)	C(12)-Si(5)-Si(2)	109.55(6)
C(7)-C(8)	1.529(3)	C(20)-Si(6)-C(25)	105.13(10)
C(7)-C(10)	1.538(3)	C(20)-Si(6)-C(21)	106.67(9)
C(7)-C(9)	1.548(3)	C(25)-Si(6)-C(21)	114.00(9)
C(12)-C(15)	1.528(3)	C(20)-Si(6)-Si(3)	102.79(7)
C(12)-C(13)	1.534(3)	C(25)-Si(6)-Si(3)	114.61(6)
C(12)-C(14)	1.546(3)	C(21)-Si(6)-Si(3)	112.36(6)
C(16)-C(18)	1.532(3)	C(29)-Si(7)-C(30)	106.12(9)
C(16)-C(19)	1.530(3)	C(29)-Si(7)-C(34)	105.63(8)
C(16)-C(17)	1.542(3)	C(30)-Si(7)-C(34)	113.66(8)
C(21)-C(23)	1.529(3)	C(29)-Si(7)-Si(3)	107.67(7)
C(21)-C(22)	1.534(3)	C(30)-Si(7)-Si(3)	108.89(6)
C(21)-C(24)	1.551(3)	C(34)-Si(7)-Si(3)	114.35(6)
C(25)-C(26)	1.520(3)	C(1)-N(1)-C(38)	125.51(15)
C(25)-C(28)	1.539(3)	N(1)-C(1)-Si(1)	135.10(14)
C(25)-C(27)	1.544(3)	N(1)-C(1)-Si(3)	120.66(13)
C(30)-C(32)	1.538(3)	Si(1)-C(1)-Si(3)	103.72(8)
C(30)-C(33)	1.539(3)	C(5)-C(3)-C(6)	108.69(19)
C(30)-C(31)	1.538(3)	C(5)-C(3)-C(4)	108.63(17)
C(34)-C(37)	1.535(3)	C(6)-C(3)-C(4)	107.65(18)
C(34)-C(35)	1.533(3)	C(5)-C(3)-Si(4)	113.39(14)
C(34)-C(36)	1.541(3)	C(6)-C(3)-Si(4)	111.02(14)
C(38)-C(39)	1.410(3)	C(4)-C(3)-Si(4)	107.27(15)
C(38)-C(43)	1.410(3)	C(8)-C(7)-C(10)	108.84(18)
C(39)-C(40)	1.397(3)	C(8)-C(7)-C(9)	108.55(18)
C(39)-C(44)	1.509(3)	C(10)-C(7)-C(9)	107.56(17)
C(40)-C(41)	1.385(3)	C(8)-C(7)-Si(4)	113.47(14)
C(41)-C(42)	1.385(3)	C(10)-C(7)-Si(4)	108.64(14)
C(42)-C(43)	1.389(3)		

C(9)-C(7)-Si(4)	109.60(14)	C(32)-C(30)-C(33)	108.21(17)
C(15)-C(12)-C(13)	107.72(18)	C(32)-C(30)-C(31)	108.26(16)
C(15)-C(12)-C(14)	108.80(18)	C(33)-C(30)-C(31)	107.88(17)
C(13)-C(12)-C(14)	107.76(17)	C(32)-C(30)-Si(7)	112.56(13)
C(15)-C(12)-Si(5)	112.42(14)	C(33)-C(30)-Si(7)	113.00(14)
C(13)-C(12)-Si(5)	109.26(13)	C(31)-C(30)-Si(7)	106.74(13)
C(14)-C(12)-Si(5)	110.74(15)	C(37)-C(34)-C(35)	107.85(15)
C(18)-C(16)-C(19)	107.64(17)	C(37)-C(34)-C(36)	106.90(16)
C(18)-C(16)-C(17)	108.74(16)	C(35)-C(34)-C(36)	108.44(16)
C(19)-C(16)-C(17)	108.04(17)	C(37)-C(34)-Si(7)	109.99(13)
C(18)-C(16)-Si(5)	112.89(13)	C(35)-C(34)-Si(7)	112.99(13)
C(19)-C(16)-Si(5)	108.05(13)	C(36)-C(34)-Si(7)	110.44(13)
C(17)-C(16)-Si(5)	111.30(14)	C(39)-C(38)-C(43)	120.15(17)
C(23)-C(21)-C(22)	108.28(16)	C(39)-C(38)-N(1)	121.62(16)
C(23)-C(21)-C(24)	107.76(16)	C(43)-C(38)-N(1)	117.64(16)
C(22)-C(21)-C(24)	106.47(17)	C(40)-C(39)-C(38)	118.42(18)
C(23)-C(21)-Si(6)	110.13(13)	C(40)-C(39)-C(44)	118.08(17)
C(22)-C(21)-Si(6)	110.05(14)	C(38)-C(39)-C(44)	123.48(17)
C(24)-C(21)-Si(6)	113.94(13)	C(41)-C(40)-C(39)	121.65(19)
C(26)-C(25)-C(28)	108.81(17)	C(40)-C(41)-C(42)	119.25(18)
C(26)-C(25)-C(27)	107.52(18)	C(41)-C(42)-C(43)	121.32(19)
C(28)-C(25)-C(27)	108.31(18)	C(42)-C(43)-C(38)	119.14(18)
C(26)-C(25)-Si(6)	107.71(14)	C(42)-C(43)-C(45)	120.78(18)
C(28)-C(25)-Si(6)	111.30(14)	C(38)-C(43)-C(45)	120.08(17)
C(27)-C(25)-Si(6)	113.05(14)		

Symmetry transformations used to generate equivalent atoms:

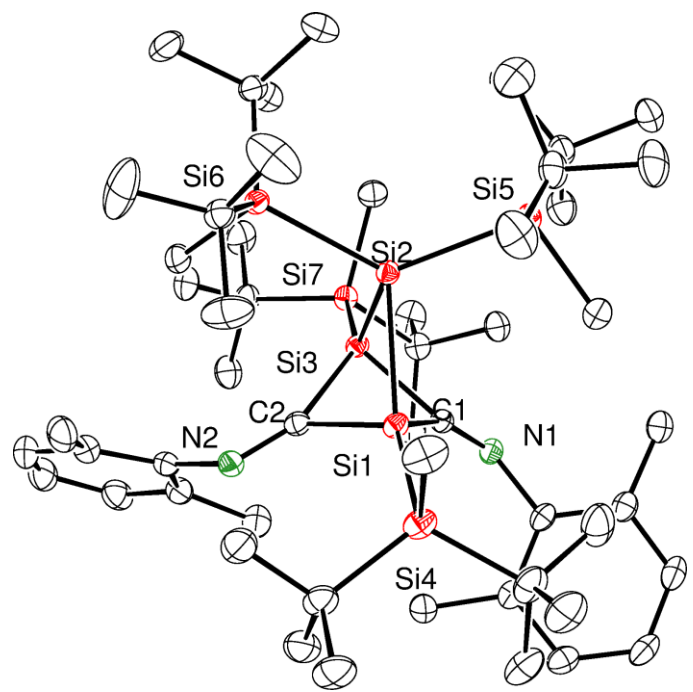


Figure 1-5-4. ORTEP drawing of compound **17** (H atoms are omitted for clarity)

Table 1-5-10. Crystal data and structure refinement for compound **17**.

Identification code	(tBu ₂ MeSi)Si ₃ + 2XylNC		
Empirical formula	C ₅₉ H ₁₁₄ N ₂ Si ₇		
Formula weight	1048.15		
Temperature	120(1) K		
Wavelength	0.71073 Å		
Crystal system	Triclinic		
Space group	P-1		
Unit cell dimensions	a = 12.3120(6) Å	α = 80.810(1) deg.	
	b = 13.0946(6) Å	β = 88.378(1) deg.	
	c = 22.2223(10) Å	γ = 65.370(1) deg.	
Volume	3212.0(3) Å ³		
Z	2		
Density (calculated)	1.084 Mg/m ³		
Absorption coefficient	0.184 mm ⁻¹		
F(000)	1160		
Crystal size	0.47 x 0.22 x 0.13 mm ³		
Theta range for data collection	1.73 to 27.48°		
Index ranges	-15≤h≤15, -16≤k≤16, -28≤l≤28		
Reflections collected	36436		
Independent reflections	14310 [R(int) = 0.0212]		
Completeness to theta = 27.48 deg	97.4 %		
Absorption correction	Empirical		
Max. and min. transmission	0.9759 and 0.9184		
Refinement method	Full-matrix least-squares on F ²		
Data / restraints / parameters	14310 / 0 / 613		
Goodness-of-fit on F ²	1.026		
Final R indices [I>2sigma(I)]	R1 = 0.0474, wR2 = 0.1284		
R indices (all data)	R1 = 0.0560, wR2 = 0.1352		
Largest diff. peak and hole	1.399 and -0.770 e. Å ⁻³		

Table 1-5-11. Atomic coordinates ($\times 10^4$) and equivalent isotropic displacement parameters ($\text{\AA}^2 \times 10^3$)for compound **17**. $U(\text{eq})$ is defined as one third of the trace of the orthogonalized U^{ij} tensor.

	x	y	z	$U(\text{eq})$
Si(1)	4857(1)	7648(1)	2840(1)	17(1)
Si(2)	3718(1)	7179(1)	2121(1)	15(1)
Si(3)	5813(1)	6590(1)	1883(1)	15(1)
Si(4)	4307(1)	8447(1)	3791(1)	23(1)
Si(5)	2254(1)	8978(1)	1577(1)	20(1)
Si(6)	3423(1)	5429(1)	2421(1)	16(1)
Si(7)	6866(1)	5928(1)	960(1)	18(1)
N(1)	6157(1)	8657(1)	1866(1)	18(1)
N(2)	6730(2)	5363(1)	3221(1)	20(1)
C(1)	5693(2)	8003(2)	2119(1)	16(1)
C(2)	6107(2)	6142(2)	2788(1)	17(1)
C(3)	2745(2)	8584(2)	3954(1)	35(1)
C(4)	5349(2)	7379(2)	4449(1)	27(1)
C(5)	5126(2)	6295(2)	4535(1)	33(1)
C(6)	6685(2)	7030(2)	4342(1)	33(1)
C(7)	5044(2)	7884(2)	5046(1)	36(1)
C(8)	4207(2)	9972(2)	3741(1)	30(1)
C(9)	5412(2)	9990(2)	3881(1)	35(1)
C(10)	3299(2)	10609(2)	4196(1)	37(1)
C(11)	3742(3)	10649(2)	3103(1)	40(1)
C(12)	2757(2)	10074(2)	1760(1)	32(1)
C(13)	700(2)	9396(2)	1914(1)	26(1)
C(14)	875(2)	9187(2)	2611(1)	41(1)
C(15)	-81(2)	10681(2)	1727(1)	38(1)
C(16)	3(2)	8750(2)	1733(1)	36(1)
C(17)	2266(2)	9104(2)	704(1)	24(1)
C(18)	1296(2)	10240(2)	386(1)	31(1)
C(19)	2125(2)	8145(2)	453(1)	30(1)
C(20)	3491(2)	9089(2)	530(1)	30(1)
C(21)	4977(2)	4293(2)	2582(1)	24(1)
C(22)	2602(2)	5361(2)	3169(1)	22(1)
C(23)	3186(3)	5716(3)	3644(1)	41(1)
C(24)	1269(2)	6122(3)	3117(1)	50(1)
C(25)	2763(3)	4142(2)	3415(1)	56(1)
C(26)	2814(2)	5022(2)	1750(1)	21(1)
C(27)	1575(2)	5894(2)	1490(1)	30(1)
C(28)	2747(2)	3864(2)	1927(1)	31(1)
C(29)	3699(2)	4908(2)	1236(1)	26(1)
C(30)	5636(2)	6096(2)	410(1)	24(1)
C(31)	7959(2)	4338(2)	1054(1)	24(1)
C(32)	7473(2)	3654(2)	1526(1)	28(1)
C(33)	8031(2)	3895(2)	446(1)	33(1)
C(34)	9241(2)	4091(2)	1258(1)	29(1)
C(35)	7570(2)	6929(2)	602(1)	22(1)
C(36)	8219(2)	6533(2)	21(1)	32(1)
C(37)	8449(2)	7033(2)	1038(1)	26(1)
C(38)	6566(2)	8127(2)	408(1)	26(1)
C(39)	6294(2)	9558(2)	2089(1)	19(1)
C(40)	7107(2)	9307(2)	2581(1)	21(1)

C(41)	7339(2)	10182(2)	2750(1)	25(1)
C(42)	6802(2)	11284(2)	2436(1)	28(1)
C(43)	6049(2)	11508(2)	1933(1)	27(1)
C(44)	5796(2)	10663(2)	1745(1)	22(1)
C(45)	7804(2)	8102(2)	2896(1)	27(1)
C(46)	5026(2)	10949(2)	1175(1)	29(1)
C(47)	7693(2)	4302(2)	3160(1)	21(1)
C(48)	7673(2)	3296(2)	3485(1)	26(1)
C(49)	8635(2)	2260(2)	3441(1)	32(1)
C(50)	9634(2)	2212(2)	3124(1)	34(1)
C(51)	9692(2)	3213(2)	2854(1)	29(1)
C(52)	8735(2)	4265(2)	2866(1)	23(1)
C(53)	6695(2)	3293(2)	3908(1)	33(1)
C(54)	8876(2)	5340(2)	2628(1)	28(1)
C(61)	8988(4)	9371(3)	4480(2)	85(1)
C(62)	9344(5)	8033(5)	4660(2)	101(2)
C(63)	10453(4)	7516(5)	4986(2)	94(2)
C(64)	10912(3)	6182(3)	5153(2)	59(1)
C(65)	10150(3)	5824(3)	5592(2)	61(1)

Table 1-5-12. Bond lengths [Å] and angles [deg] for compound.

Si(1)-C(2)	1.9504(19)	C(8)-C(10)	1.548(3)
Si(1)-C(1)	1.9773(19)	C(13)-C(16)	1.531(3)
Si(1)-Si(2)	2.4595(7)	C(13)-C(14)	1.536(3)
Si(1)-Si(4)	2.4602(7)	C(13)-C(15)	1.543(3)
Si(1)-Si(3)	2.6964(7)	C(17)-C(19)	1.528(3)
Si(2)-Si(3)	2.4337(7)	C(17)-C(20)	1.540(3)
Si(2)-Si(5)	2.4365(7)	C(17)-C(18)	1.540(3)
Si(2)-Si(6)	2.4537(7)	C(22)-C(24)	1.520(3)
Si(3)-C(1)	1.9488(19)	C(22)-C(23)	1.525(3)
Si(3)-C(2)	2.0032(19)	C(22)-C(25)	1.533(3)
Si(3)-Si(7)	2.4745(7)	C(26)-C(27)	1.533(3)
Si(4)-C(3)	1.885(2)	C(26)-C(29)	1.537(3)
Si(4)-C(4)	1.922(2)	C(26)-C(28)	1.541(3)
Si(4)-C(8)	1.935(2)	C(31)-C(34)	1.539(3)
Si(5)-C(12)	1.883(2)	C(31)-C(32)	1.540(3)
Si(5)-C(17)	1.919(2)	C(31)-C(33)	1.541(3)
Si(5)-C(13)	1.923(2)	C(35)-C(37)	1.533(3)
Si(6)-C(21)	1.870(2)	C(35)-C(38)	1.540(3)
Si(6)-C(22)	1.930(2)	C(35)-C(36)	1.544(3)
Si(6)-C(26)	1.930(2)	C(39)-C(40)	1.406(3)
Si(7)-C(30)	1.890(2)	C(39)-C(44)	1.409(3)
Si(7)-C(35)	1.918(2)	C(40)-C(41)	1.397(3)
Si(7)-C(31)	1.931(2)	C(40)-C(45)	1.506(3)
N(1)-C(1)	1.271(2)	C(41)-C(42)	1.384(3)
N(1)-C(39)	1.422(2)	C(42)-C(43)	1.385(3)
N(2)-C(2)	1.276(2)	C(43)-C(44)	1.393(3)
N(2)-C(47)	1.425(2)	C(44)-C(46)	1.506(3)
C(4)-C(6)	1.535(3)	C(47)-C(48)	1.406(3)
C(4)-C(5)	1.537(3)	C(47)-C(52)	1.409(3)
C(4)-C(7)	1.544(3)	C(48)-C(49)	1.396(3)
C(8)-C(11)	1.531(3)	C(48)-C(53)	1.508(3)
C(8)-C(9)	1.534(3)	C(49)-C(50)	1.384(4)

C(50)-C(51)	1.381(3)	N(2)-C(2)-Si(1)	128.62(14)
C(51)-C(52)	1.395(3)	N(2)-C(2)-Si(3)	145.38(15)
C(52)-C(54)	1.501(3)	Si(1)-C(2)-Si(3)	85.99(8)
		C(6)-C(4)-C(5)	107.71(19)
C(2)-Si(1)-C(1)	79.13(8)	C(6)-C(4)-C(7)	108.94(18)
C(2)-Si(1)-Si(2)	84.71(6)	C(5)-C(4)-C(7)	107.86(18)
C(1)-Si(1)-Si(2)	85.85(6)	C(6)-C(4)-Si(4)	114.09(15)
C(2)-Si(1)-Si(4)	124.39(6)	C(5)-C(4)-Si(4)	108.43(15)
C(1)-Si(1)-Si(4)	132.66(6)	C(7)-C(4)-Si(4)	109.63(16)
Si(2)-Si(1)-Si(4)	131.81(3)	C(11)-C(8)-C(9)	108.7(2)
C(2)-Si(1)-Si(3)	47.83(6)	C(11)-C(8)-C(10)	106.7(2)
C(1)-Si(1)-Si(3)	46.18(5)	C(9)-C(8)-C(10)	108.23(19)
Si(2)-Si(1)-Si(3)	56.105(19)	C(11)-C(8)-Si(4)	110.04(15)
Si(4)-Si(1)-Si(3)	170.83(3)	C(9)-C(8)-Si(4)	112.92(16)
Si(3)-Si(2)-Si(5)	118.45(3)	C(10)-C(8)-Si(4)	110.00(16)
Si(3)-Si(2)-Si(6)	106.55(2)	C(16)-C(13)-C(14)	109.5(2)
Si(5)-Si(2)-Si(6)	126.01(3)	C(16)-C(13)-C(15)	107.87(19)
Si(3)-Si(2)-Si(1)	66.88(2)	C(14)-C(13)-C(15)	106.18(19)
Si(5)-Si(2)-Si(1)	106.94(3)	C(16)-C(13)-Si(5)	114.60(15)
Si(6)-Si(2)-Si(1)	117.54(3)	C(14)-C(13)-Si(5)	107.52(15)
C(1)-Si(3)-C(2)	78.54(8)	C(15)-C(13)-Si(5)	110.81(15)
C(1)-Si(3)-Si(2)	87.18(6)	C(19)-C(17)-C(20)	108.62(18)
C(2)-Si(3)-Si(2)	84.31(6)	C(19)-C(17)-C(18)	107.74(18)
C(1)-Si(3)-Si(7)	120.84(6)	C(20)-C(17)-C(18)	107.67(17)
C(2)-Si(3)-Si(7)	137.12(6)	C(19)-C(17)-Si(5)	114.98(14)
Si(2)-Si(3)-Si(7)	130.47(3)	C(20)-C(17)-Si(5)	105.45(14)
C(1)-Si(3)-Si(1)	47.06(6)	C(18)-C(17)-Si(5)	112.10(15)
C(2)-Si(3)-Si(1)	46.18(6)	C(24)-C(22)-C(23)	108.9(2)
Si(2)-Si(3)-Si(1)	57.019(19)	C(24)-C(22)-C(25)	107.9(2)
Si(7)-Si(3)-Si(1)	167.76(3)	C(23)-C(22)-C(25)	106.8(2)
C(3)-Si(4)-C(4)	107.31(11)	C(24)-C(22)-Si(6)	114.37(15)
C(3)-Si(4)-C(8)	104.91(11)	C(23)-C(22)-Si(6)	107.25(14)
C(4)-Si(4)-C(8)	113.64(10)	C(25)-C(22)-Si(6)	111.38(16)
C(3)-Si(4)-Si(1)	107.08(8)	C(27)-C(26)-C(29)	107.90(17)
C(4)-Si(4)-Si(1)	108.90(7)	C(27)-C(26)-C(28)	107.57(17)
C(8)-Si(4)-Si(1)	114.48(7)	C(29)-C(26)-C(28)	107.62(17)
C(12)-Si(5)-C(17)	105.37(10)	C(27)-C(26)-Si(6)	114.54(14)
C(12)-Si(5)-C(13)	104.41(10)	C(29)-C(26)-Si(6)	107.29(13)
C(17)-Si(5)-C(13)	115.03(9)	C(28)-C(26)-Si(6)	111.65(14)
C(12)-Si(5)-Si(2)	104.34(7)	C(34)-C(31)-C(32)	108.91(17)
C(17)-Si(5)-Si(2)	114.46(7)	C(34)-C(31)-C(33)	107.42(18)
C(13)-Si(5)-Si(2)	111.84(7)	C(32)-C(31)-C(33)	107.55(18)
C(21)-Si(6)-C(22)	105.63(9)	C(34)-C(31)-Si(7)	114.03(14)
C(21)-Si(6)-C(26)	104.43(9)	C(32)-C(31)-Si(7)	108.72(14)
C(22)-Si(6)-C(26)	114.32(9)	C(33)-C(31)-Si(7)	110.01(14)
C(21)-Si(6)-Si(2)	103.79(7)	C(37)-C(35)-C(38)	107.69(17)
C(22)-Si(6)-Si(2)	115.05(6)	C(37)-C(35)-C(36)	109.01(17)
C(26)-Si(6)-Si(2)	112.17(6)	C(38)-C(35)-C(36)	107.34(17)
C(30)-Si(7)-C(35)	107.35(9)	C(37)-C(35)-Si(7)	113.50(14)
C(30)-Si(7)-C(31)	105.26(9)	C(38)-C(35)-Si(7)	108.70(13)
C(35)-Si(7)-C(31)	113.25(9)	C(36)-C(35)-Si(7)	110.39(14)
C(30)-Si(7)-Si(3)	104.33(7)	C(40)-C(39)-C(44)	119.78(17)
C(35)-Si(7)-Si(3)	109.86(6)	C(40)-C(39)-N(1)	119.70(17)
C(31)-Si(7)-Si(3)	115.93(7)	C(44)-C(39)-N(1)	119.40(17)
C(1)-N(1)-C(39)	128.99(17)	C(41)-C(40)-C(39)	119.22(18)
C(2)-N(2)-C(47)	126.74(17)	C(41)-C(40)-C(45)	119.25(19)
N(1)-C(1)-Si(3)	127.55(14)	C(39)-C(40)-C(45)	121.35(17)
N(1)-C(1)-Si(1)	145.23(15)	C(42)-C(41)-C(40)	121.3(2)
Si(3)-C(1)-Si(1)	86.75(7)	C(41)-C(42)-C(43)	118.85(19)

C(42)-C(43)-C(44)	121.9(2)	C(49)-C(48)-C(53)	118.40(19)
C(43)-C(44)-C(39)	118.73(19)	C(47)-C(48)-C(53)	122.90(19)
C(43)-C(44)-C(46)	119.14(19)	C(50)-C(49)-C(48)	121.5(2)
C(39)-C(44)-C(46)	122.11(18)	C(51)-C(50)-C(49)	119.3(2)
C(48)-C(47)-C(52)	119.82(19)	C(50)-C(51)-C(52)	121.1(2)
C(48)-C(47)-N(2)	118.57(18)	C(51)-C(52)-C(47)	119.11(19)
C(52)-C(47)-N(2)	120.80(17)	C(51)-C(52)-C(54)	119.69(19)
C(49)-C(48)-C(47)	118.6(2)	C(47)-C(52)-C(54)	120.86(18)

Symmetry transformations used to generate equivalent atoms:

References

- 1) Reviews on disilenes: (a) G. Raabe, J. Michl, *Chem. Rev.* **1985**, *85*, 419; (b) R. West, *Angew. Chem., Int. Ed.* **1987**, *26*, 1201; (c) J. Barrau, J. Escudie, J. Satge, *Chem. Rev.* **1990**, *90*, 283; (d) T. Tsumuraya, S. A. Batcheller, S. Masamune, *Angew. Chem., Int. Ed.* **1991**, *30*, 902; (e) R. Okazaki, R. West, *Adv. Organomet. Chem.* **1996**, *39*, 231; (f) M. Kira, T. Iwamoto, *Adv. Organomet. Chem.* **2006**, *54*, 73; (g) T. L. Morking, T. R. Owens, W. J. Leigh, in *The Chemistry of Organic Silicon Compounds Vol. 3*, (Ed. by Z. Rappoport, Y. Apeloig) John Wiley & Sons, Ltd, Chichester, 2001, chap 17.
- 2) A. Sekiguchi, V. Ya. Lee, *Chem. Rev.* **2003**, *103*, 1429.
- 3) (a) A. Sekiguchi, T. Matsuno, M. Ichinohe, *J. Am. Chem. Soc.* **2000**, *122*, 11250. (b) M. Ichinohe, M. Igarashi, K. Sanuki, A. Sekiguchi, *J. Am. Chem. Soc.* **2005**, *127*, 9978.
- 4) (a) M. Karni, J. Kapp, P. v. R. Schleyer, Y. Apeloig in *The Chemistry of Organic Silicon Compounds Vol. 3*, (Ed. by Z. Rappoport, Y. Apeloig) John Wiley & Sons, Ltd, Chichester, 2001 chap. 1; (b) M. Rohmer, M. Bénard, *Chem. Soc. Rev.* **2001**, *30*, 340; (c) M. Kira, *Organometallics* **2014**, *33*, 644; (d) T. Müller in *Organosilicon Chemistry IV From Molecules to Materials*, (Ed. by N. Auner and J. Weis) Wiley-VCH, Ltd, 2000, 110.
- 5) (a) S. Masamune, Y. Kabe, S. Collins, *J. Am. Chem. Soc.* **1985**, *107*, 5552; (b) R. Jones, D. Williams, Y. Kabe, S. Masamune, *Angew. Chem., Int. Ed.* **1986**, *25*, 173.
- 6) (a) V. Ya. Lee, H. Yasuda, A. Sekiguchi, *A. J. Am. Chem. Soc.* **2007**, *129*, 2436; (b) T. Iwamoto, D. Yin, C. Kabuto, M. Kira, *J. Am. Chem. Soc.* **2001**, *123*, 12730; (c) T. Iwamoto, D. Yin, S. Boomgaarden, C. Kabuto, M. Kira, *Chem. Lett.* **2008**, *37*, 520.
- 7) P. v. R. Schleyer, A. F. Sax, J. Kalcher, R. Janoschek, *Angew. Chem., Int. Ed. Engl.* **1987**, *26*, 364.
- 8) (a) A. Rauk, T. S. Sorensen, F. Sun, *J. Am. Chem. Soc.* **1995**, *117*, 4506; (b) P. H. M. Budzelaar, E. Kraka, D. Cremer, P v. R. Schleyer, *J. Am. Chem. Soc.* **1986**, *108*, 561.
- 9) V. Ya. Lee, S. Miyazaki, H. Yasuda, A. Sekiguchi, *J. Am. Chem. Soc.* **2008**, *130*, 2758
- 10) H. B. Yokelson, A. J. Millevolte, K. J. Haller, K. J. R. West, *Chem. Commun.* **1987**, *21*, 1605.
- 11) A. G. Brook, C. Golino, E. Matern, *Can. J. Chem.* **1978**, *56*, 2286.
- 12) M. Kira, T. Iwamoto, C. Kabuto, *J. Am. Chem. Soc.* **1996**, *118*, 10303.
- 13) M. Raban, E. Carlson, *J. Am. Chem. Soc.* **1971**, *93*, 685.
- 14) K. Ueba-Ohshima, T. Iwamoto, M. Kira, *Organometallics* **2008**, *27*, 320.

Chapter 2

Reaction of Cyclotrisilene Isocyanide Adduct with Methanol: Synthesis Structure and Properties of *C*-amino and *C*-hydroxyl Silenes

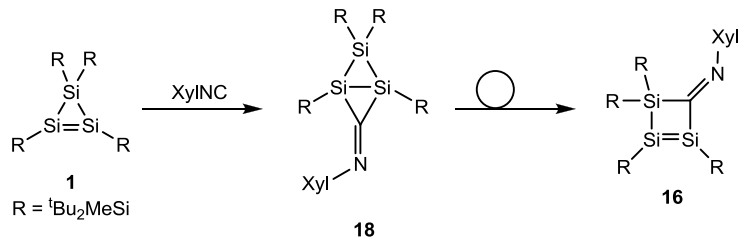
2-1. Summary

Xylyliminotrisilabicyclo[1.1.0]butane, prepared by the reaction of cyclotrisilene and xylylisocyanide, reacted with MeOH to give cyclic sila-enamine (*C*-xylylaminosilene). The reaction of **1** with CO in the presence of MeOH afforded related sila-enol (*C*-hydroxylsilene). The molecular structures of both compounds were determined by crystallographic and spectroscopic methods, indicating the conjugation between Si=C double bond and the lone pair on N or O atom. Theoretical calculations using model compounds showed elevation of HOMO (Si=C π orbital) energy level of sila-enamine caused by the interaction with non-bonding orbital on nitrogen. Thermal reaction of sila-enamine afforded bis-silene via α -elimination of $^t\text{Bu}_2\text{MeSiOMe}$ and following intermolecular N-H insertion of the silylenes.

2-2. Introduction

Since the first synthesis of disilene¹ and silene² in 1981, the chemistry of low-valent silicon compounds have been well established.³ Accompanying with a number of isolable unsaturated silicon compounds, fundamental and applied properties of Si=Si double bond have been studied for decades.⁴ Due to the high-lying π orbital and low-lying π^* orbital of silicon multiple bond, disilenes showed a variety of reactivity toward small, and even stable molecules without catalyst.

Sekiguchi et al. synthesized a silicon analogue of cyclopropene ring, cyclotrisilene **1**⁵ by the reduction of dibromosilanes, RSiBr₂ and RSiBr₃ (R = ^tBu₂MeSi). Because of the strained three-membered skeleton as well as reactive Si=Si double bond, **1** had a notable potential leading to the unsaturated silicon small rings with special electronic and structural properties (e.g. aromatic and homoaromatic rings).⁶ Recently, hetero-hybrid Si₃X trisilabicyclo[1.1.0]butanes (X = CH₂, S, Se, Te), which have highly strained non-classical bonds, are also synthesized using cyclotrisilene **1** as a precursor. For example, elemental chalcogen atoms were smoothly introduced to cyclotrisilene **1** to give Si₃X (X = S, Se, Te) trisilabicyclo[1.1.0]butanes via [1 + 2]cycloaddition.⁷



In the previous chapter, the author described the reaction of **1** with isocyanide affording iminotrisilabicyclo[1.1.0]butane. Depending on the substituent group on imine, the thermal stability of iminotrisilabicyclo[1.1.0]butanes are dramatically affected. Thus, cyclohexyliminotrisilabicyclo[1.1.0]butane is isolable in an ambient condition, while xylyliminotrisilabicyclo[1.1.0]butane **18** isomerized to iminotrisilabicyclo[1.1.0]butane **16** at the same condition. The considerable transition state from **18** to **16** is a planar biradical species, which is stabilized by electron delocalization through arylimino group. However, a clear-cut structural and spectroscopic analysis of **18** are still lack, because of the thermal instability of **18**. Investigation of the interaction between banana Si-Si single bond and C=N π orbital of **18** could offer a novel aspect of heavy bicyclo[1.1.0]butanes.

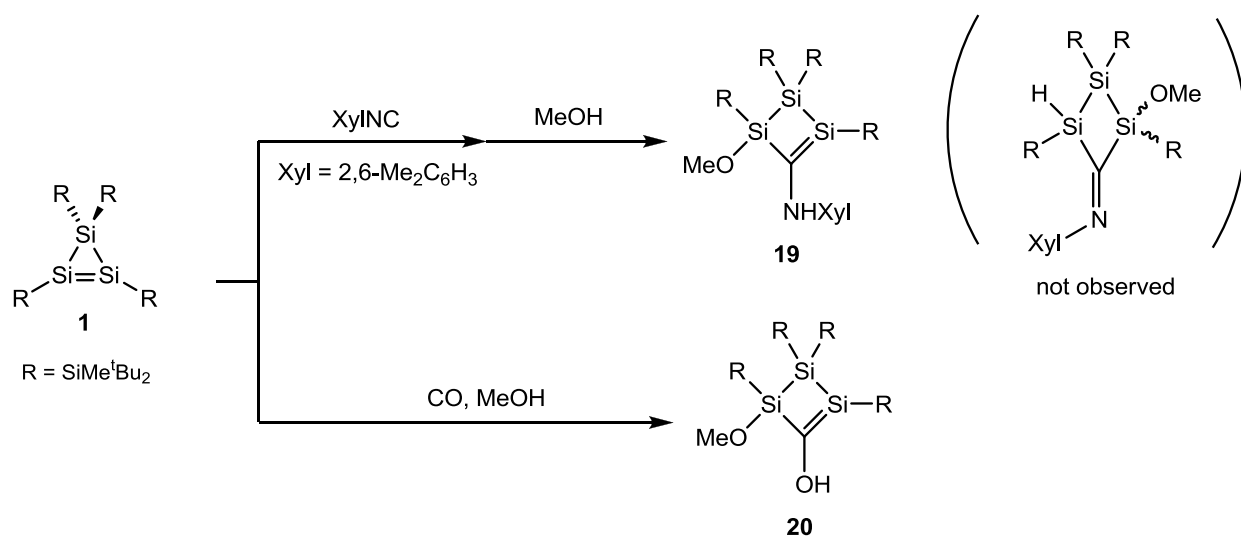
In this chapter, the author describes the reaction of iminotrisilabicyclo[1.1.0]butane **18** with methanol, which gives unexpected functionalized cyclsilene named sila-enamine. Encouraged by the reactivity of **18**, the author also describes the reaction of cyclotrisilene **1** with isoelectronic carbon monoxide in the presence of methanol, affording similar cyclic silene named sila-enol. The structural and spectroscopic properties of the silenes are discussed in detail.

2-3. Result and Discussion

2-3-1 Synthesis of Cyclic Sila-enamine and Sila-enol

Benzene solution of **1** was added to xylylisocyanide to afford **18**. Immediate addition of methanol to the reaction mixture resulted in the bright yellow solution. After washing the resulting solid with hexane, air- and moisture sensitive yellow crystals of sila-enamine **19** were obtained in 43% yield (Scheme 2-3-1). Methanol adduct to the Si-Si bridge bond of **18** was not detected by any spectroscopic methods, in contrast to the methanol addition of bicyclo[1.1.0]tetrasilane and bicyclo[1.1.0]butanone.^{9,10}

Scheme 2-3-1



Carbon monoxide, which is an isoelectronic species of isocyanide, was also reacted with cyclotrisilene **1** in the presence of MeOH, giving cyclic sila-enol **20**. Reaction of **1** with CO in the absence of MeOH did not afford any product even at high temperature.

The plausible formation mechanism of **19** and **20** is shown in Scheme 2-3-2. In the reaction of **1** with isocyanide and carbon monoxide, both reactions involve [1 + 2]cycloaddition toward Si=Si double bond by isocyanide or CO. The resulting trisilabicyclo[1.1.0]butane derivative **18** and **21** can lead the product **19** and **20** via the following two possible reaction pathways. In the former pathway (i), protonation to the lone pair on the heteroatom proceeds to give cationic intermediate **22**, with a stable homoaromatic system.⁶ Following methoxylation to silicon skeletal will give the products **19** or **20**. In contrast, the latter path (ii) started from nucleophilic addition of methoxy group to Si-Si bridge bond, affording allylanion intermediate **23**. The protonation of heteroatom X of **23** would give the product, silaenamine **19** and **20**. However, allyl intermediate **23** can also react with H⁺ at Si1 atom, giving silylimine **24** and silylketone **25** (Figure 2-3-1). Because these thermally favorable isomers **24** and **25** were not observed spectroscopically, the author concludes that the formation of cyclic sila-enamine **19** and sila-enol **20** prefers path (i) to path (ii), although the

possibility of path (ii) under kinetic control cannot be excluded. Scheschkeitz's group recently reported remarkable zwitterionic oxyallyl, by the reaction of peraryl substituted cyclotrisilene with carbon monoxide and strong Lewis acidic borane. Such isolable zwitterionic oxyallyl structure may be a possible intermediate **22** in path (i).¹¹

Scheme 2-3-2

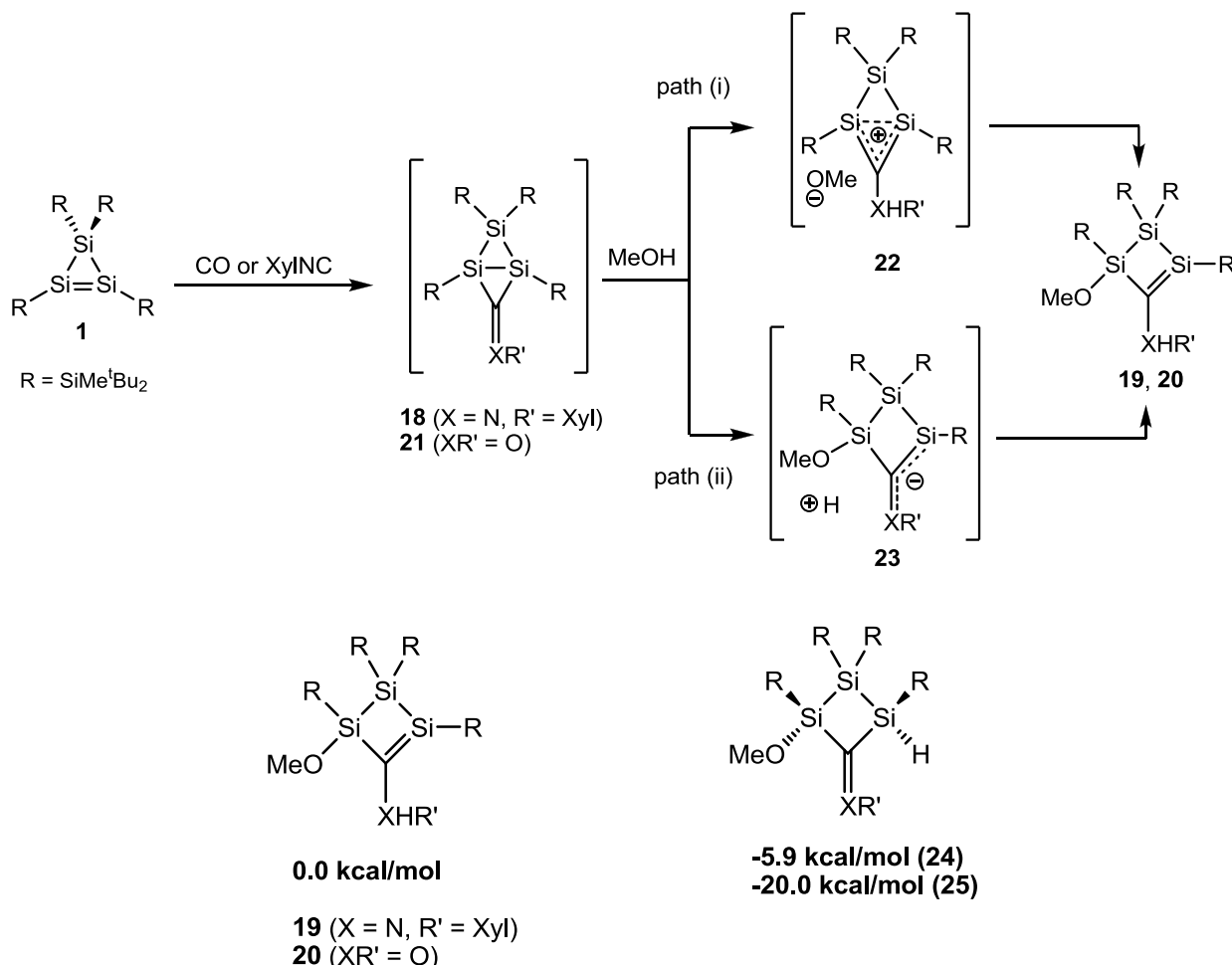


Figure 2-3-1. Relative energies for cyclic sila-enamine **19**, sila-enol **20** and tautomers **24**, **25** (B3LYP/6-31G(d)).

2-3-2. Structural Property of Sila-enamine and Sila-enol.

The molecular structure of sila-enamine **19** and enol **20** were determined by X-ray single crystal diffraction analysis (Figure 2-3-2). The sum of the internal angles of sila-enamine **19** (356.4°) suggests the slightly distorted four-membered plane due to the xylyl group, while **20** has a nearly planar four-membered skeleton (sum of the internal angles = 358.9°). Both four-membered ring **19** and **20** have planar geometry around sp^2 carbon and silicon atoms, with the sum of the bonding angles $358\text{--}360^\circ$. Si1-C1 bond length of **19** ($1.7871(18)$ Å) is longer than that of corresponding Si=C bond in sila-enol **20** ($1.7638(16)$ Å). Particularly, Si1-C1 bond length of **19** lies in the upper limit of Si=C double bond region ($1.702(5)\text{--}1.775(3)$ Å). This elongation can be explained by the conjugation between Si=C bond and lone pair on N1

atom (Chart 2-3-1), which enhances the single bond character to the Si=C bond.¹² Although C1-N1 bond length in **19** (1.387 (2) Å) and C1-O1 bond length in **20** (1.3876(19) Å) fall in the typical single bond region, the remarkable elongation of Si=C bond in **19** compared with related cyclic silene without hetero atom substituent (1.7459(15) Å)¹³ indicates the contribution of zwitterionic resonance form **B**.

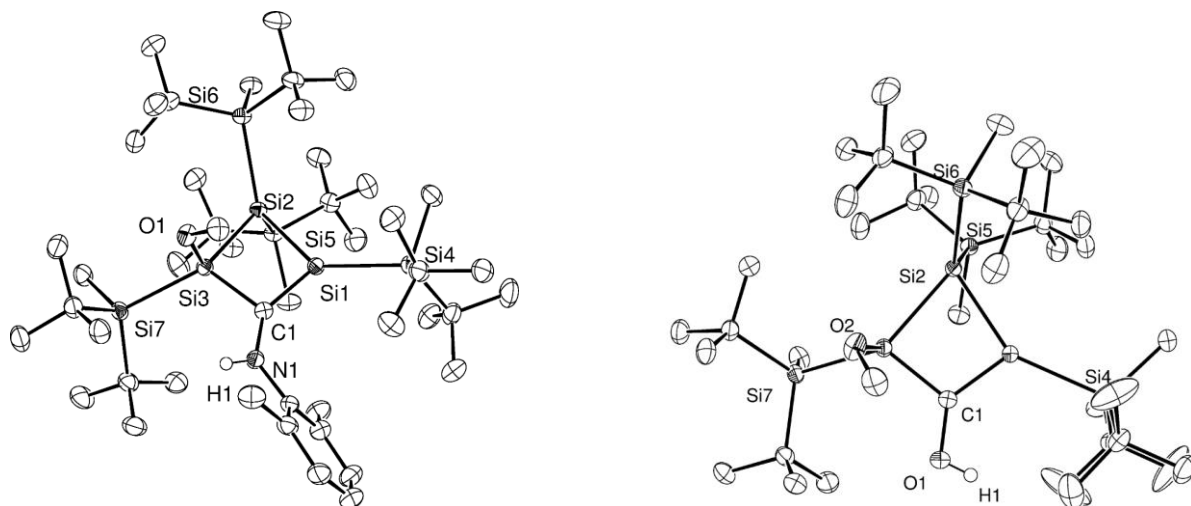


Figure 2-3-2. ORTEP drawing of sila-enamine **19** (left) and sila-enol **20** (right). Selected structural parameters for **19**: Si1-C1 1.7871(18) Å, Si1-Si2 2.3922(7) Å, Si2-Si3 2.4080(7) Å, Si3-C1 1.8741(18) Å, C1-N1 1.387(2) Å; for **20**: Si1-C1 1.7638(16) Å, Si1-Si2 2.3666(6) Å, Si2-Si3 2.4481(7) Å, Si3-C1 1.8754(16) Å, C1-O1 1.3876(19) Å.

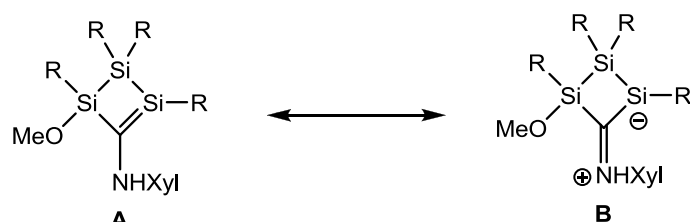


Chart 2-3-1. Resonance structures of cyclic sila-enamine **19**.

2-3-2. NMR Spectroscopic Analysis of Sila-enamine and Sila-enol.

The NMR spectra of sila-enamine **19** and sila-enol **20** reflect the structural characteristics. In the ¹H NMR spectrum, NH proton signal of **19** was observed at 6.42 ppm, and OH proton signal of **20** was observed at 5.64 ppm. Two methyl groups of the xylyl group in **19** appeared independently at 2.33 and 2.68 ppm, suggesting that rotation of N-Ar bond is prevented by the steric hindrance between xylyl and neighboring Si^tBu₂Me groups. In the ¹³C NMR spectrum, the silene carbon atoms appeared at 185.8 ppm (**19**) and 211.0 ppm (**20**) respectively. The low field shifted ¹³C chemical shift of silene carbon in **20** reflects an inductive effect of oxygen atom. The sp² silicon atom of sila-enamine **19** was detected at 51.7 ppm, which is within the range for the ²⁹Si chemical shift of typical silenes. However, the doubly bonded silicon atom of **19** is significantly higher shifted compared with other cyclic silenes (**20**: 89.2 ppm; cf. cyclic silenes without

hetero atom substituent: 98.2-139.1 ppm).¹³ The difference of chemical shifts can be regarded as the electronic situation on sp^2 silicon atom. Therefore, the silene silicon of **19** is more negative than that of sila-enol **20** by the π -donation from nitrogen lone-pair.

2-3-3. Molecular Orbital of Sila-enamine and Sila-enol.

Conjugation between Si=C bond and the lone-pair electrons can be seen in the molecular orbital of model compounds (Figure 2-3-3). Both model compounds **19'**, **20'**(R = SiMe₃) optimized at B3LYP/6-31G(d) level are in agreement with experimental data. Both LUMOs are mainly formed by π^* orbital of Si=C bond with nearly same energy levels (2.18 and 2.20 eV respectively). On the other hand, the HOMOs of **19'** and **20'** show interactions between Si=C π orbital and non-bonding orbital of O or N atom. In addition, the energy level of HOMO of sila-enamine **19'** (-6.23 eV) is higher than that of sila-enol **20'** (-6.88 eV), due to the greater π -donor ability of nitrogen atom than oxygen atom. The resulting decreased HOMO-LUMO gap of **19'** can be confirmed in UV-Vis spectra. The maximum absorption wavelength corresponding to the Si=C π - π^* transition of sila-enamine **19** was observed at 421 nm, which is 50 nm red-shifted than that of sila-enol **20** (369 nm).

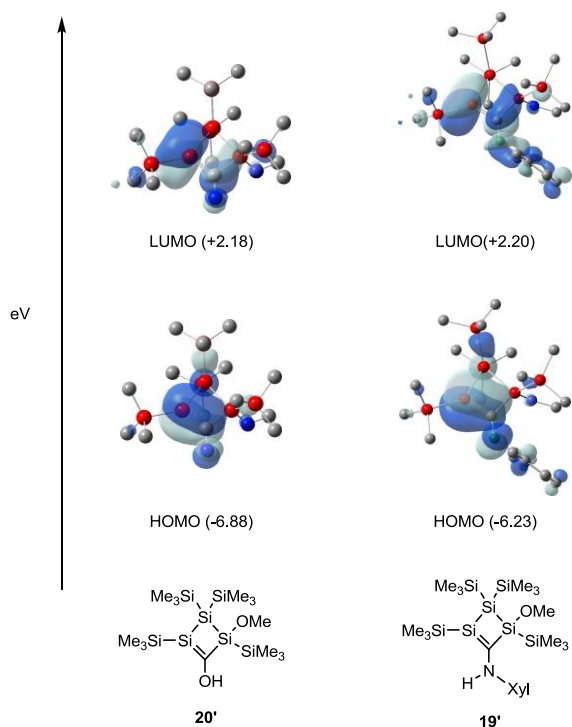
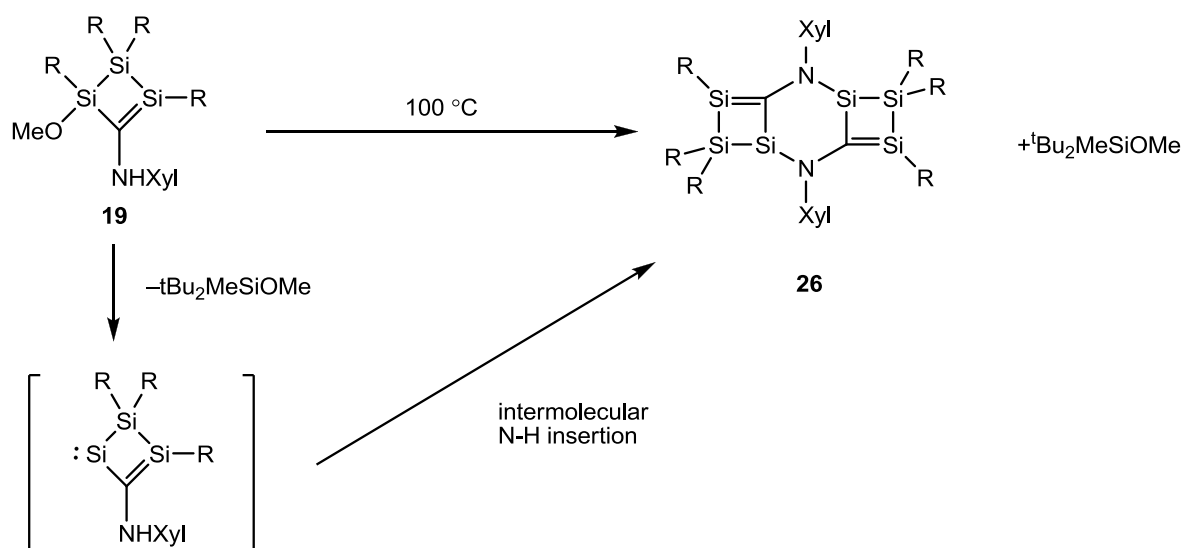


Figure 2-3-3. HOMO and LUMO energy diagram of model compound **19'** and **20'** (calculated at B3LYP/6-31G(d) level).

2-3-4. Thermal Reaction of Sila-enamine and Sila-enol.

The possibility of thermal tautomeric behavior of sila-enamine **19** and sila-enol **20** was studied (Scheme 2-3-3). As is often found for the carbon analogues, computation using B3LYP/6-31G(d) level reveals that sila-enamine **19** and sila-enol **20** are 5.9 and 20.0 kcal/mol less stable than corresponding tautomers **24** and **25**, respectively. Therefore, the thermal isomerization seems to be possible. However, thermal reaction of **19** at 100 °C afforded unexpected t Bu₂MeSiOMe and poorly-soluble crystals of bis-silene **26**, which was characterized by ¹H NMR spectrum and X-ray crystallography. Thermal reaction of sila-enol **20** gave only complex mixture including t Bu₂MeSiOMe. The elimination of t Bu₂MeSiOMe (thermal α -elimination of methoxysilane, known as a method for silylene generation) might proceed in the first reaction step. Resulting cyclic silylene intermediate would dimerize via intermolecular N-H insertion, giving of bis-silene **26**.¹⁴

Scheme 2-3-3



To gain insight into the tautomerism of sila-enamine, a transition state for the isomerization of sila-enamine to silyl-imine was investigated by simple model compounds (Figure 2-3-4). Theoretical calculations at B3LYP/6-31G(d) level reveal 35.5 kcal/mol energy barrier of conversion process under catalyst-free condition. Moreover, the calculated transition state **TS1** had twisted Si-C bond with a torsional angle $\angle H_{Si-H}-Si-C-N = 126.3^\circ$. Such twisted transition state should be further unfavorable for cyclic sila-enamine **19**, where the Si=C bond is incorporated in the rigid four-membered ring. Instead, the steric hindrance in sila-enamine **19** leads to the elongation of Si3-Si7 (2.4643(7) Å) and Si3-O1 bond (1.6774(14) Å) compared with typical bond length (Si-Si 2.359 Å and Si-O 1.631 Å). This elongation in **19** would allow the thermal α -elimination of methoxysilane at relatively low temperature.

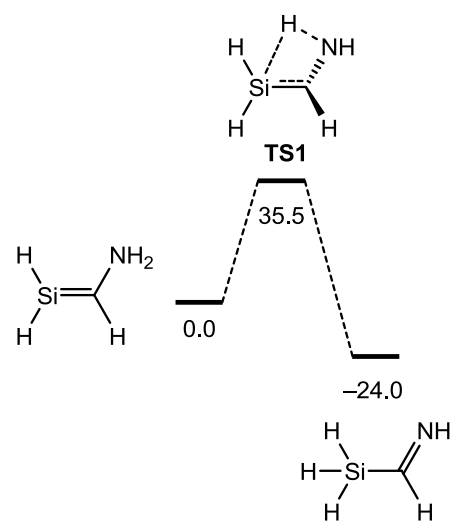


Figure 2-3-4. Transition state from model sila-enamine to silylimine (calculated at B3LYP/6-31G(d) level).

2-4. Conclusion

In summary, the author described the reaction of cyclotrisilene-isocyanide adduct with methanol, giving cyclic sila-enamine **19**. Using carbon monoxide instead of isocyanide resulted in sila-enol **20**. Structural analysis of **19** shows the characteristic long Si=C double bond due to the conjugation between Si=C and lone-pair on N. The conjugation between Si=C π orbital and non-bonding orbital of nitrogen was also investigated by spectroscopic and theoretical methods, showing anionic character of sp^2 silicon atom in **19**. Thermal tautomerization of sila-enamine **19** and sila-enol **20** was failed, but gave bis-silene **26** via thermal α -elimination of methoxysilane.

2-5. Experimental Section

General Procedure. All experiments were performed using high-vacuum line techniques or in an argon atmosphere using MBRAUN MB 150B-G glove box. All solvents were dried and degassed over potassium mirror in vacuum prior to use. NMR spectra were recorded on Bruker AC-300FT NMR (¹H NMR at 300.1 MHz; ¹³C NMR at 75.5 MHz; ²⁹Si NMR at 59.6 MHz), AV-400FT NMR (¹H NMR at 400 MHz; ¹³C NMR at 100.6 MHz; ²⁹Si NMR at 79.5 MHz) spectrometers. High-resolution mass spectra were measured on Bruker Daltonics microTOF-TU mass spectrometer with APCI (atmospheric pressure chemical ionization method). UV-Vis spectra were recorded on Simadzu UV-3150 UV-Vis spectrophotometer. IR spectra were recorded on Shimadzu IR Prestige-21 FT/IR spectrophotometer. All computations were carried out using the Gaussian 03 and 98 suite of programs B3LYP level at 6-31G(d) basis set. Tetrakis[di-*tert*-butyl(methyl)silyl]cyclotrisilene **1** was prepared according to the published procedure.

Experimental Procedure and Spectral Data of

1,3,4,4-tetrakis[di-*tert*-butyl(methyl)silyl]-2-xylylamino-3-methoxy-1,3,4-trisilacyclobutene **19**.

Dry oxygen-free C₆H₆ (3.0 ml) was added by vacuum transfer to mixture of 1,2,3,3-tetrakis[di-*tert*-butyl(methyl)silyl]cyclotrisilene **1** (100 mg, 0.14 mmol) and xylyl isocyanide (18 mg, 0.14 mmol) and stirred at room temperature for 5 min. The solution color changed to dark red from orange of **1**. Then, dry methanol (1 ml, excess) was added to the reaction mixture. After 24 h stirring, the solvent and methanol were removed by vacuo. Then, washing the resulting solid with hexane gave **19** as yellow powder (53 mg, 43% yield); mp = 97.0-97.5 °C (dec); ¹H NMR (toluene-*d*₈, δ) 0.24 (s, 3 H, SiMe), 0.39 (s, 3 H, SiMe), 0.56 (s, 3 H, SiMe), 0.64 (s, 3 H, SiMe), 0.97 (s, 9 H, Si*t*Bu₂), 0.97 (s, 9 H, Si*t*Bu₂), 1.17 (s, 9 H, Si*t*Bu₂), 1.23 (s, 9 H, Si*t*Bu₂), 1.31 (s, 9 H, Si*t*Bu₂), 1.31 (s, 9 H, Si*t*Bu₂), 1.32 (s, 9 H, Si*t*Bu₂), 1.33 (s, 9 H, Si*t*Bu₂), 2.33 (s, 3 H, ArMe), 2.68 (s, 3 H, ArMe), 3.81 (s, 3 H, OMe), 6.42 (s, 1 H, NH), 6.88-6.92 (m, 3 H, ArH); ¹³C NMR (toluene-*d*₈, δ) -3.8 (SiMe), -3.8 (SiMe), -0.5 (SiMe), 1.4 (SiMe), 19.3 (ArMe), 21.4 (ArMe), 21.6 (CMe₃), 21.7 (CMe₃), 22.0 (CMe₃), 22.3 (CMe₃), 22.4 (CMe₃), 22.5 (CMe₃), 22.5 (CMe₃), 29.6 (CMe₃), 30.0 (CMe₃), 30.4 (CMe₃), 30.6 (CMe₃), 31.0 (CMe₃), 31.2 (CMe₃), 31.5 (CMe₃), 32.0 (CMe₃), 50.3 (MeO), 124.9 (Ar), 128.4 (Ar), 130.5 (Ar), 132.6 (Ar), 133.1 (Ar), 141.8 (Ar), 185.8 (Si=C); ²⁹Si NMR (toluene-*d*₈, δ) -80.8 (skeletal sp³ Si), 10.5 (Si*t*Bu₂Me), 16.8 (Si*t*Bu₂Me), 20.1 (Si*t*Bu₂Me), 20.3 (Si*t*Bu₂Me), 21.1 (Si-OMe), 51.7 (Si=C); HRMS: *m/z* calcd for C₄₆H₉₈NOSi₇ (M+H)⁺ 876.6028, found 876.6029; UV/Vis (hexane): λ_{max} / nm (ε): 421 (8400); IR (toluene): 3370 cm⁻¹ (NH).

The single crystals of **19** for X-ray diffraction analysis were grown from a toluene solution. Diffraction data were collected at 120 K on a Bruker AXS APEX II CCD X-ray diffractometer (Mo- *Kα* radiation, *l* = 0.71073 Å, 50 kV, 30

mA). The structure was solved by the direct method, using SIR-92 program, and refined by the full-matrix least-squares method by SHELXL-97 program. Crystal data for **19** at 120 K: MF = C₄₆H₉₇ONSi₇ + C₇H₈, MW = 969.01, monoclinic, space group *P* 2₁/n, *a* = 15.7196(8) Å, *b* = 19.2672(10) Å, *c* = 19.6765(10) Å, β = 91.9600(10)°, *V* = 5956.0(5) Å³, *Z* = 4, D_{calcd} = 1.081 g/cm³, The final *R* factor was 0.0445 (*R*_w = 0.1351 for all data) for 13580 reflections with *I* > 2σ(*I*), GOF = 1.042.

Experimental Procedure and Spectral Data of 1,3,4,4-tetrakis[di-*tert*-butyl(methyl)silyl]-2-hydroxy-3-methoxy-1,3,4-trisilacyclobutene **20**.

Dry oxygen-free C₆H₆ (5.0 ml) and methanol (1.0 ml) were added by vacuum transfer to 1,2,3,3-tetrakis[di-*tert*-butyl(methyl)silyl]cyclotrisilene **1** (140 mg, 0.20 mmol), and then CO gas were bubbled to the reaction glass via KOH and CaCl₂ tubes for 1 h. The solution color changed to pale yellow from orange of **1**. After removal of the solvent, the reaction mixture was purified by a short column to give **20** as pale yellow crystals (110 mg, 70% yield); mp = 114.0-115.0 °C; ¹H NMR (C₆D₆, δ) 0.17 (s, 3 H, SiMe), 0.45 (s, 3 H, SiMe), 0.51 (s, 3 H, SiMe), 0.55 (s, 3 H, SiMe), 1.14 (s, 9 H, Si'*t*Bu₂), 1.19 (s, 9 H, Si'*t*Bu₂), 1.21 (s, 9 H, Si'*t*Bu₂), 1.26 (s, 9 H, Si'*t*Bu₂), 1.27 (s, 9 H, Si'*t*Bu₂), 1.29 (s, 9 H, Si'*t*Bu₂), 1.29 (s, 9 H, Si'*t*Bu₂), 1.30 (s, 9 H, Si'*t*Bu₂), 3.60 (s, 3 H, OMe), 5.79 (s, 1 H, OH); ¹³C NMR (C₆D₆, δ) -6.1 (SiMe), -4.0 (SiMe), -1.1 (SiMe), 0.4 (SiMe), 21.9 (CMe₃), 21.9 (CMe₃), 22.0 (CMe₃), 22.2 (CMe₃), 22.5 (CMe₃), 22.6 (CMe₃), 22.8 (CMe₃), 23.0, 29.6 (CMe₃), 29.9 (CMe₃), 30.2 (CMe₃), 30.2 (CMe₃), 30.4 (CMe₃), 30.7 (CMe₃), 31.1 (CMe₃), 32.3 (CMe₃), 51.7 (MeO), 207.5 (Si=C); ²⁹Si NMR (C₆D₆, δ) -95.3 (skeletal sp³ Si), 9.2 (Si'*t*Bu₂Me), 16.1 (Si'*t*Bu₂Me), 18.8 (Si'*t*Bu₂Me), 18.8 (Si'*t*Bu₂Me), 21.4 (Si-OMe), 90.2 (Si=C); HRMS: *m/z* calcd for C₃₈H₈₉O₂Si₇ (M+H)⁺ 773.5242, found 773.5241; UV/Vis (hexane): λ_{max} / nm (ε): 369 (3870); IR (nujol): 3578 cm⁻¹ (OH).

The single crystals of **20** for X-ray diffraction analysis were grown from a pentane solution. Diffraction data were collected at 120 K on a Bruker AXS APEX II CCD X-ray diffractometer (Mo- *Kα* radiation, *l* = 0.71073 Å, 50 kV, 30 mA). The structure was solved by the direct method, using SIR-92 program, and refined by the full-matrix least-squares method by SHELXL-97 program. Crystal data for **20** at 120 K: MF = C₃₈H₈₈O₂Si₇, MW = 773.71, Orthorhombic, space group Pbca, *a* = 17.0076(11) Å, *b* = *b* = 17.1760(11) Å, *c* = *c* = 33.624(2) Å, β = 90°, *V* = 9822.3(11) Å³, *Z* = 8, D_{calcd} = 1.046 g/cm³, The final *R* factor was 0.0368 (*R*_w = 0.1014 for all data) for 11249 reflections with *I* > 2σ(*I*), GOF = 1.039.

**Experimental Procedure and Spectral Data of
4,5,5,9,10,10-hexakis(di-*tert*-butylmethylsilyl)-2,7-bis(2,6-xylol)-2,7-aza-1,4,5,6,9,10-hexasilatricyclo[6.2.0.0^{3,6}]dec
a-3,8-diene (26).**

Toluene solution of compound **19** (100 mg, 0.114 mmol) was placed at 100 °C for 48 hours. After evaporation, the resulting residue was washed by hexane. Recrystallization from THF at 80 °C with slow cooling to room temperature gave **26** as yellow crystals (30 mg, 35% yield); mp = 276.1-277.0 °C; ¹H NMR (toluene-*d*₈, δ) 0.19 (s, 6 H, Si*Me* × 2), 0.50 (s, 6 H, Si*Me* × 2), 0.55 (s, 6 H, Si*Me* × 2), 0.94 (s, 18 H, Si*tBu*₂ × 2), 1.02 (s, 18 H, Si*tBu*₂ × 2), 1.22 (s, 18 H, x 2), 1.26 (s, 18 H, Si*tBu*₂ × 2), 1.27 (s, 18 H, Si*tBu*₂ × 2), 1.34 (s, 18 H, Si*tBu*₂ × 2), 2.76 (s, 6 H, Ar*Me*), 2.78 (s, 6 H, Ar*Me*), 5.97 (s, 2 H, Si*H* × 2), 7.00-7.09 (m, 6 H, Ar*H*). HRMS: *m/z* calcd for C₇₂H₁₄₆N₂Si₁₂ (M+H)⁺ 1374.8712, found 1374.8714.

The single crystals of **26** for X-ray diffraction analysis were grown from a THF solution. Diffraction data were collected at 120 K on a Bruker AXS APEX II CCD X-ray diffractometer (Mo- *Kα* radiation, *l* = 0.71073 Å, 50 kV, 30 mA). The structure was solved by the direct method, using SIR-92 program, and refined by the full-matrix least-squares method by SHELXL-97 program. Crystal data for **26** at 120 K: MF = C₇₂H₁₄₆N₂Si₁₂ + (C₄H₈O)₂, MW = 1521.20, monoclinic, space group *P*-1, *a* = 16.2994(14) Å, *b* = 17.1566(15) Å, *c* = 18.729(3) Å, β = 100.8050(10)°, *V* = 4614.4(9) Å³, *Z* = 2, D_{calcd} = 1.095 g/cm³, The final *R* factor was 0.0560 (*R*_w = 0.1702 for all data) for 51564 reflections with *I* > 2σ(*I*), GOF = 1.020.

Crystal Data

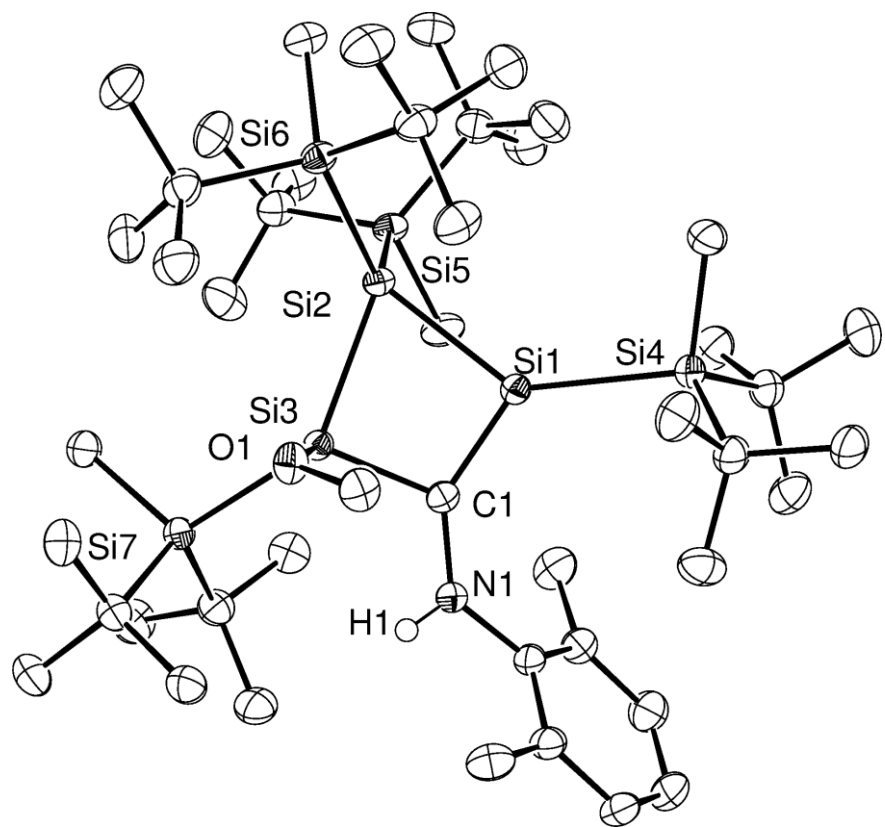


Figure 2-5-1. ORTEP drawing of Compound **19**.

Table 2-5-1. Crystal data and structure refinement for compound **19**.

Identification code	(tBu2MeSi)4Si3 + CNXyl + MeOH		
Empirical formula	C53 H105 N O Si7		
Formula weight	969.01		
Temperature	120(1) K		
Wavelength	0.71073 Å		
Crystal system	Monoclinic		
Space group	P2(1)/n		
Unit cell dimensions	a = 15.7196(8) Å	α= 90 deg.	
	b = 19.2672(10) Å	β= 91.9600(10) deg.	
	c = 19.6765(10) Å	γ = 90 deg.	
Volume	5956.0(5) Å ³		
Z	4		
Density (calculated)	1.081 Mg/m ³		
Absorption coefficient	0.195 mm ⁻¹		
F(000)	2144		
Crystal size	0.35 x 0.28 x 0.12 mm ³		
Theta range for data collection	1.63 to 27.48°.		
Index ranges	-20≤h≤20, -24≤k≤25, -25≤l≤25		
Reflections collected	66429		
Independent reflections	13580 [R(int) = 0.0311]		
Completeness to theta = 27.48 deg	99.5 %		
Absorption correction	Empirical		
Max. and min. transmission	0.9770 and 0.9350		
Refinement method	Full-matrix least-squares on F ²		
Data / restraints / parameters	13580 / 0 / 564		
Goodness-of-fit on F ²	1.008		
Final R indices [I>2sigma(I)]	R1 = 0.0432, wR2 = 0.1204		
R indices (all data)	R1 = 0.0551, wR2 = 0.1307		
Extinction coefficient	0.0001(2)		
Largest diff. peak and hole	1.012 and -0.541 e.Å ⁻³		

Table 2-5-2. Atomic coordinates ($\times 10^4$) and equivalent isotropic displacement parameters ($\text{\AA}^2 \times 10^3$) for compound **19**. U(eq) is defined as one third of the trace of the orthogonalized U^{ij} tensor.

	x	y	z	U(eq)
Si(1)	874(1)	6556(1)	1800(1)	19(1)
Si(2)	-327(1)	7311(1)	1652(1)	18(1)
Si(3)	392(1)	7249(1)	593(1)	18(1)
Si(4)	1300(1)	5654(1)	2590(1)	22(1)
Si(5)	-11(1)	8280(1)	2422(1)	21(1)
Si(6)	-1820(1)	6955(1)	1544(1)	20(1)
Si(7)	658(1)	8102(1)	-308(1)	22(1)
O(1)	-88(1)	6649(1)	95(1)	25(1)
N(1)	2047(1)	6705(1)	642(1)	22(1)
C(1)	1334(1)	6818(1)	1023(1)	19(1)
C(2)	333(1)	5494(1)	3101(1)	32(1)
C(3)	1492(1)	4816(1)	2085(1)	26(1)
C(4)	650(1)	4593(1)	1729(1)	35(1)
C(5)	2152(2)	4910(1)	1538(1)	35(1)
C(6)	1772(1)	4222(1)	2568(1)	35(1)
C(7)	2213(1)	5899(1)	3227(1)	30(1)
C(8)	3094(1)	5790(1)	2941(1)	37(1)
C(9)	2152(2)	5459(2)	3879(1)	46(1)
C(10)	2126(2)	6661(1)	3443(1)	38(1)
C(11)	1184(1)	8328(1)	2412(1)	30(1)
C(12)	-287(1)	8110(1)	3360(1)	28(1)
C(13)	-311(2)	7324(1)	3482(1)	38(1)
C(14)	413(2)	8422(1)	3841(1)	41(1)
C(15)	-1143(1)	8411(1)	3580(1)	36(1)
C(16)	-403(1)	9176(1)	2114(1)	28(1)
C(17)	-128(1)	9752(1)	2619(1)	34(1)
C(18)	-1371(1)	9219(1)	1988(1)	36(1)
C(19)	15(2)	9322(1)	1437(1)	42(1)
C(20)	-2409(1)	7501(1)	2166(1)	28(1)
C(21)	-2022(1)	6012(1)	1819(1)	27(1)
C(22)	-1423(1)	5502(1)	1471(1)	32(1)
C(23)	-1868(1)	5961(1)	2589(1)	35(1)
C(24)	-2950(1)	5788(1)	1663(1)	35(1)
C(25)	-2327(1)	7172(1)	659(1)	27(1)
C(26)	-3295(1)	7294(1)	708(1)	36(1)
C(27)	-1942(1)	7856(1)	411(1)	35(1)

C(28)	-2190(1)	6616(1)	115(1)	35(1)
C(29)	-133(1)	8842(1)	-307(1)	30(1)
C(30)	1775(1)	8528(1)	-216(1)	29(1)
C(31)	1782(2)	9245(1)	-563(1)	41(1)
C(32)	2497(1)	8098(1)	-516(1)	35(1)
C(33)	1984(1)	8637(1)	544(1)	34(1)
C(34)	470(1)	7653(1)	-1179(1)	27(1)
C(35)	-481(1)	7476(1)	-1276(1)	33(1)
C(36)	696(2)	8148(1)	-1762(1)	36(1)
C(37)	993(1)	6982(1)	-1252(1)	32(1)
C(38)	2868(1)	6427(1)	797(1)	22(1)
C(39)	3169(1)	5910(1)	360(1)	26(1)
C(40)	3996(1)	5662(1)	469(1)	33(1)
C(41)	4511(1)	5913(1)	994(1)	39(1)
C(42)	4212(1)	6428(1)	1412(1)	38(1)
C(43)	3394(1)	6702(1)	1320(1)	29(1)
C(44)	2609(1)	5622(1)	-206(1)	34(1)
C(45)	3120(1)	7303(1)	1750(1)	37(1)
C(46)	28(1)	5917(1)	108(1)	27(1)
C(47)	5317(2)	8951(2)	591(2)	79(1)
C(48)	6062(2)	9325(2)	730(2)	67(1)
C(49)	6457(2)	9307(2)	1358(2)	61(1)
C(50)	6107(2)	8938(2)	1872(2)	61(1)
C(51)	5367(2)	8558(2)	1734(2)	72(1)
C(52)	4991(2)	8566(2)	1120(2)	72(1)
C(53)	4877(4)	8984(4)	-51(3)	137(2)

Table 2-5-3. Bond lengths [\AA] and angles [deg] for compound **19**.

Si(1)-C(1)	1.7871(18)	C(21)-C(22)	1.537(3)
Si(1)-Si(2)	2.3922(7)	C(21)-C(24)	1.542(3)
Si(1)-Si(4)	2.4112(7)	C(25)-C(28)	1.535(3)
Si(1)-Si(3)	2.8063(7)	C(25)-C(27)	1.537(3)
Si(2)-Si(3)	2.4080(7)	C(25)-C(26)	1.545(3)
Si(2)-Si(5)	2.4439(7)	C(30)-C(33)	1.535(3)
Si(2)-Si(6)	2.4475(7)	C(30)-C(32)	1.540(3)
Si(3)-O(1)	1.6774(14)	C(30)-C(31)	1.542(3)
Si(3)-C(1)	1.8741(18)	C(34)-C(35)	1.538(3)
Si(3)-Si(7)	2.4643(7)	C(34)-C(37)	1.540(3)
Si(4)-C(2)	1.877(2)	C(34)-C(36)	1.542(3)
Si(4)-C(3)	1.925(2)	C(38)-C(43)	1.401(3)
Si(4)-C(7)	1.931(2)	C(38)-C(39)	1.408(3)
Si(5)-C(11)	1.882(2)	C(39)-C(40)	1.395(3)
Si(5)-C(16)	1.924(2)	C(39)-C(44)	1.503(3)
Si(5)-C(12)	1.940(2)	C(40)-C(41)	1.379(3)
Si(6)-C(20)	1.881(2)	C(41)-C(42)	1.381(3)
Si(6)-C(21)	1.926(2)	C(42)-C(43)	1.396(3)
Si(6)-C(25)	1.935(2)	C(43)-C(45)	1.507(3)
Si(7)-C(29)	1.891(2)	C(1)-Si(1)-Si(2)	93.74(6)
Si(7)-C(34)	1.933(2)	C(1)-Si(1)-Si(4)	130.03(6)
Si(7)-C(30)	1.941(2)	Si(2)-Si(1)-Si(4)	135.83(3)
O(1)-C(46)	1.421(2)	C(1)-Si(1)-Si(3)	41.12(6)
N(1)-C(1)	1.387(2)	Si(2)-Si(1)-Si(3)	54.487(18)
N(1)-C(38)	1.420(2)	Si(4)-Si(1)-Si(3)	161.67(3)
N(1)-H(1)	0.80(2)	Si(1)-Si(2)-Si(3)	71.55(2)
C(3)-C(5)	1.531(3)	Si(1)-Si(2)-Si(5)	104.23(2)
C(3)-C(4)	1.538(3)	Si(3)-Si(2)-Si(5)	118.86(2)
C(3)-C(6)	1.542(3)	Si(1)-Si(2)-Si(6)	126.23(3)
C(7)-C(8)	1.527(3)	Si(3)-Si(2)-Si(6)	112.81(2)
C(7)-C(10)	1.536(3)	Si(5)-Si(2)-Si(6)	116.22(2)
C(7)-C(9)	1.544(3)	O(1)-Si(3)-C(1)	106.91(7)
C(12)-C(13)	1.532(3)	O(1)-Si(3)-Si(2)	108.98(5)
C(12)-C(15)	1.541(3)	C(1)-Si(3)-Si(2)	91.04(6)
C(12)-C(14)	1.548(3)	O(1)-Si(3)-Si(7)	97.09(5)
C(16)-C(19)	1.531(3)	C(1)-Si(3)-Si(7)	117.98(6)
C(16)-C(18)	1.534(3)	Si(2)-Si(3)-Si(7)	133.32(3)
C(16)-C(17)	1.541(3)	O(1)-Si(3)-Si(1)	105.66(5)
C(21)-C(23)	1.529(3)	C(1)-Si(3)-Si(1)	38.83(6)

Si(2)-Si(3)-Si(1)	53.962(18)	C(10)-C(7)-C(9)	106.65(18)
Si(7)-Si(3)-Si(1)	151.48(3)	C(8)-C(7)-Si(4)	113.01(14)
C(2)-Si(4)-C(3)	106.45(9)	C(10)-C(7)-Si(4)	110.02(14)
C(2)-Si(4)-C(7)	106.83(10)	C(9)-C(7)-Si(4)	109.80(16)
C(3)-Si(4)-C(7)	114.42(9)	C(13)-C(12)-C(15)	107.58(18)
C(2)-Si(4)-Si(1)	104.55(7)	C(13)-C(12)-C(14)	107.98(19)
C(3)-Si(4)-Si(1)	108.53(6)	C(15)-C(12)-C(14)	106.96(17)
C(7)-Si(4)-Si(1)	115.21(7)	C(13)-C(12)-Si(5)	108.86(14)
C(11)-Si(5)-C(16)	105.20(9)	C(15)-C(12)-Si(5)	115.42(15)
C(11)-Si(5)-C(12)	105.86(9)	C(14)-C(12)-Si(5)	109.79(14)
C(16)-Si(5)-C(12)	111.78(9)	C(19)-C(16)-C(18)	107.59(19)
C(11)-Si(5)-Si(2)	102.35(6)	C(19)-C(16)-C(17)	107.96(17)
C(16)-Si(5)-Si(2)	115.78(7)	C(18)-C(16)-C(17)	108.70(17)
C(12)-Si(5)-Si(2)	114.41(6)	C(19)-C(16)-Si(5)	107.14(14)
C(20)-Si(6)-C(21)	104.78(9)	C(18)-C(16)-Si(5)	113.86(14)
C(20)-Si(6)-C(25)	105.59(9)	C(17)-C(16)-Si(5)	111.36(15)
C(21)-Si(6)-C(25)	112.95(9)	C(23)-C(21)-C(22)	108.76(17)
C(20)-Si(6)-Si(2)	106.17(7)	C(23)-C(21)-C(24)	107.27(17)
C(21)-Si(6)-Si(2)	113.97(6)	C(22)-C(21)-C(24)	108.84(17)
C(25)-Si(6)-Si(2)	112.45(6)	C(23)-C(21)-Si(6)	108.44(14)
C(29)-Si(7)-C(34)	104.97(9)	C(22)-C(21)-Si(6)	111.64(13)
C(29)-Si(7)-C(30)	105.90(9)	C(24)-C(21)-Si(6)	111.76(14)
C(34)-Si(7)-C(30)	112.52(9)	C(28)-C(25)-C(27)	108.05(18)
C(29)-Si(7)-Si(3)	111.93(7)	C(28)-C(25)-C(26)	108.15(17)
C(34)-Si(7)-Si(3)	108.32(6)	C(27)-C(25)-C(26)	106.76(17)
C(30)-Si(7)-Si(3)	112.94(6)	C(28)-C(25)-Si(6)	114.44(14)
C(46)-O(1)-Si(3)	128.14(12)	C(27)-C(25)-Si(6)	108.47(13)
C(1)-N(1)-C(38)	133.55(16)	C(26)-C(25)-Si(6)	110.67(14)
C(1)-N(1)-H(1)	116.6(17)	C(33)-C(30)-C(32)	108.17(18)
C(38)-N(1)-H(1)	109.1(17)	C(33)-C(30)-C(31)	107.72(18)
N(1)-C(1)-Si(1)	140.93(14)	C(32)-C(30)-C(31)	107.11(17)
N(1)-C(1)-Si(3)	117.85(13)	C(33)-C(30)-Si(7)	108.21(13)
Si(1)-C(1)-Si(3)	100.05(9)	C(32)-C(30)-Si(7)	114.45(14)
C(5)-C(3)-C(4)	107.79(18)	C(31)-C(30)-Si(7)	110.95(15)
C(5)-C(3)-C(6)	109.64(17)	C(35)-C(34)-C(37)	108.81(17)
C(4)-C(3)-C(6)	107.27(17)	C(35)-C(34)-C(36)	107.04(17)
C(5)-C(3)-Si(4)	112.63(14)	C(37)-C(34)-C(36)	108.18(17)
C(4)-C(3)-Si(4)	108.74(13)	C(35)-C(34)-Si(7)	109.12(14)
C(6)-C(3)-Si(4)	110.59(14)	C(37)-C(34)-Si(7)	113.07(13)
C(8)-C(7)-C(10)	108.92(19)	C(36)-C(34)-Si(7)	110.44(14)
C(8)-C(7)-C(9)	108.22(18)	C(43)-C(38)-C(39)	120.89(17)

C(43)-C(38)-N(1)	121.60(17)	C(38)-C(43)-C(45)	122.02(18)
C(39)-C(38)-N(1)	117.21(17)	C(52)-C(47)-C(48)	117.2(3)
C(40)-C(39)-C(38)	118.68(19)	C(52)-C(47)-C(53)	120.6(4)
C(40)-C(39)-C(44)	120.40(18)	C(48)-C(47)-C(53)	122.1(4)
C(38)-C(39)-C(44)	120.91(17)	C(49)-C(48)-C(47)	121.2(4)
C(41)-C(40)-C(39)	121.0(2)	C(50)-C(49)-C(48)	120.0(3)
C(40)-C(41)-C(42)	119.73(19)	C(49)-C(50)-C(51)	119.0(3)
C(41)-C(42)-C(43)	121.6(2)	C(52)-C(51)-C(50)	120.9(4)
C(42)-C(43)-C(38)	118.07(19)	C(51)-C(52)-C(47)	121.7(4)
C(42)-C(43)-C(45)	119.81(19)		

Symmetry transformations used to generate equivalent atoms:

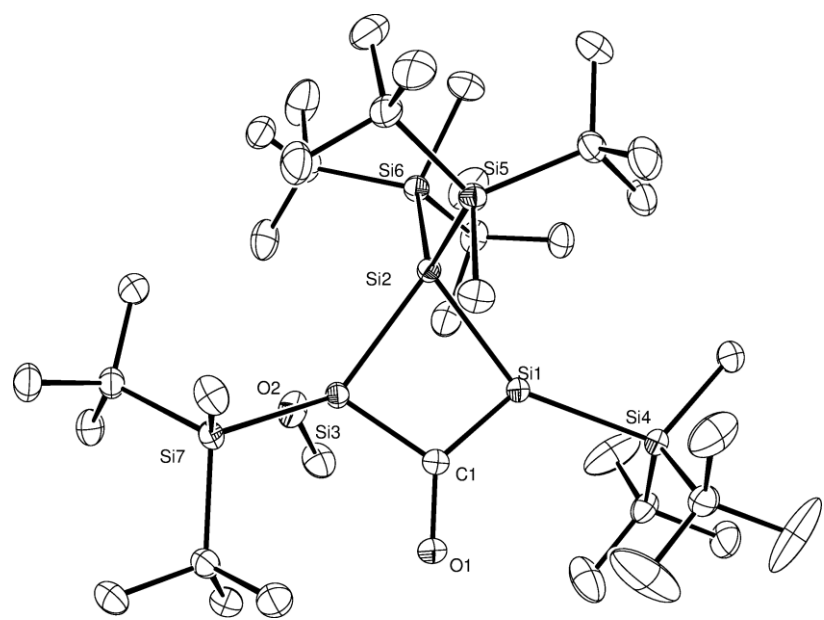


Figure 2-5-2. ORTEP drawing of cyclic sila-enol **20**.

Table 2-5-4. Crystal data and structure refinement for compound **20**.

Identification code	(tBu2MeSi)4Si3 + CO + MeOH		
Empirical formula	C38 H88 O2 Si7		
Formula weight	773.71		
Temperature	120.0(5) K		
Wavelength	0.71073 Å		
Crystal system	Orthorhombic		
Space group	Pbca		
Unit cell dimensions	a = 17.0076(11) Å	α= 90 deg.	
	b = 17.1760(11) Å	β= 90 deg.	
	c = 33.624(2) Å	γ = 90 deg.	
Volume	9822.3(11) Å ³		
Z	8		
Density (calculated)	1.046 Mg/m ³		
Absorption coefficient	0.222 mm ⁻¹		
F(000)	3440		
Crystal size	0.38 x 0.35 x 0.34 mm ³		
Theta range for data collection	1.21 to 27.48°.		
Index ranges	-22<=h<=22, -22<=k<=22, -43<=l<=43		
Reflections collected	106536		
Independent reflections	11249 [R(int) = 0.0361]		
Completeness to theta = 27.48 deg	99.9 %		
Absorption correction	Empirical		
Max. and min. transmission	0.9279 and 0.9211		
Refinement method	Full-matrix least-squares on F ²		
Data / restraints / parameters	11249 / 0 / 429		
Goodness-of-fit on F ²	1.039		
Final R indices [I>2sigma(I)]	R1 = 0.0368, wR2 = 0.0962		
R indices (all data)	R1 = 0.0442, wR2 = 0.1014		
Extinction coefficient	0.00000(5)		
Largest diff. peak and hole	0.687 and -0.601 e.Å ⁻³		

Table 2-5-5. Atomic coordinates (x 10⁴) and equivalent isotropic displacement parameters (Å²x 10³) for compound **20**. U(eq) is defined as one third of the trace of the orthogonalized U^{ij} tensor.

	x	y	z	U(eq)
Si(1)	5853(1)	4089(1)	1222(1)	17(1)
Si(2)	4643(1)	3535(1)	1424(1)	15(1)
Si(3)	4864(1)	3106(1)	739(1)	17(1)
Si(4)	6938(1)	4933(1)	1387(1)	19(1)
Si(5)	5032(1)	2639(1)	1942(1)	18(1)
Si(6)	3548(1)	4405(1)	1551(1)	19(1)
Si(7)	4728(1)	1863(1)	406(1)	18(1)
O(1)	6394(1)	3523(1)	459(1)	32(1)
O(2)	4301(1)	3613(1)	426(1)	28(1)
C(1)	5862(1)	3567(1)	771(1)	21(1)
C(2)	6802(1)	5443(1)	1877(1)	28(1)
C(3)	7875(1)	4304(1)	1430(1)	26(1)
C(4)	7765(1)	3712(1)	1762(1)	48(1)
C(5)	8585(1)	4798(2)	1542(1)	82(1)
C(6)	8043(2)	3835(2)	1056(1)	95(1)
C(7)	6957(1)	5738(1)	988(1)	25(1)
C(8)	7607(1)	6333(1)	1071(1)	37(1)
C(9)	7065(2)	5419(1)	567(1)	47(1)
C(10)	6176(1)	6174(2)	1004(1)	60(1)
C(11)	5888(1)	2131(1)	1697(1)	25(1)
C(12)	5435(1)	3134(1)	2420(1)	24(1)
C(13)	6133(1)	2657(1)	2582(1)	34(1)
C(14)	5745(1)	3947(1)	2317(1)	30(1)
C(15)	4829(1)	3220(1)	2755(1)	35(1)
C(16)	4280(1)	1837(1)	2061(1)	25(1)
C(17)	4101(1)	1413(1)	1671(1)	36(1)
C(18)	3500(1)	2130(1)	2236(1)	36(1)
C(19)	4632(1)	1235(1)	2349(1)	35(1)
C(20)	3345(1)	4378(1)	2104(1)	32(1)
C(21)	3826(1)	5466(1)	1433(1)	25(1)
C(22)	4523(1)	5689(1)	1701(1)	30(1)
C(23)	4072(1)	5578(1)	998(1)	34(1)
C(24)	3150(1)	6030(1)	1525(1)	44(1)
C(25)	2599(1)	4054(1)	1294(1)	25(1)
C(26)	2617(1)	4165(1)	843(1)	35(1)
C(27)	1862(1)	4470(1)	1457(1)	49(1)

C(28)	2487(1)	3184(1)	1385(1)	29(1)
C(29)	4994(1)	997(1)	724(1)	28(1)
C(30)	5448(1)	1850(1)	-38(1)	23(1)
C(31)	6280(1)	1706(1)	127(1)	31(1)
C(32)	5458(1)	2610(1)	-278(1)	28(1)
C(33)	5258(1)	1172(1)	-323(1)	31(1)
C(34)	3645(1)	1725(1)	249(1)	22(1)
C(35)	3409(1)	2236(1)	-107(1)	28(1)
C(36)	3469(1)	867(1)	147(1)	30(1)
C(37)	3119(1)	1949(1)	602(1)	30(1)
C(38)	4514(1)	4279(1)	205(1)	31(1)

Table 2-5-6. Bond lengths [Å] and angles [deg] for compound **20**.

Si(1)-C(1)	1.7638(16)	C(21)-C(22)	1.536(2)
Si(1)-Si(2)	2.3666(6)	C(25)-C(26)	1.531(3)
Si(1)-Si(4)	2.4098(6)	C(25)-C(28)	1.538(2)
Si(2)-Si(5)	2.4165(6)	C(25)-C(27)	1.541(2)
Si(2)-Si(6)	2.4257(6)	C(30)-C(32)	1.535(2)
Si(2)-Si(3)	2.4481(6)	C(30)-C(31)	1.540(2)
Si(3)-O(2)	1.6673(12)	C(30)-C(33)	1.543(2)
Si(3)-C(1)	1.8754(16)	C(34)-C(37)	1.535(2)
Si(3)-Si(7)	2.4216(6)	C(34)-C(35)	1.537(2)
Si(4)-C(2)	1.8831(17)	C(34)-C(36)	1.543(2)
Si(4)-C(7)	1.9261(17)		
Si(4)-C(3)	1.9299(18)	C(1)-Si(1)-Si(2)	92.80(5)
Si(5)-C(11)	1.8869(17)	C(1)-Si(1)-Si(4)	119.81(5)
Si(5)-C(16)	1.9215(17)	Si(2)-Si(1)-Si(4)	147.34(2)
Si(5)-C(12)	1.9423(17)	Si(1)-Si(2)-Si(5)	102.97(2)
Si(6)-C(20)	1.8886(18)	Si(1)-Si(2)-Si(6)	118.10(2)
Si(6)-C(21)	1.9258(17)	Si(5)-Si(2)-Si(6)	118.33(2)
Si(6)-C(25)	1.9273(17)	Si(1)-Si(2)-Si(3)	73.637(18)
Si(7)-C(29)	1.8874(17)	Si(5)-Si(2)-Si(3)	116.37(2)
Si(7)-C(30)	1.9284(17)	Si(6)-Si(2)-Si(3)	118.04(2)
Si(7)-C(34)	1.9306(16)	O(2)-Si(3)-C(1)	109.60(7)
O(1)-C(1)	1.3876(19)	O(2)-Si(3)-Si(7)	96.57(5)
O(1)-H(1)	0.78(3)	C(1)-Si(3)-Si(7)	119.02(5)
O(2)-C(38)	1.411(2)	O(2)-Si(3)-Si(2)	110.34(5)
C(3)-C(6)	1.521(3)	C(1)-Si(3)-Si(2)	87.56(5)
C(3)-C(4)	1.523(3)	Si(7)-Si(3)-Si(2)	133.32(2)
C(3)-C(5)	1.523(3)	C(2)-Si(4)-C(7)	106.12(8)
C(7)-C(10)	1.526(3)	C(2)-Si(4)-C(3)	107.21(8)
C(7)-C(9)	1.530(3)	C(7)-Si(4)-C(3)	116.08(8)
C(7)-C(8)	1.531(2)	C(2)-Si(4)-Si(1)	112.78(6)
C(12)-C(14)	1.533(2)	C(7)-Si(4)-Si(1)	106.57(5)
C(12)-C(15)	1.535(2)	C(3)-Si(4)-Si(1)	108.23(6)
C(12)-C(13)	1.543(2)	C(11)-Si(5)-C(16)	105.83(8)
C(16)-C(17)	1.530(2)	C(11)-Si(5)-C(12)	106.87(8)
C(16)-C(18)	1.536(3)	C(16)-Si(5)-C(12)	112.08(7)
C(16)-C(19)	1.538(2)	C(11)-Si(5)-Si(2)	101.06(6)
C(21)-C(23)	1.534(3)	C(16)-Si(5)-Si(2)	115.16(6)
C(21)-C(24)	1.535(2)	C(12)-Si(5)-Si(2)	114.46(5)

C(20)-Si(6)-C(21)	105.76(8)	C(15)-C(12)-Si(5)	114.38(12)
C(20)-Si(6)-C(25)	106.25(8)	C(13)-C(12)-Si(5)	109.49(12)
C(21)-Si(6)-C(25)	114.14(8)	C(17)-C(16)-C(18)	108.22(16)
C(20)-Si(6)-Si(2)	107.42(6)	C(17)-C(16)-C(19)	107.29(15)
C(21)-Si(6)-Si(2)	110.94(5)	C(18)-C(16)-C(19)	108.34(15)
C(25)-Si(6)-Si(2)	111.81(5)	C(17)-C(16)-Si(5)	107.13(12)
C(29)-Si(7)-C(30)	106.12(8)	C(18)-C(16)-Si(5)	114.81(12)
C(29)-Si(7)-C(34)	106.64(8)	C(19)-C(16)-Si(5)	110.76(12)
C(30)-Si(7)-C(34)	113.14(7)	C(23)-C(21)-C(24)	108.52(16)
C(29)-Si(7)-Si(3)	114.19(6)	C(23)-C(21)-C(22)	108.50(15)
C(30)-Si(7)-Si(3)	107.89(5)	C(24)-C(21)-C(22)	107.61(15)
C(34)-Si(7)-Si(3)	108.97(5)	C(23)-C(21)-Si(6)	112.53(12)
C(1)-O(1)-H(1)	110(2)	C(24)-C(21)-Si(6)	111.78(13)
C(38)-O(2)-Si(3)	127.43(11)	C(22)-C(21)-Si(6)	107.73(12)
O(1)-C(1)-Si(1)	133.14(12)	C(26)-C(25)-C(28)	108.70(15)
O(1)-C(1)-Si(3)	121.58(11)	C(26)-C(25)-C(27)	108.13(17)
Si(1)-C(1)-Si(3)	104.90(8)	C(28)-C(25)-C(27)	106.20(16)
C(6)-C(3)-C(4)	106.0(2)	C(26)-C(25)-Si(6)	112.88(12)
C(6)-C(3)-C(5)	110.5(2)	C(28)-C(25)-Si(6)	108.54(12)
C(4)-C(3)-C(5)	106.73(19)	C(27)-C(25)-Si(6)	112.13(13)
C(6)-C(3)-Si(4)	112.97(13)	C(32)-C(30)-C(31)	108.31(14)
C(4)-C(3)-Si(4)	109.09(12)	C(32)-C(30)-C(33)	108.49(14)
C(5)-C(3)-Si(4)	111.20(14)	C(31)-C(30)-C(33)	107.19(14)
C(10)-C(7)-C(9)	108.23(19)	C(32)-C(30)-Si(7)	113.81(11)
C(10)-C(7)-C(8)	107.09(17)	C(31)-C(30)-Si(7)	107.88(11)
C(9)-C(7)-C(8)	108.77(16)	C(33)-C(30)-Si(7)	110.93(12)
C(10)-C(7)-Si(4)	108.23(12)	C(37)-C(34)-C(35)	107.80(14)
C(9)-C(7)-Si(4)	112.93(12)	C(37)-C(34)-C(36)	107.27(14)
C(8)-C(7)-Si(4)	111.38(12)	C(35)-C(34)-C(36)	108.77(14)
C(14)-C(12)-C(15)	107.95(15)	C(37)-C(34)-Si(7)	108.38(11)
C(14)-C(12)-C(13)	107.33(15)	C(35)-C(34)-Si(7)	113.09(11)
C(15)-C(12)-C(13)	107.85(15)	C(36)-C(34)-Si(7)	111.31(11)
C(14)-C(12)-Si(5)	109.59(11)		

Symmetry transformations used to generate equivalent atoms:

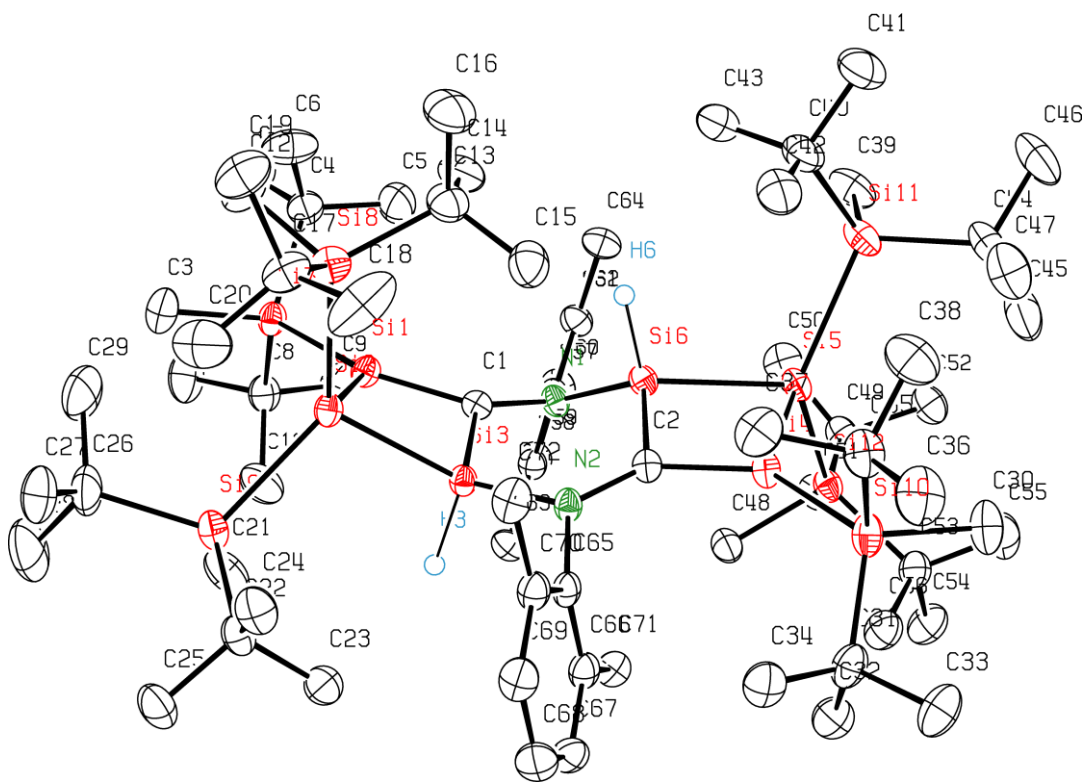


Figure 2-5-3. ORTEP drawing of **26**.

Table 2-5-7. Crystal data and structure refinement for compound **26**.

Identification code	2,7-diaza-1,4,5,6,9,10-hexasilatricyclo[6.2.0.0(3,6)]deca-3,8-diene		
Empirical formula	C ₇₂ H ₁₄₆ N ₂ Si ₁₂ (C ₄ H ₈ O) ₂		
Formula weight	1521.20		
Temperature	120 K		
Wavelength	0.71073 Å		
Crystal system	Triclinic		
Space group	P-1		
Unit cell dimensions	a = 16.2994(14) Å	α = 104.3210(10) deg.	
	b = 17.1566(15) Å	β = 100.8050(10) deg.	
	c = 18.729(3) Å	γ = 108.2740(10) deg.	
Volume	4614.4(9) Å ³		
Z	2		
Density (calculated)	1.095 Mg/m ³		
Absorption coefficient	0.210 mm ⁻¹		
F(000)	1680		
Crystal size	0.30 x 0.26 x 0.21 mm ³		
Theta range for data collection	1.17 to 27.48°.		
Index ranges	-21≤h≤21, -22≤k≤22, -24≤l≤24		
Reflections collected	51564		
Independent reflections	20495 [R(int) = 0.0344]		
Completeness to theta = 27.48 deg	96.8 %		
Absorption correction	Empirical		
Max. and min. transmission	0.9568 and 0.9389		
Refinement method	Full-matrix least-squares on F ²		
Data / restraints / parameters	20495 / 165 / 958		
Goodness-of-fit on F ²	1.020		
Final R indices [I>2sigma(I)]	R1 = 0.0560, wR2 = 0.1519		
R indices (all data)	R1 = 0.0779, wR2 = 0.1702		
Largest diff. peak and hole	1.466 and -0.819 e.Å ⁻³		

Table 2-5-8. Atomic coordinates ($\times 10^4$) and equivalent isotropic displacement parameters ($\text{\AA}^2 \times 10^3$) for compound **26**. U(eq) is defined as one third of the trace of the orthogonalized U^{ij} tensor.

	x	y	z	U(eq)
Si(1)	2420(1)	7374(1)	2420(1)	22(1)
Si(2)	1733(1)	7233(1)	3438(1)	21(1)
Si(3)	1359(1)	5851(1)	2534(1)	20(1)
Si(4)	1953(1)	3396(1)	2342(1)	24(1)
Si(5)	3066(1)	3657(1)	1658(1)	24(1)
Si(6)	2794(1)	4955(1)	2093(1)	21(1)
Si(7)	2969(1)	8652(2)	2030(1)	24(1)
Si(7)	3018(2)	8414(2)	1801(2)	27(1)
Si(8)	2986(1)	7796(1)	4616(1)	30(1)
Si(9)	345(1)	7534(1)	3262(1)	28(1)
Si(10)	1324(1)	2210(1)	2818(1)	29(1)
Si(11)	4650(1)	3874(1)	2240(1)	33(1)
Si(12)	2292(1)	2913(1)	283(1)	25(1)
N(1)	2551(1)	5671(1)	1611(1)	21(1)
N(2)	1238(1)	4814(1)	2630(1)	22(1)
C(1)	2282(2)	6253(2)	2100(1)	21(1)
C(2)	1808(2)	4400(2)	2405(1)	22(1)
C(3)	2747(3)	9529(3)	2681(3)	38(1)
C(4)	4253(2)	9030(3)	2229(3)	34(1)
C(5)	4544(4)	8307(3)	1854(4)	53(2)
C(6)	4680(8)	9325(8)	3101(5)	50(4)
C(7)	4637(4)	9813(3)	1964(4)	47(1)
C(8)	2328(4)	8496(4)	1001(2)	31(2)
C(9)	2672(4)	8008(3)	398(3)	40(1)
C(10)	1321(5)	7964(5)	832(6)	43(2)
C(11)	2422(5)	9379(4)	898(4)	49(2)
C(3)	3672(4)	7992(4)	1189(4)	40(2)
C(4)	3879(4)	9464(3)	2578(3)	41(2)
C(5)	3470(6)	9863(5)	3172(4)	52(2)
C(6)	4290(7)	10140(5)	2210(5)	63(3)
C(7)	4620(12)	9217(14)	2977(9)	53(5)
C(8)	2072(4)	8547(5)	1120(3)	33(2)
C(9)	1666(5)	9158(4)	1531(4)	41(2)
C(10)	2422(6)	8893(6)	508(5)	50(2)
C(11)	1333(7)	7643(5)	715(7)	37(2)
C(12)	3648(2)	8961(2)	4708(2)	41(1)

C(13)	3808(2)	7202(2)	4559(2)	36(1)
C(14)	4321(2)	7399(2)	3969(2)	42(1)
C(15)	3315(2)	6218(2)	4351(2)	43(1)
C(16)	4535(2)	7532(2)	5341(2)	52(1)
C(17)	2608(2)	7869(2)	5540(2)	35(1)
C(18)	2333(3)	7035(2)	5733(2)	66(1)
C(19)	3349(2)	8586(2)	6243(2)	47(1)
C(20)	1804(2)	8159(3)	5437(2)	56(1)
C(21)	82(2)	7408(2)	2207(2)	42(1)
C(22)	-691(2)	6682(2)	3367(2)	30(1)
C(23)	-986(2)	5817(2)	2719(2)	37(1)
C(24)	-513(2)	6519(2)	4138(2)	38(1)
C(25)	-1506(2)	6963(2)	3274(2)	42(1)
C(26)	481(2)	8711(2)	3796(2)	48(1)
C(27)	246(3)	8861(2)	4564(2)	64(1)
C(28)	-144(3)	8988(3)	3269(3)	70(1)
C(29)	1460(3)	9317(2)	3931(3)	74(1)
C(30)	1665(2)	1313(2)	2328(2)	42(1)
C(31)	29(2)	1706(2)	2569(2)	33(1)
C(32)	-405(2)	1586(2)	1726(2)	38(1)
C(33)	-283(2)	796(2)	2656(2)	46(1)
C(34)	-344(2)	2261(2)	3085(2)	38(1)
C(35)	1918(2)	2601(2)	3904(2)	36(1)
C(36)	1493(3)	1956(2)	4301(2)	49(1)
C(37)	1906(2)	3492(2)	4311(2)	43(1)
C(38)	2900(2)	2690(3)	4014(2)	52(1)
C(39)	5390(2)	4302(2)	1645(2)	45(1)
C(40)	5195(2)	4739(2)	3259(2)	40(1)
C(41)	6068(2)	4670(3)	3677(2)	58(1)
C(42)	4570(2)	4657(2)	3777(2)	44(1)
C(43)	5461(2)	5652(2)	3195(2)	45(1)
C(44)	4747(2)	2776(2)	2210(2)	41(1)
C(45)	4254(3)	2136(3)	1398(2)	63(1)
C(46)	5714(3)	2804(3)	2382(2)	62(1)
C(47)	4302(3)	2428(3)	2773(2)	56(1)
C(48)	1493(2)	3475(2)	102(2)	29(1)
C(49)	3049(2)	3125(2)	-384(2)	29(1)
C(50)	3727(2)	4063(2)	-37(2)	37(1)
C(51)	2495(2)	3042(2)	-1182(2)	36(1)
C(52)	3557(2)	2507(2)	-509(2)	36(1)
C(53)	1536(2)	1696(2)	4(2)	31(1)

C(54)	1097(2)	1296(2)	-870(2)	42(1)
C(55)	2001(2)	1124(2)	260(2)	46(1)
C(56)	767(2)	1639(2)	382(2)	37(1)
C(57)	2777(2)	5830(2)	943(1)	22(1)
C(58)	2072(2)	5690(2)	302(1)	23(1)
C(59)	2277(2)	5796(2)	-368(2)	28(1)
C(60)	3161(2)	6045(2)	-404(2)	32(1)
C(61)	3848(2)	6194(2)	232(2)	32(1)
C(62)	3670(2)	6086(2)	908(2)	27(1)
C(63)	1107(2)	5412(2)	318(2)	27(1)
C(64)	4431(2)	6226(2)	1583(2)	32(1)
C(65)	357(2)	4352(2)	2689(1)	23(1)
C(66)	-350(2)	3837(2)	2013(2)	26(1)
C(67)	-1227(2)	3496(2)	2067(2)	31(1)
C(68)	-1404(2)	3670(2)	2773(2)	36(1)
C(69)	-702(2)	4176(2)	3434(2)	33(1)
C(70)	186(2)	4526(2)	3408(2)	27(1)
C(71)	-193(2)	3669(2)	1235(1)	28(1)
C(72)	932(2)	5087(2)	4130(2)	32(1)
O(81)	2845(3)	442(2)	5983(3)	116(1)
C(82)	2463(5)	529(4)	6583(4)	133(3)
C(83)	2920(4)	1436(3)	7130(3)	112(2)
C(84)	3375(5)	1922(4)	6640(4)	121(2)
C(85)	3062(5)	1231(3)	5878(4)	120(2)
O(86)	7133(4)	707(4)	1898(4)	172(2)
C(87)	6905(4)	1180(4)	1469(3)	87(2)
C(88)	6064(4)	717(4)	786(4)	144(3)
C(89)	6118(4)	-213(4)	620(4)	112(2)
C(90)	6868(4)	-19(4)	1307(3)	113(2)

Table 2-5-9. Bond lengths [Å] and angles [deg] for compound **26**.

Si(1)-C(1)	1.793(2)	Si(12)-C(53)	1.939(3)
Si(1)-Si(2)	2.4087(9)	N(1)-C(1)	1.414(3)
Si(1)-Si(7)	2.416(3)	N(1)-C(57)	1.433(3)
Si(1)-Si(7)	2.440(2)	N(2)-C(2)	1.400(3)
Si(2)-Si(3)	2.3625(9)	N(2)-C(65)	1.445(3)
Si(2)-Si(8)	2.4475(10)	C(4)-C(5)	1.524(5)
Si(2)-Si(9)	2.4556(10)	C(4)-C(6)	1.533(7)
Si(3)-N(2)	1.787(2)	C(4)-C(7)	1.536(5)
Si(3)-C(1)	1.866(2)	C(8)-C(9)	1.534(5)
Si(3)-H(3)	1.4750	C(8)-C(10)	1.533(6)
Si(4)-C(2)	1.789(2)	C(8)-C(11)	1.537(6)
Si(4)-Si(5)	2.4037(10)	C(4)-C(5)	1.529(6)
Si(4)-Si(10)	2.4328(10)	C(4)-C(7)	1.528(7)
Si(5)-Si(6)	2.3819(9)	C(4)-C(6)	1.532(6)
Si(5)-Si(12)	2.4485(10)	C(8)-C(11)	1.529(6)
Si(5)-Si(11)	2.4766(10)	C(8)-C(9)	1.534(6)
Si(6)-N(1)	1.789(2)	C(8)-C(10)	1.536(6)
Si(6)-C(2)	1.870(2)	C(13)-C(15)	1.534(4)
Si(6)-H(6)	1.4750	C(13)-C(16)	1.545(4)
Si(7)-C(3)	1.867(5)	C(13)-C(14)	1.546(4)
Si(7)-C(4)	1.917(4)	C(17)-C(18)	1.516(4)
Si(7)-C(8)	1.921(4)	C(17)-C(20)	1.536(5)
Si(7)-C(3)	1.872(7)	C(17)-C(19)	1.542(4)
Si(7)-C(4)	1.919(4)	C(22)-C(24)	1.529(4)
Si(7)-C(8)	1.920(4)	C(22)-C(23)	1.533(4)
Si(8)-C(12)	1.896(3)	C(22)-C(25)	1.545(4)
Si(8)-C(13)	1.925(3)	C(26)-C(27)	1.538(5)
Si(8)-C(17)	1.930(3)	C(26)-C(28)	1.548(5)
Si(9)-C(21)	1.884(3)	C(26)-C(29)	1.540(5)
Si(9)-C(22)	1.935(3)	C(31)-C(34)	1.528(4)
Si(9)-C(26)	1.940(3)	C(31)-C(32)	1.538(4)
Si(10)-C(30)	1.883(3)	C(31)-C(33)	1.543(4)
Si(10)-C(35)	1.924(3)	C(35)-C(38)	1.528(5)
Si(10)-C(31)	1.926(3)	C(35)-C(37)	1.538(4)
Si(11)-C(39)	1.894(3)	C(35)-C(36)	1.542(4)
Si(11)-C(44)	1.927(3)	C(40)-C(43)	1.531(5)
Si(11)-C(40)	1.942(3)	C(40)-C(42)	1.531(4)
Si(12)-C(48)	1.876(3)	C(40)-C(41)	1.545(4)
Si(12)-C(49)	1.934(3)	C(44)-C(47)	1.524(5)

C(44)-C(45)	1.525(5)	Si(7)-Si(1)-Si(7)	12.99(5)
C(44)-C(46)	1.532(4)	Si(3)-Si(2)-Si(1)	69.72(3)
C(49)-C(50)	1.527(4)	Si(3)-Si(2)-Si(8)	120.95(4)
C(49)-C(51)	1.541(4)	Si(1)-Si(2)-Si(8)	105.68(4)
C(49)-C(52)	1.539(4)	Si(3)-Si(2)-Si(9)	106.04(3)
C(53)-C(55)	1.527(4)	Si(1)-Si(2)-Si(9)	112.52(3)
C(53)-C(54)	1.537(4)	Si(8)-Si(2)-Si(9)	127.15(4)
C(53)-C(56)	1.539(4)	N(2)-Si(3)-C(1)	112.21(10)
C(57)-C(62)	1.403(3)	N(2)-Si(3)-Si(2)	132.73(7)
C(57)-C(58)	1.409(3)	C(1)-Si(3)-Si(2)	93.51(8)
C(58)-C(59)	1.397(3)	C(2)-Si(4)-Si(5)	94.23(8)
C(58)-C(63)	1.502(3)	C(2)-Si(4)-Si(10)	133.79(8)
C(59)-C(60)	1.388(4)	Si(5)-Si(4)-Si(10)	131.92(4)
C(60)-C(61)	1.382(4)	Si(6)-Si(5)-Si(4)	71.43(3)
C(61)-C(62)	1.393(4)	Si(6)-Si(5)-Si(12)	110.29(3)
C(62)-C(64)	1.507(4)	Si(4)-Si(5)-Si(12)	107.76(4)
C(65)-C(70)	1.406(3)	Si(6)-Si(5)-Si(11)	111.45(4)
C(65)-C(66)	1.404(4)	Si(4)-Si(5)-Si(11)	121.64(4)
C(66)-C(67)	1.398(4)	Si(12)-Si(5)-Si(11)	122.69(4)
C(66)-C(71)	1.501(3)	N(1)-Si(6)-C(2)	110.66(10)
C(67)-C(68)	1.386(4)	N(1)-Si(6)-Si(5)	132.12(7)
C(68)-C(69)	1.382(4)	C(2)-Si(6)-Si(5)	92.86(8)
C(69)-C(70)	1.397(4)	C(3)-Si(7)-C(4)	106.7(2)
C(70)-C(72)	1.497(4)	C(3)-Si(7)-C(8)	106.3(2)
O(81)-C(85)	1.363(5)	C(4)-Si(7)-C(8)	114.5(3)
O(81)-C(82)	1.381(5)	C(3)-Si(7)-Si(1)	106.14(18)
C(82)-C(83)	1.493(6)	C(4)-Si(7)-Si(1)	109.28(16)
C(83)-C(84)	1.527(6)	C(8)-Si(7)-Si(1)	113.4(2)
C(84)-C(85)	1.488(6)	C(3)-Si(7)-C(4)	105.8(3)
O(86)-C(90)	1.328(6)	C(3)-Si(7)-C(8)	106.4(3)
O(86)-C(87)	1.357(6)	C(4)-Si(7)-C(8)	115.7(4)
C(87)-C(88)	1.518(6)	C(3)-Si(7)-Si(1)	108.6(2)
C(87)-C(90)	1.983(8)	C(4)-Si(7)-Si(1)	108.6(2)
C(88)-C(89)	1.581(6)	C(8)-Si(7)-Si(1)	111.5(3)
C(89)-C(90)	1.484(6)	C(12)-Si(8)-C(13)	106.38(15)
		C(12)-Si(8)-C(17)	105.29(13)
C(1)-Si(1)-Si(2)	93.90(8)	C(13)-Si(8)-C(17)	112.06(13)
C(1)-Si(1)-Si(7)	124.72(11)	C(12)-Si(8)-Si(2)	105.80(10)
Si(2)-Si(1)-Si(7)	141.20(9)	C(13)-Si(8)-Si(2)	112.83(9)
C(1)-Si(1)-Si(7)	137.71(10)	C(17)-Si(8)-Si(2)	113.70(10)
Si(2)-Si(1)-Si(7)	128.29(6)	C(21)-Si(9)-C(22)	105.49(14)

C(21)-Si(9)-C(26)	106.13(16)	C(9)-C(8)-C(10)	107.4(5)
C(22)-Si(9)-C(26)	111.66(13)	C(9)-C(8)-C(11)	108.7(4)
C(21)-Si(9)-Si(2)	99.90(10)	C(10)-C(8)-C(11)	107.9(5)
C(22)-Si(9)-Si(2)	115.88(8)	C(9)-C(8)-Si(7)	111.8(4)
C(26)-Si(9)-Si(2)	115.94(11)	C(10)-C(8)-Si(7)	110.3(5)
C(30)-Si(10)-C(35)	108.18(14)	C(11)-C(8)-Si(7)	110.7(4)
C(30)-Si(10)-C(31)	105.55(14)	C(5)-C(4)-C(7)	109.4(7)
C(35)-Si(10)-C(31)	113.22(13)	C(5)-C(4)-C(6)	108.7(6)
C(30)-Si(10)-Si(4)	105.31(10)	C(7)-C(4)-C(6)	109.3(8)
C(35)-Si(10)-Si(4)	107.31(10)	C(5)-C(4)-Si(7)	112.8(5)
C(31)-Si(10)-Si(4)	116.70(9)	C(7)-C(4)-Si(7)	106.1(9)
C(39)-Si(11)-C(44)	104.52(15)	C(6)-C(4)-Si(7)	110.4(5)
C(39)-Si(11)-C(40)	104.42(15)	C(11)-C(8)-C(9)	109.1(5)
C(44)-Si(11)-C(40)	112.78(13)	C(11)-C(8)-C(10)	108.5(6)
C(39)-Si(11)-Si(5)	110.39(10)	C(9)-C(8)-C(10)	108.3(5)
C(44)-Si(11)-Si(5)	110.35(10)	C(11)-C(8)-Si(7)	106.9(6)
C(40)-Si(11)-Si(5)	113.80(9)	C(9)-C(8)-Si(7)	113.7(5)
C(48)-Si(12)-C(49)	105.28(12)	C(10)-C(8)-Si(7)	110.3(5)
C(48)-Si(12)-C(53)	105.41(12)	C(15)-C(13)-C(16)	108.0(3)
C(49)-Si(12)-C(53)	112.68(12)	C(15)-C(13)-C(14)	110.2(3)
C(48)-Si(12)-Si(5)	101.85(9)	C(16)-C(13)-C(14)	106.1(3)
C(49)-Si(12)-Si(5)	114.60(9)	C(15)-C(13)-Si(8)	111.4(2)
C(53)-Si(12)-Si(5)	115.35(9)	C(16)-C(13)-Si(8)	110.4(2)
C(1)-N(1)-C(57)	120.55(19)	C(14)-C(13)-Si(8)	110.6(2)
C(1)-N(1)-Si(6)	108.58(15)	C(18)-C(17)-C(20)	108.9(3)
C(57)-N(1)-Si(6)	129.24(16)	C(18)-C(17)-C(19)	108.1(3)
C(2)-N(2)-C(65)	123.08(19)	C(20)-C(17)-C(19)	105.8(3)
C(2)-N(2)-Si(3)	120.68(16)	C(18)-C(17)-Si(8)	115.4(2)
C(65)-N(2)-Si(3)	112.76(15)	C(20)-C(17)-Si(8)	107.2(2)
N(1)-C(1)-Si(1)	141.78(18)	C(19)-C(17)-Si(8)	111.1(2)
N(1)-C(1)-Si(3)	121.27(17)	C(24)-C(22)-C(23)	108.5(2)
Si(1)-C(1)-Si(3)	96.35(11)	C(24)-C(22)-C(25)	108.4(2)
N(2)-C(2)-Si(4)	138.82(18)	C(23)-C(22)-C(25)	105.9(2)
N(2)-C(2)-Si(6)	121.57(17)	C(24)-C(22)-Si(9)	113.3(2)
Si(4)-C(2)-Si(6)	99.54(12)	C(23)-C(22)-Si(9)	109.75(18)
C(5)-C(4)-C(6)	107.8(5)	C(25)-C(22)-Si(9)	110.74(19)
C(5)-C(4)-C(7)	109.3(4)	C(27)-C(26)-C(28)	106.3(3)
C(6)-C(4)-C(7)	107.1(5)	C(27)-C(26)-C(29)	109.3(3)
C(5)-C(4)-Si(7)	112.4(3)	C(28)-C(26)-C(29)	107.6(3)
C(6)-C(4)-Si(7)	108.3(5)	C(27)-C(26)-Si(9)	116.4(2)
C(7)-C(4)-Si(7)	111.8(3)	C(28)-C(26)-Si(9)	108.8(3)

C(29)-C(26)-Si(9)	108.1(2)	C(59)-C(58)-C(63)	119.5(2)
C(34)-C(31)-C(32)	108.6(2)	C(57)-C(58)-C(63)	121.5(2)
C(34)-C(31)-C(33)	107.8(2)	C(60)-C(59)-C(58)	120.9(2)
C(32)-C(31)-C(33)	106.8(2)	C(61)-C(60)-C(59)	119.6(2)
C(34)-C(31)-Si(10)	112.4(2)	C(60)-C(61)-C(62)	121.3(2)
C(32)-C(31)-Si(10)	110.33(19)	C(61)-C(62)-C(57)	119.1(2)
C(33)-C(31)-Si(10)	110.7(2)	C(61)-C(62)-C(64)	120.0(2)
C(38)-C(35)-C(37)	108.3(3)	C(57)-C(62)-C(64)	120.9(2)
C(38)-C(35)-C(36)	107.4(3)	C(70)-C(65)-C(66)	120.5(2)
C(37)-C(35)-C(36)	108.6(2)	C(70)-C(65)-N(2)	119.5(2)
C(38)-C(35)-Si(10)	108.4(2)	C(66)-C(65)-N(2)	119.3(2)
C(37)-C(35)-Si(10)	111.3(2)	C(67)-C(66)-C(65)	119.0(2)
C(36)-C(35)-Si(10)	112.7(2)	C(67)-C(66)-C(71)	119.2(2)
C(43)-C(40)-C(42)	108.4(3)	C(65)-C(66)-C(71)	121.7(2)
C(43)-C(40)-C(41)	106.8(3)	C(68)-C(67)-C(66)	120.9(3)
C(42)-C(40)-C(41)	107.3(3)	C(67)-C(68)-C(69)	119.6(2)
C(43)-C(40)-Si(11)	109.9(2)	C(68)-C(69)-C(70)	121.5(2)
C(42)-C(40)-Si(11)	113.1(2)	C(69)-C(70)-C(65)	118.5(2)
C(41)-C(40)-Si(11)	111.1(2)	C(69)-C(70)-C(72)	120.5(2)
C(47)-C(44)-C(45)	108.8(3)	C(65)-C(70)-C(72)	121.0(2)
C(47)-C(44)-C(46)	109.0(3)	C(85)-O(81)-C(82)	104.1(5)
C(45)-C(44)-C(46)	106.1(3)	O(81)-C(82)-C(83)	109.3(5)
C(47)-C(44)-Si(11)	109.8(2)	C(82)-C(83)-C(84)	102.1(5)
C(45)-C(44)-Si(11)	108.3(2)	C(85)-C(84)-C(83)	102.4(5)
C(46)-C(44)-Si(11)	114.6(3)	O(81)-C(85)-C(84)	109.0(5)
C(50)-C(49)-C(51)	106.2(2)	C(90)-O(86)-C(87)	95.2(6)
C(50)-C(49)-C(52)	109.5(2)	O(86)-C(87)-C(88)	117.5(5)
C(51)-C(49)-C(52)	107.7(2)	O(86)-C(87)-C(90)	41.8(3)
C(50)-C(49)-Si(12)	108.44(18)	C(88)-C(87)-C(90)	82.3(4)
C(51)-C(49)-Si(12)	111.31(18)	C(87)-C(88)-C(89)	96.1(4)
C(52)-C(49)-Si(12)	113.46(19)	C(90)-C(89)-C(88)	98.9(5)
C(55)-C(53)-C(54)	108.1(2)	O(86)-C(90)-C(89)	120.4(6)
C(55)-C(53)-C(56)	106.9(2)	O(86)-C(90)-C(87)	43.0(3)
C(54)-C(53)-C(56)	107.1(2)	C(89)-C(90)-C(87)	82.0(4)
C(55)-C(53)-Si(12)	115.8(2)		
C(54)-C(53)-Si(12)	110.66(19)		
C(56)-C(53)-Si(12)	107.82(18)		
C(62)-C(57)-C(58)	120.1(2)		
C(62)-C(57)-N(1)	121.4(2)		
C(58)-C(57)-N(1)	118.4(2)		
C(59)-C(58)-C(57)	119.0(2)		

Symmetry transformations used to generate equivalent atoms:

References

- 1) R. West, M. J. Fink, J. Michl, *Science* **1981**, *214*, 1343.
- 2) A. G. Brook, F. Abdesaken, B. Gutekunst, G. Gutekunst, R. K. Kallury, *J. Chem. Soc., Chem. Commun.* **1981**, 191
- 3) For reviews on heavier Group 14 elements, see: (a) The Chemistry of Organic Silicon Compounds, S. Patai and Z. Rappoport, Eds.; John Wiley & Sons Ltd.: 1989. (b) The Chemistry of Organic Silicon Compounds, Volume 2, Z. Rappoport and Y. Apeloig, Eds.; John Wiley & Sons Ltd.: 1998. (c) The Chemistry of Organic Silicon Compounds, Z. Rappoport and Y. Apeloig, Eds.; John Wiley & Sons Ltd.: 2001. (d) Organometallic Compounds of Low-Coordinate Si, Ge, Sn and Pb, V. Ya. Lee and A. Sekiguchi, Eds.; John Wiley & Sons Ltd.: 2010.
- 4) For reviews on disilenes, see: (a) R. West, *Angew. Chem. Int. Ed. Engl.* **1987**, *26*, 1201. (b) J. Barrau, J. Escudie, and J. Satge, *Chem. Rev.* **1990**, *90*, 283. (c) T. Tsumuraya, S. A. Batcheller, and S. Masamune, *Angew. Chem. Int. Ed. Engl.* **1991**, *30*, 902. (d) R. Okazaki and R. West, *Adv. Organomet. Chem.* **1996**, *39*, 231. (e) G. Raabe and J. Michl, in The Chemistry of Organic Silicon Compounds, Volume 1, Part 2, Z. Rappoport, Y. Apeloig, Eds. John Wiley & Sons Ltd. 1989, Chap 17. (f) H. Sakurai, in The Chemistry of Organic Silicon Compounds, Volume 2, Part 1, Z. Rappoport, Y. Apeloig, Eds. John Wiley & Sons Ltd. 1998, Chap 15. (g) T. L. Morkin, T. R. Owens, and W. J. Leigh, in The Chemistry of Organic Silicon Compounds, Volume 3, Z. Rappoport, Y. Apeloig, Eds. John Wiley & Sons Ltd. 2001, Chap 17.
- 5) M. Ichinohe, T. Matsuno, A. Sekiguchi, *Angew. Chem., Int. Ed.* **1999**, *38*, 2194.
- 6) (a) A. Sekiguchi, T. Matsuno, M. Ichinohe, *J. Am. Chem. Soc.* **2000**, *122*, 11250; (b) M. Ichinohe, M. Igarashi, K. Sanuki, A. Sekiguchi, *J. Am. Chem. Soc.* **2005**, *127*, 9978.
- 7) (a) V. Ya. Lee, S. Miyazaki, H. Yasuda, and A. Sekiguchi, *J. Am. Chem. Soc.* **2008**, *130*, 2758; (b) V. Ya. Lee, O. A. Gapurenko, S. Miyazaki, A. Sekiguchi, R. M. Minyaev, V. I. Minkin, and H. Gornitzka, *Angew. Chem., Int. Ed.* **2015**, *127*, 14324
- 8) In the carbon chemistry, for example M. Nakamoto, Y. Inagaki, M. Nishina, A. Sekiguchi, *J. Am. Chem. Soc.* **2009**, *131*, 3172.
- 9) S. Masamune, Y. Kabe, S. Collins, *J. Am. Chem. Soc.* **1985**, *107*, 5552.
- 10) A. Rauk, T. S. Sorensen, F. Sun, *J. Am. Chem. Soc.* **1995**, *117*, 4506
- 11) M. J. Cowley, V. Huch, D. Scheschkewitz, *Chem. Eur. J.* **2014**, *20*, 9221.
- 12) Y. Apeloig, M. Karni, *J. Am. Chem. Soc.* **1984**, *106*, 6676.
- 13) I. Bejan, S. Inoue, M. Ichinohe, A. Sekiguchi, D. Scheschkewitz, *Chem. Eur. J.* **2008**, *14*, 7119.
- 14) (a) W. H. Atwell, D. R. Weyenberg, *J. Organomet. Chem.* **1966**, *5*, 594; (b) W. H. Atwell, D. R. Weyenberg, *J. Am.*

Chem. Soc. **1968**, *90*, 3438; (c) W. H. Atwell, D. R. Weyenberg, *Angew. Chem., Int. Ed.* **1969**, *8*, 469.

Chapter 3

**Reaction of Cyclotrisilene with Azides: Synthesis, Structure, and Properties of
Azatrisilabicyclo[1.1.0]butane and Amide-substituted Cyclotrisilene**

3-1. Summary

Cyclotrisilene reacted with trimethylsilylazide, giving azatrisilabicyclo[1.1.0]butane derivative, which was characterized by spectroscopic and crystallographic methods. On the other hand, the reaction of cyclotrisilene with metal azide MN_3 ($M = Na, K$) gave amide-substituted cyclotrisilene via formally metallonitrene insertion into $Si_{sp}^2-SiMe^tBu_2$ bond. Spectroscopic and structural characterization revealed the silylanion contribution of amide-substituted cyclotrisilene. When the alkali metal ion was separated by the solvation of THF or 222-cryptand, cation free anion was formed. Structural analysis and theoretical calculations revealed that *bent* allylanion form is dominantly contributed to molecular structure of cation free anion.

3-2. Introduction

Since the first isolation of disilene¹ and silene² in 1981, the chemistry of unsaturated silicon compounds have been well established.³ In particular, bicyclo[1.1.0]tetrasilane Si₄H₆ **I** and its derivatives are energetically studied compounds, because of the highly strained framework including non-classical banana bond.⁴ In addition to bicyclo[1.1.0]tetrasilane **I**, Si₄H₆ valence isomers, tetrasilacyclobutene **II**, cyclotrisilenes **III**, **IV**, and planar *trans*-isomer **V** are also attractive compounds in the view of the isomeric interplays. For example, per-silyl substituted bicyclo[1.1.0]tetrasilane (type **I**) reported by Kira et al. shows a reversible conversion toward tetrasilacyclobutene derivative (type **II**). In contrast, Sekiguchi et al. reported thermal conversions of Si₃X (X = CH₂, S) hybrid trisilabicyclo[1.1.0]butane derivatives (type **I**) toward cyclotrisilenes type **IV**.^{5,6} The author also describes the chemistry of iminotrisilabicyclo[1.1.0]butane (type **I**), prepared from cyclotrisilene⁷ and isocyanide, in chapter 1. While cyclohexyliminotrisilabicyclo[1.1.0]butane is thermally stable, *N*-arylimino derivative easily transforms to iminotrisilacyclobutene (type **II**) at room temperature. The isomeric behaviors of bicyclo[1.1.0]butane heavy analogues above suggest that the thermal stability of valence isomers (type **I**–**V**) depend on both the constituent elements and substituent in the framework.

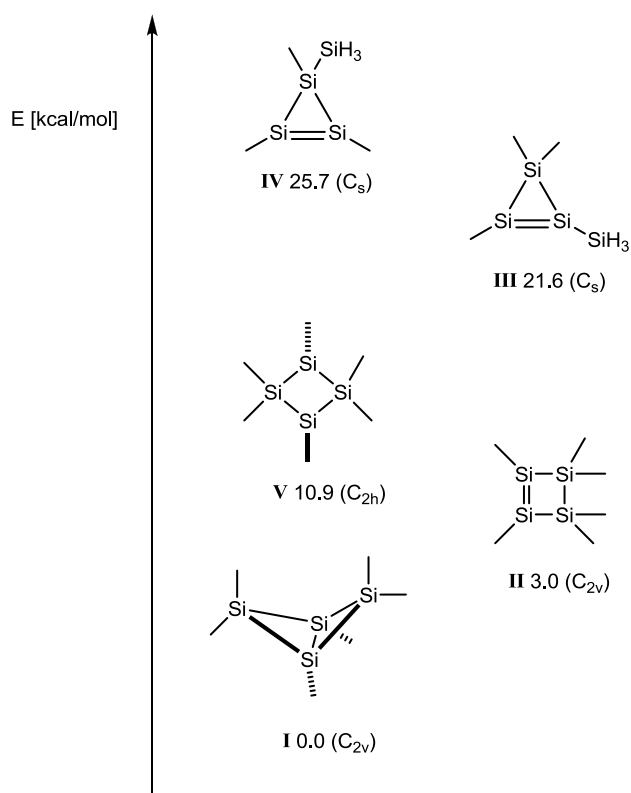
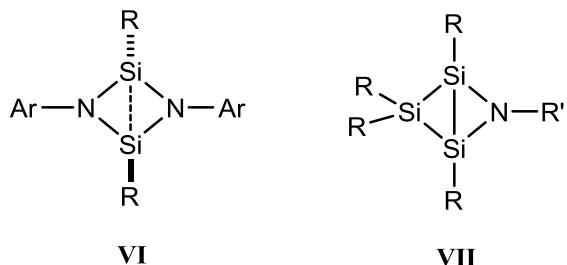


Chart. Relative energies of Si₄H₆ isomers.



Recently, Sekiguchi et al. reported Si_2N_2 biradicaloid **VI** by the reaction of silicon-silicon triple bonded disilyne $\text{RSi}\equiv\text{SiR}$ ⁸ ($\text{R} = \text{Si}^{\text{i}}\text{PrDsi}_2$) with azobenzenes $\text{ArN}=\text{NAr}$ ($\text{Ar} = \text{phenyl}, 3,5\text{-dimethylphenyl}$).⁹ Biradicaloid character of Si_2N_2 ring **VI** was clearly characterized by the reactivity toward both CCl_4 (radical abstraction of chlorine) and MeOH (polar addition) to the silicon centers. Introduction of N atoms into four-membered silicon ring would stabilize the biradicaloid structure of **VI** with the 6π aromatic ring.

Because biradicaloid **VI** has the perfectly planar centrosymmetric four-membered ring plane, one could regard **VI** as type **V** isomer ($\text{C}_{2\text{h}}$ symmetry). The structure and electronic property of Si_2N_2 four-membered ring **VI** encouraged the author to synthesis Si_3N trisilabicyclo[1.1.0]butane derivative **VII**. In this chapter, the author describes the reaction of cyclotrisilene with azides that is known as a divalent nitrene source, aiming formal [1 + 2]cycloaddition of nitrene with Si=Si double bond. In order to investigate the substituent effect of azide, the reaction with trimethylsilylazide and metal azide will be described

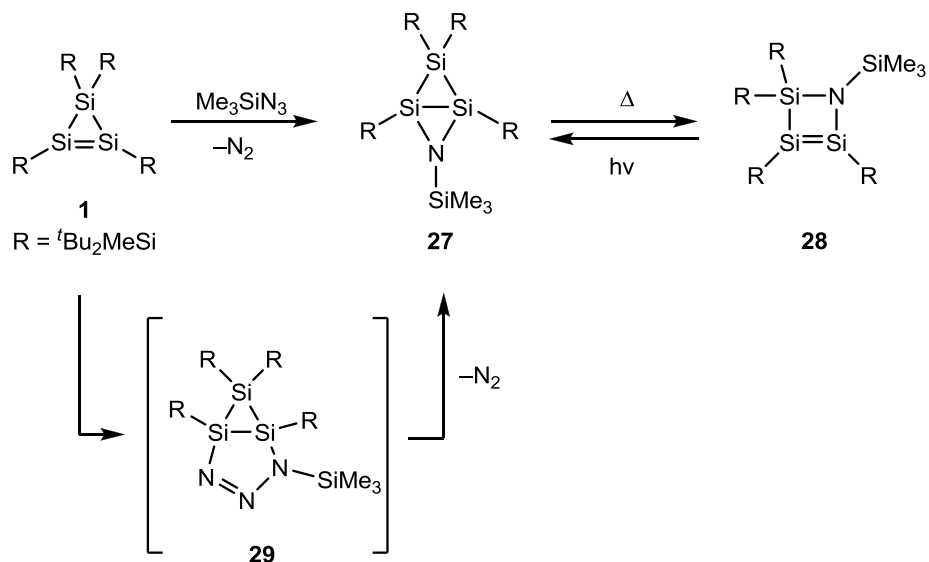
.

3-3. Result and Discussion

3-3-1. Reaction of Cyclotrisilene with Trimethylsilylazide

Cyclotrisilene **1** immediately reacted with trimethylsilylazide at -78°C to afford deep red solution of azatrisilabicyclo[1.1.0]butane derivative **27**, accompanied with N_2 elimination. Following recrystallization from pentane solution gave dark red crystals of **27** in 40% yields. Although azatrisilabicyclo[1.1.0]butane **27** is stable at room temperature, thermal reaction of **27** at 100°C gave azatrisilacyclobutene derivative **28**, as seen in the other silicon-based bicyclo[1.1.0]butanes (Scheme 3-3-1). Notably, azatrisilacyclobutene **28** could be reversely converted to **27** under photo irradiation. Similar thermal and photochemical conversion between bicyclo[1.1.0]butane and cyclobutene structure was previously reported by Kira's group.¹⁰

Scheme 3-3-1



The plausible reaction pathway to **27** begins by sila-Huisgen cycloaddition. Resulting [2 + 3]cycloadduct **29** would form additional Si–N bond with elimination of N_2 gas, leading to product **27**. Because this case is the first example of reactivity of Si=Si double bond toward azide, theoretical calculations using model compounds were performed to evaluate the reaction pathway (Figure 3-3-1). As expected, [2 + 3]cycloaddition process is greatly exothermic in spite of the highly strain of **Int 1**, due to the formation of two strong Si–N bonds by the cleavage of weak Si=Si π bond. The generation of azatrisilabicyclo[1.1.0]butane **27'** accompanied with N_2 elimination, as well as isomerization to cyclobutene **28'**, possess energetically reasonable values.

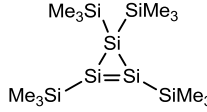
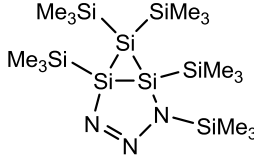
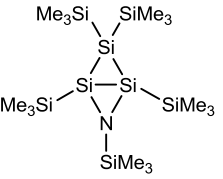
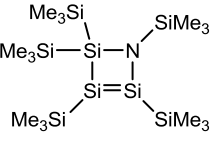
			
+ Me ₃ SiN ₃	Int 1	+ N ₂	+ N ₂
		27'	28'
Relative Energy (kcal/mol)	0.0	-44.0	-69.0
			-81.7

Figure 3-3-1. Relative energies of azatrisilabicyclo[1.1.0]butane, azatrisilabicyclo[1.1.0]butene and related compounds, using model compounds.

3-3-2. Structural Property of Azatrisilabicyclo[1.1.0]butane

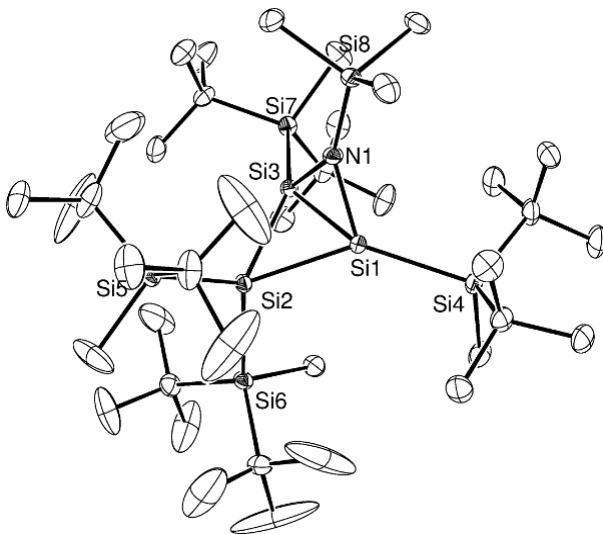


Figure 3-3-2. ORTEP drawing of azatrisilabicyclo[1.1.0]butane **27**. Selected structural parameters: Si1-Si2 2.4024(8) Å, Si1-Si3 2.2453(8) Å, Si2-Si3 2.3877(8) Å, Si1-N1 1.796(2) Å, Si3-N1 1.8128(19) Å, N1-Si1-Si3 51.86(6)°, N1-Si1-Si4 124.17(7)°, Si3-Si1-Si4 140.59(4)°, N1-Si1-Si2 92.88(7)°, Si3-Si1-Si2 61.72(3)°, Si4-Si1-Si2 142.94(3)°, N1-Si3-Si1 51.19(6)°, N1-Si3-Si2 92.94(7)°, Si1-Si3-Si2 62.38(3)°, N1-Si3-Si7 119.48(7)°, Si1-Si3-Si7 143.26(4)°, Si2-Si3-Si7 146.89(3)°.

The molecular structure of azatrisilabicyclo[1.1.0]butane **27** shown in Figure 3-3-2 has butterfly-type skeleton with greatly short bridge bond. The bridging Si1-Si3 bond (2.2453(8) Å) is the shortest one among the reported trisilabicyclo[1.1.0]butane derivatives (2.2616(19)–2.367(1) Å),^{5,6} and lies in the typical Si=Si double bond range (2.13–2.26 Å). The conformations around Si1 and Si3 atoms excluding a bridging bond are nearly trigonal planar with sum of the bonding angles 360.0° and 359.3° (ignoring bridge Si1-Si3 bond), indicating the high p character of Si1-Si3 bond. These structural characteristics can be recognized as the result of banana bond formation (Chart 3-3-1). In order to gain orbital overlap, Si1 and Si3 atoms approach closely keeping planar conformation. Then, the approximate Si1 and Si3 atom form banana bond with p orbitals, resulting very short bridge bond of **27**. Because similar short Si-Si bridge bond were previously reported in methylene bridged trisilabicyclo[1.1.0]butane derivative (2.2664(9) Å),⁵ the introduction of nitrogen atom into the trisilabicyclo[1.1.0]butane had only a small influence on the molecular structure of **27**.

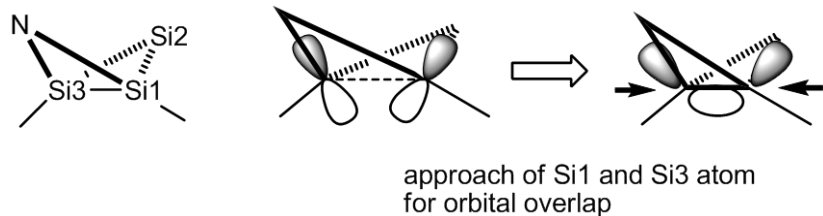


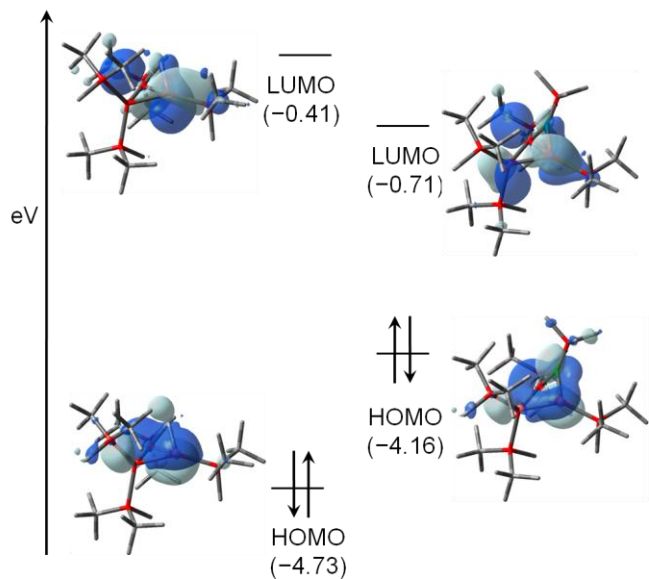
Chart 3-3-1. Short banana bond formation between Si1 and Si3 atom.

3-3-3. Spectroscopic Properties of Azatrisilabicyclo[1.1.0]butane

The ^{29}Si NMR spectrum of **27** exhibits four substitutional signals at -0.6 ppm (SiMe_3), 12.1 , 19.2 , and 28.9 ppm ($^t\text{Bu}_2\text{MeSi}$) and two skeletal signals at -75.8 ppm (Si1, Si3) and -12.3 ppm (Si2), respectively. The skeletal chemical shifts in high fields are typical for skeletal atoms of strained three-membered ring. The ^{29}Si chemical shifts of Si1 and Si3 atom are low field shifted than those of methylene bridged trisilabicyclo[1.1.0]butane (-132.3 ppm), due to the inductive effect of N1 atom.⁵

Notably, UV-Vis absorption spectrum of **27** reflected the influence of nitrogen atom. Thus, HOMO (σ bridge Si-Si) –LUMO (σ^* bridge Si-Si) transition of **27** (453 nm) is remarkably red-shifted than that of methylene bridged trisilabicyclo[1.1.0]butane (352 nm).

To investigate the detail of interaction between N atom and bridge Si1-Si3 bond, theoretical calculation was performed (Figure 3-3-3). HOMO (-4.73 eV) and LUMO (-0.41 eV) of methylene bridged trisilabicyclo[1.1.0]butane are composed of banana σ and σ^* orbital respectively. On the other hand, HOMO of **27'** (-4.16 eV) is formed by banana σ orbital and lone pair of N1 atom with anti-bonding interaction (also see φ_2 in Figure 3-3-4). LUMO of **27'** (-0.71 eV) is composed by mainly banana Si-Si σ^* orbital, with lower level than that of methylene bridged trisilabicyclo[1.1.0]butane, probably due to the electronegative N atom. Therefore, HOMO-LUMO gap of **27**, decreased by the interaction between nitrogen atom and Si1-Si3 banana bond, leads to the bathochromic shift of σ - σ^* absorption band.



($\text{R} = \text{tBu}_2\text{MeSi}$)



27'

Figure 3-3-3. Molecular orbitals of methylene bridged trisilabicyclo[1.1.0]butane derivative and azatrisilabicyclo[1.1.0]butane **27'** (calculated at B3LYP/6-31G(d) level).

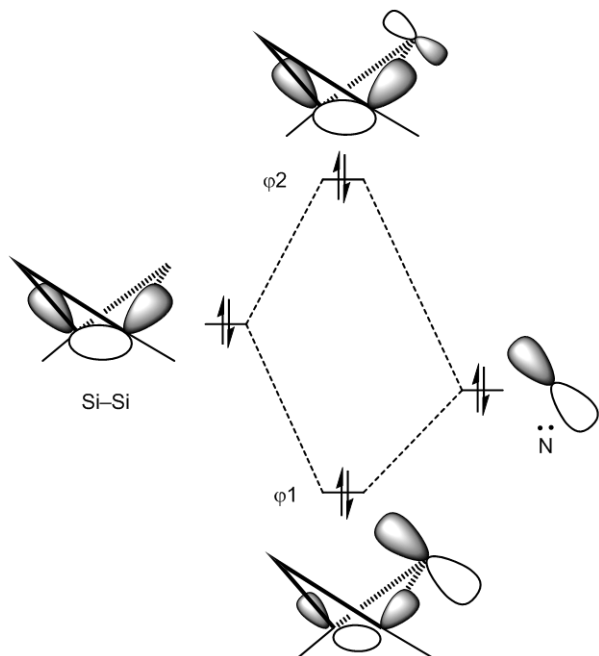
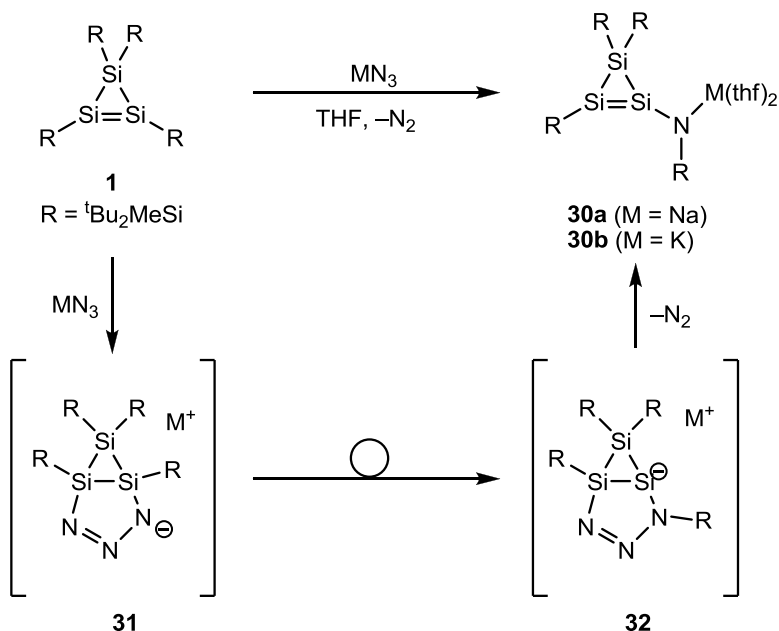


Figure 3-3-4. MO diagram of azatrisilabicyclo[1.1.0]butane **27**.

3-3-4. Reaction of Cyclotrisilene with Metal Azide

When cyclotrisilene was treated with metal azide MN_3 ($M = Na, K$) in THF, amide-substituted cyclotrisilene **30** was obtained. Compound **30** was isolated by recrystallization from toluene solution [**30a** ($M = Na$) y. = 20%; **30b** ($M = K$) y. = 19%]. The reaction in non-polar solvent (e.g. hexane, benzene and toluene) failed due to the insolubility of inorganic azide salts. Following azide addition to amide-substituted cyclotrisilene **30** was not observed when an excess amount of azide was used.

Scheme 3-3-2



Considerable reaction path way is shown in Scheme 3-3-2. As seen in the reaction of **1** with trimethylsilylazide, [2 + 3]cycloaddition between $\text{Si}=\text{Si}$ double bond and metal azide is the first step. Compared with trimethylsilylazide case, the following silyl group migration to nitrogen atom gives silylanion intermediate **32**.¹¹ Use of polar solvent would produce a solvent separated ion pair **31**, which then undergo the migration of the silyl group to the negative charged nitrogen atom. Then, an elimination of N_2 gas regenerates cyclotrisilene skeleton, giving product **30**.

3-3-4. Molecular Structure of Amide-substituted Cyclotrisilene

The molecular structure of **30a** was determined as contact ion pair, in which Na1 atom strongly binds to N1 atom (Na1-N1 2.322(3) Å) with coordination from two THF (Figure 3-3-5). The three-membered ring skeleton has a scalene triangle structure (Si1-Si3 2.3827(6) Å, Si2-Si3 2.3232(6) Å), reflecting the different substitutions on Si1 and Si2 atom. Si1-Si2 bond length (2.1629(6) Å) is slightly greater than that of **1** (2.138(2) Å), but within the typical Si=Si double bond length (2.13-2.26 Å). In contrast, Si2-N1 bond (1.6384(14) Å) is shortened compared with Si5-N1 bond (1.7046(15) Å) and typical Si-N single bond (1.748 Å), indicating some Si=N double bond character of Si2-N1 bond. Notably, Si1 atom is highly pyramidalized with the sum of the bonding angles 342.6° in spite of steric repulsion of bulky $^t\text{Bu}_2\text{MeSi}$ groups including Si4 and Si7 atom. The resulting repulsion between $^t\text{Bu}_2\text{MeSi}(4)$ and $^t\text{Bu}_2\text{MeSi}(7)$ groups lead distorted arrangement of two silyl groups on the saturated Si3 atom ($\angle\text{Si1-Si2-Si3-Si7} = \angle\text{Si2-Si1-Si3-Si6} = 113.4^\circ$). These structural characteristics suggest that the molecular structure of **30a** reflects the contribution of silylanion resonance form **B** due to the conjugation between Si=Si π -orbital and N1 lone pair (Chart 3-3-2).

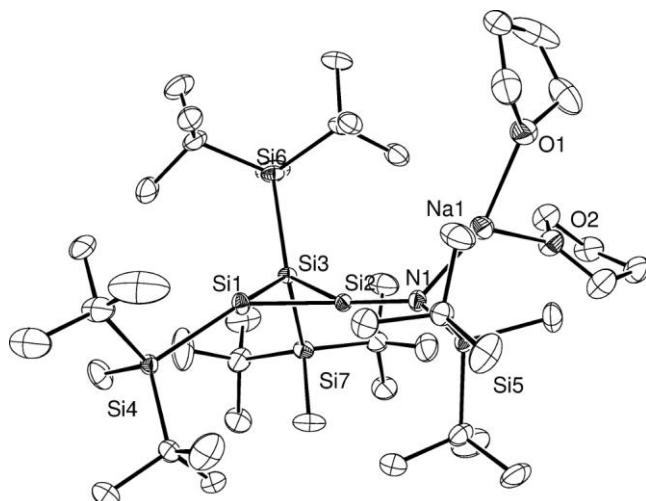


Figure 3-3-5. ORTEP drawing of sodium amide-substituted cyclotrisilene **30a**. Selected structural parameters: Si1-Si2 2.1629(6) Å, Si1-Si3 2.3827(6) Å, Si2-N1 1.6384(14) Å, Si2-Si3 2.3232(6) Å, Si5-N1 1.7046(15) Å, Na1-N1 2.3167(16) Å, Si2-Si1-Si4 145.20(3)°, Si2-Si1-Si3 61.249(19)°, Si4-Si1-Si3 136.14(3)°, N1-Si2-Si1 154.63(6)°, N1-Si2-Si3 139.47(6)°, Si1-Si2-Si3 64.05(2)°, Si2-Si3-Si1 54.705(18)°, Si2-N1-Si5 135.53(10)°, $\angle\text{Si1-Si2-Si3-Si7} = \angle\text{Si2-Si1-Si3-Si6} = 113.4^\circ$.

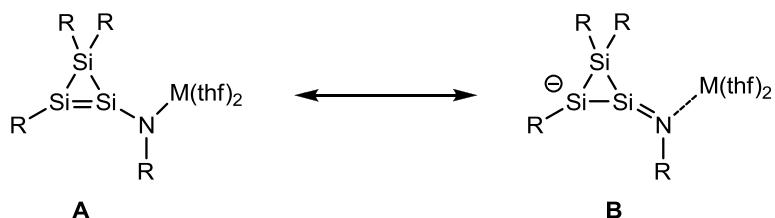


Chart 3-3-2. Resonance forms **A** and **B** of amide-substituted cyclotrisilene **30**.

3-3-5. NMR Spectroscopic Property of Amide-substituted Cyclotrisilene

The influence of the conjugation between lone pair of N1 atom and Si=Si π orbital is also significant in the NMR spectra (Table 3-3-1). In the ^{29}Si NMR spectrum of **30** in C_6D_6 , Si2 atom was observed at 96.7 ppm (**30a**) and 101.7 ppm (**30b**), which are very close to that of cyclotrisilene **1** (97.7 ppm). Similarly, the chemical shift of saturated Si3 skeletal silicon atom (-98.1 (**30a**), -98.9 (**30b**)) is close to that of **1** (-97.6 ppm). On the other hand, Si1 atoms were found in much higher region at -149.3 ppm (**30a**) and -153.5 ppm (**30b**). Such high-field chemical shift of Si1 is far from the typical sp^2 -silicon chemical shift region (50–170 ppm), indicating the great contribution of silylanion form **B** for the structure of **30**. Slightly higher field shift of Si1 atom of **30b** than that of **30a** is due to the ionic N-K bond, which should enhance the silylanion character in **30b**.

	30a	30b		
	C_6D_6	THF-d_8	C_6D_6	THF-d_8
Si1	-149.3	-179.7	-153.5	-179.6
Si2	96.7	123.8	101.7	123.6
Si3	-98.1	-132.3	-98.9	-132.1

Table 3-3-1. Selected NMR chemical shifts of amide-substituted cyclotrisilenes **30** in C_6D_6 and THF-d_8 (in ppm).

Interestingly, the NMR chemical shifts of **30** in THF-d_8 showed notable difference from those in C_6D_6 . Thus, Si1 atoms appeared at high field region -179.7 ppm (**30a**) and -179.6 (**30b**), which are comparable to silyllithium ($^t\text{Bu}_2\text{MeSi})_3\text{Li}$ (-185.0 ppm), while Si2 atoms were lower field shifted than those in C_6D_6 (123.8 ppm and 123.6 ppm respectively).¹² High field shift of Si1 atom as well as nearly same chemical shifts of **30a** and **30b** in THF-d_8 indicate the formation of solvent separated ion pair **33** in THF, which should have greater silylanion character **B** than contact ion pairs **30** (Scheme 3-3-3). It is also noted that, both in THF and C_6D_6 , the ^{29}Si chemical shifts of Si6 and Si7 atoms appeared as an equivalent signal. This result indicates the inversion at Si1 atoms occur at room temperature (Chart 3-3-3).¹³

Scheme 3-3-3

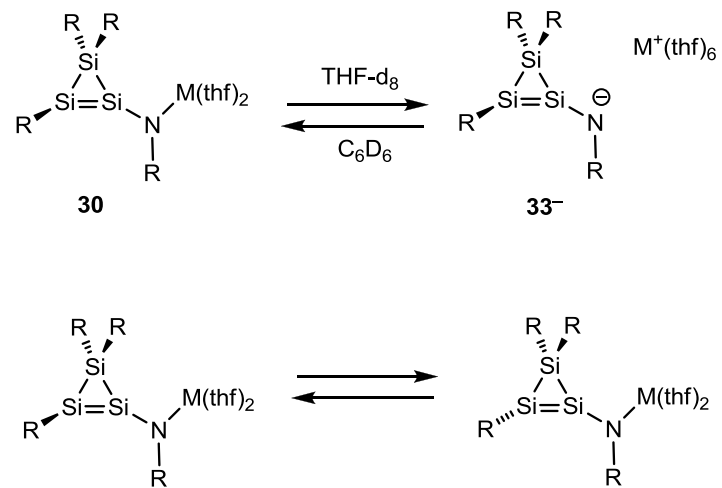


Chart 3-3-3. Inversion at Si1 atom.

3-3-5. Structural Property of Solvent Separated Ion Pair $\mathbf{33}^-$

To investigate the detail of the molecular structure of solvent separated ion pair $\mathbf{33}^-$, recrystallization from THF solution of **30** was performed. Indeed, preliminary analysis of the single crystals of **30a** grown in THF showed metal-free anionic cyclotrisilene moiety and solvent separated sodium ion coordinated by six THF molecules.

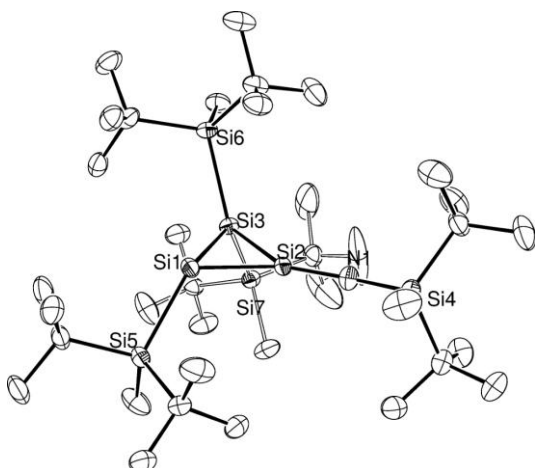


Figure 3-3-6. ORTEP drawing of solvent separated ion pair $\mathbf{33}^- \cdot [\text{K}^+(222\text{-cryptand})]$ (H atoms and cation moiety is omitted for clarity). Selected structural parameters: Si2-N1 1.593(2) Å, Si1-Si2 2.2109(9) Å, Si2-Si3 2.3123(9) Å, Si1-Si5 2.3681(9) Å, Si1-Si3 2.4465(9) Å, Si3-Si7 2.3734(9) Å, Si3-Si6 2.3778(9) Å, Si4-N1 1.663(2) Å, N1-Si2-Si1 156.61(11) °, N1-Si2-Si3 137.95(11)°, Si1-Si2-Si3 65.44(3)°, Si2-Si1-Si5 120.67(4)°, Si2-Si1-Si3 59.28(3)°, Si5-Si1-Si3 128.84(4)°, Si2-Si3-Si1 55.28(3)°, Si2-N1-Si4 158.62(19)°, $\angle \text{Si1-Si2-Si3-Si7}$ 120.5°, $\angle \text{Si2-Si1-Si3-Si6}$ 117.7°

Exact structural data of $\mathbf{33}^-$ was finally determined by using single crystal grown from diethyl ether solution of **30b** in the presence of 222-cryptand, known as a host molecule suitable for potassium ion (Figure 3-3-6). Distance between cationic potassium ion of $[\text{K}^+(222\text{-cryptand})]$ and anionic cyclotrisilene moiety is ca. 13 Å, showing that there is no interaction between them.

The molecular structure of anion part $\mathbf{33}^-$ pronounced the significant silyl anion character of resonance form **D** (Chart 3-3-3). The sum of the bonding angles around Si1 atom is 308.9°, which is remarkably smaller than that of **30a** (342.6°). Such pyramidalization is even comparable to that of $(\text{Me}_3\text{Si})_3\text{Si-Li}(\text{thf})_3$ [the sum of the bonding angle at Si = 308°(excluding Si-Li)].¹⁴ $^1\text{B}_2\text{MeSi}$ group including Si5 atom repulses another silyl group including Si7 atom, leading to the distorted arrangement at Si3 atom. As a result, Si1-Si3 (2.4465(9) Å) is greatly elongated than that of Si2-Si3 (2.3123(9) Å). Si1-Si2 bond (2.2109(9) Å) of $\mathbf{33}^-$ is longer than that of **30a** (2.1629(6) Å), while Si2-N1 bond (1.593(2)

\AA) is shortened (vs. 1.6384(14) \AA). These structural characteristics of 33^- (pyramidalization of Si1 atom, elongation of Si1-Si2 bond, and shortening of Si2-N1 bond) are consistent with the great contribution of resonance form **D**. The geometry at N1 atom shows a near linear arrangement with a bond angle of Si2-N1-Si4 158.62(19) $^\circ$, which is typical for *N*-silylsilaimines (for example, Si=N-Si 177.8 $^\circ$ in $^t\text{Bu}_2\text{Si}=\text{NSi}^t\text{Bu}_3$). This is in good agreement with the Si=N double bond character in **D**.¹⁵

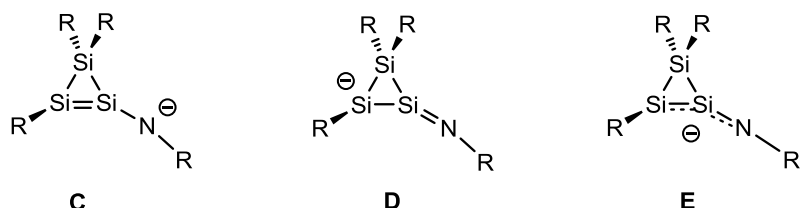
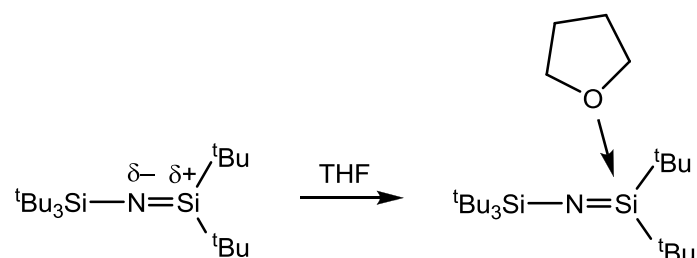


Chart 3-3-4. Plausible descriptions for 33^- , localized disil enylamide **C**, silaiminosilylanion **D** and delocalized *bent* allyl anion **E**.

However, Si1-Si2 bond is still much shorter than other Si-Si single bonds in 33^- (2.3123(9)– 2.4465(9) \AA) and lies within the typical Si=Si double bond range (2.13–2.26 \AA). Likewise, Si2-N1 bond is still longer than that of free silaimine $^t\text{Bu}_2\text{Si}=\text{NSi}^t\text{Bu}_3$ (1.568(3) \AA). Instead, the bond length of Si2-N1 lies in the donor stabilized silaimine region (1.596–1.611 \AA , Scheme 3-3-4). Such bonding properties suggest that 33^- should be described as *bent* allylanion **E** rather than the localized anion form **C** and **D**.

Scheme 3-3-4



3-3-6. Theoretical Calculations

To get insight of the structural property of 33^- , DFT calculations at B3LYP/6-31+G(d) level were performed. Optimized structures of contact ion pair $30\text{a}'$ and cation free anion 33^- reproduced the experimental data. HOMO of $30\text{a}'$ is composed of Si=Si π orbital with anti-bonding interaction from small N (n) orbital. The lone-pair of N atom is mainly located at HOMO-3, which is slightly expanded to Si2 atom (Figure 3-3-7). In contrast, a clear Si=N π interaction can be seen in HOMO-3 of 33^- . HOMO of 33^- is mainly formed by the p orbital of Si1 atom with slight π bonding interaction toward Si2 atom.

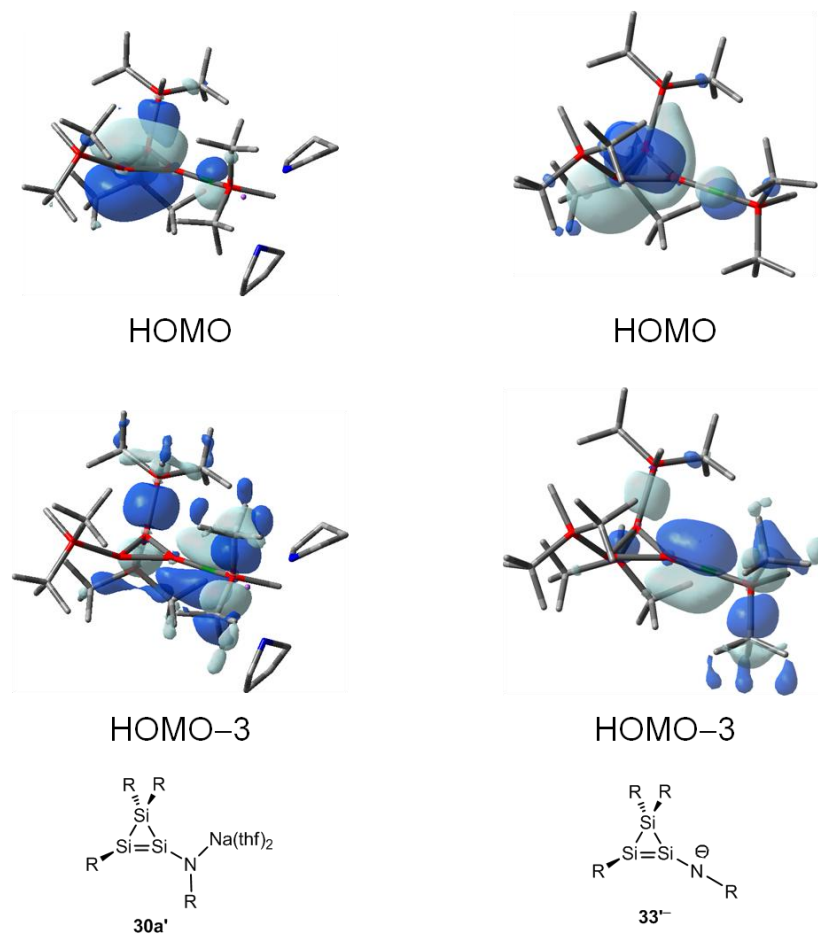


Figure 3-3-7. Molecular orbitals of optimized structure, amide-substituted cyclotrisilene $30\text{a}'$ and cation free anion 33^- .

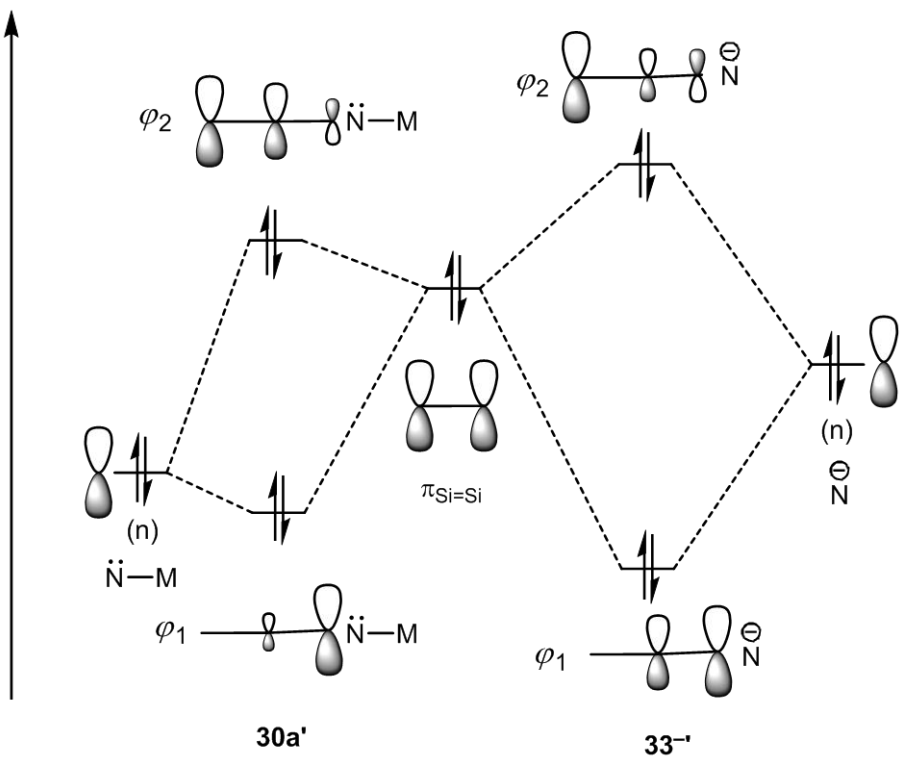


Figure 3-3-8. MO diagram of **30a'** and cation free anion **33⁻**.

The molecular orbitals of **30a'** and **33⁻** can be explained by the MO diagram in Figure 3-3-8. In this diagram, only simple interactions between Si=Si π orbital and non-bonding orbital on N atom are shown. Because the non-bonding orbital on N atom of **30a'** locates at much lower level than that of Si=Si π orbital, the energy splitting of the interaction should be small. Therefore, the bonding orbital (φ_1) is mainly composed by the lone-pair of N atom, while the Si=Si π orbital is dominant in anti-bonding orbital (φ_2). Drawings of φ_1 and φ_2 of **30a'** are consistent with the HOMO and HOMO-3 of **30a'** in Figure 3-3-6. In contrast, the energy level of anionic N atom of **33⁻** is much higher than that of **30a'**. Thus, the interaction between non-bonding orbital of N and Si=Si π orbital in **33⁻** is effective, accompanying with large orbital energy splitting. As a result, Si=Si π orbital of **33⁻**, especially internal Si2 atom close to nitrogen atom, contributes to bonding orbital (φ_1) of **33⁻**. Because Si-Si bond is much longer than Si-N bond, the contribution of terminal Si1 atom of **33⁻** to φ_1 is limited. Instead, Si1 is mainly contributed to the anti-bonding orbital (φ_2) of **33⁻**. Orbital coefficients of internal Si2 atom in φ_2 of **33⁻** are less for the contribution to φ_1 . In total, **33⁻** would have half π bond in the Si-Si-N fragment.

Finally, Wiberg Bond Index (WBI) of the model compound **33⁻** is investigated. The calculated values are 1.325 for Si1-Si2 and 1.082 for Si2-N1, respectively. Both values are less than those of corresponding double bonds (Si=Si in **1**: 1.817, Si=Si in **30a'**: 1.491, Si=N in $^t\text{Bu}_2\text{Si}=\text{NSi}^t\text{Bu}_3$: 1.368), but greater than single bonds (Si-Si single bond in **33⁻**: 0.895–0.951, Si-N2; 0.732). This result clearly suggests allyl-like delocalization of Si1-Si2-N1 fragment in **33⁻**.

3-4. Conclusion

In this chapter, the reaction of cyclotrisilene **1** with azide was performed. Reaction with trimethylsilylazide gave azatrisilabicyclo[1.1.0]butane **27** derivative as [1 + 2]cycloadduct with trimethylsilylnitrene. The molecular structure of **27** showed greatly short bridge Si-Si bond. On the other hand, reaction with metal azide MN_3 ($M = Na, K$) gave amide-substituted cyclotrisilene **30**, which was solvated to give cation free allylanion **33⁻** by THF or 222-cryptand. Structural and theoretical analysis revealed that the contact ion pair **30** had a Si=Si double bond conjugating with lone-pair on N atom, while cation free anion **33⁻** showed delocalized allylanion structure **E** with highly pyramidalized terminal Si1 atom.

3-5. Experimental Section

General Procedure. All experiments were performed using high-vacuum line techniques or in an argon atmosphere using MBRAUN MB 150B-G glove box. All solvents were dried and degassed over potassium mirror in vacuum prior to use. NMR spectra were recorded on Bruker AC-300FT NMR (¹H NMR at 300.1 MHz; ¹³C NMR at 75.5 MHz; ²⁹Si NMR at 59.6 MHz), AV-400FT NMR (¹H NMR at 400 MHz; ¹³C NMR at 100.6 MHz; ²⁹Si NMR at 79.5 MHz) spectrometers. High-resolution mass spectra were measured on Bruker Daltonics microTOF-TU mass spectrometer with APCI (atmospheric pressure chemical ionization method). UV-Vis spectra were recorded on Simadzu UV-3150 UV-Vis spectrophotometer. All computations were carried out using the Gaussian 03 and 98 suite of programs B3LYP level at 6-31G(d) and 6-31+G(d) basis set. Tetrakis[di-*tert*-butyl(methyl)silyl]cyclotrisilene **1** was prepared according to the published procedure.

Experimental	Procedure	and	Spectral	Data	of
1,2,2,3-tetrakis(di-<i>tert</i>-butylmethylsilyl)-4-trimethylsilylaza-1,2,3-trisilabicyclo[1.1.0]butane 27.					

Trimethylsilylazide (22.3 μ L, 19.6 mg, 0.17 mmol) was added to benzene solution of cyclotrisilene **1** (100 mg, 0.14 mmol) and then stirred for 1 hour. After the evaporation of solvent and excess azide, the residue was filtered in hexane. Recrystallization of resulting mixture in pentane at -30 °C gave air- and moisture sensitive dark red crystals of title compound **27**(45 mg, 0.056 mmol, 40% yields); mp = 171.2–172.0 °C; ¹H NMR (C₆D₆, δ) 0.40 (s, 9 H, NSiMe₃), 0.44 (s, 6 H, ^tBu₂MeSi x 2), 0.46 (s, 3 H, ^tBu₂MeSi), 0.64 (s, 3 H, ^tBu₂MeSi), 1.20 (s, 18 H, ^tBu₂MeSi), 1.22 (s, 18 H, ^tBu₂MeSi), 1.24 (s, 18 H, ^tBu₂MeSi), 1.28 (s, 18 H, ^tBu₂MeSi); ¹³C NMR (C₆D₆, δ) -3.1 (^tBu₂MeSi x 2), -2.4 (^tBu₂MeSi), -0.7 (^tBu₂MeSi), 5.9 (SiMe₃), 21.1 (CMe₃), 21.8 (CMe₃), 21.9 (CMe₃), 22.4 (CMe₃), 30.1 (CMe₃), 30.8 (CMe₃), 30.9 (CMe₃) 31.2 (CMe₃); ²⁹Si NMR (C₆D₆, δ) -75.8 (bridgehead Si x 2), -12.3 (SiSi₄), -0.6 (SiMe₃), 12.1 (^tBu₂MeSi), 19.2 (^tBu₂MeSi), 28.9 (^tBu₂MeSi x 2); HRMS: *m/z* calcd for C₃₉H₉₃NSi₈ M⁺ 799.5457, found 799.5451; UV/Vis (hexane): λ_{max} / nm (ϵ): 453 (2300).

The single crystals of **27** for X-ray diffraction analysis were grown from a pentane solution. Diffraction data were collected at 100 K on a Bruker AXS APEX II CCD X-ray diffractometer (Mo-K α radiation, l = 0.71073 Å, 50 kV, 600 μ A). The structure was solved by the direct method, using SHELXT program, and refined by the full-matrix least-squares method by SHELXL-97 program. Crystal data for **27** at 100 K: MF = C₃₈H₉₃NSi₈, MW = 800.86, monoclinic, space group P 1 21 /n 1, a = 11.9717(7) Å, b = 19.3345(11) Å, c = 22.1927(12) Å, β = 92.338(1) $^\circ$, V = 5132.6(5) Å³, Z = 4, D_{calcd} = 1.036 g/cm³, The final *R* factor was 0.0595 (*R*_w = 0.1409 for all data) for 10594 reflections with $I > 2\sigma(I)$, GOF = 1.042.

Experimental Procedure and Spectral Data of

1,2,3,3-tetrakis(di-*tert*-butylmethyldisilyl)-4-trimethylsilylaza-1,2,3-trisilacyclobutene 28.

Trimethylsilylazide (9.2 μ L, 10.5 mg, 0.07 mmol) was added to benzene solution of cyclotrisilene **1** (50 mg, 0.07 mmol) and then stirred for 1 hour. After the evaporation of solvent and excess azide, dried benzene was transferred and heated at 100 °C in the sealed reaction tube. After 10 hour heating, the resulting solid was recrystallized in pentane and gave air- and moisture sensitive dark red crystals of title compound (29 mg, 0.036 mmol, 51% yields).; mp = 168.5-169.0 °C; ^1H NMR (C_6D_6 , δ) 0.42 (s, 3 H, $^1\text{Bu}_2\text{MeSi}$), 0.46 (s, 3 H, $^1\text{Bu}_2\text{MeSi}$), 0.51 (s, 6 H, $^1\text{Bu}_2\text{MeSi} \times 2$), 0.54 (s, 9 H, NSiMe_3), 1.23 (s, 18 H, $^1\text{Bu}_2\text{MeSi}$), 1.28 (s, 18 H, $^1\text{Bu}_2\text{MeSi}$), 1.29 (s, 18 H, $^1\text{Bu}_2\text{MeSi}$), 1.33 (s, 18 H, $^1\text{Bu}_2\text{MeSi}$); ^{13}C NMR (C_6D_6 , δ) -3.6 ($^1\text{Bu}_2\text{MeSi}$), -3.0 ($^1\text{Bu}_2\text{MeSi}$), -1.3 ($^1\text{Bu}_2\text{MeSi} \times 2$), 6.9 (SiMe_3), 22.4 (CMe_3), 22.7 (CMe_3), 24.1 (CMe_3), 24.4 (CMe_3), 30.2 (CMe_3), 30.5 (CMe_3), 31.6 (CMe_3) 31.8 (CMe_3); ^{29}Si NMR (C_6D_6 , δ) 0.4 (NSiMe_3), 8.72 ($^1\text{Bu}_2\text{MeSi} \times 2$), 9.4 ($^1\text{Bu}_2\text{MeSi}$), 24.5 (SiSi_4), 25.6 ($^1\text{Bu}_2\text{MeSi}$), 66.1 (Si=Si-N), 165.9 (Si=Si-N); HRMS: m/z calcd for $\text{C}_{39}\text{H}_{94}\text{NSi}_8$ (M+H^+) 800.5535, found 800.5532; UV/Vis (hexane): λ_{max} / nm (ϵ): 477 (6300).

The single crystals of **28** for X-ray diffraction analysis were grown from a pentane solution. Diffraction data were collected at 100 K on a Bruker AXS APEX II CCD X-ray diffractometer (Mo- $K\alpha$ radiation, $l = 0.71073 \text{ \AA}$, 50 kV, 600 μA). The structure was solved by the direct method, using SHELXT program, and refined by the full-matrix least-squares method by SHELXL-97 program. Crystal data for **28** at 100 K: MF = $\text{C}_{39}\text{H}_{93}\text{NSi}_8$, MW = 800.86, monoclinic, space group C 1 c 1, $a = 11.3187(6) \text{ \AA}$, $b = 25.5654(13) \text{ \AA}$, $c = 18.4956(10) \text{ \AA}$, $\beta = 106.299(1)^\circ$, $V = 5136.9(5) \text{ \AA}^3$, $Z = 4$, $D_{\text{calcd}} = 1.036 \text{ g/cm}^3$, The final R factor was 0.0221 ($R_w = 0.0618$ for all data) for 11417 reflections with $I > 2\sigma(I)$, GOF = 1.039.

Experimental Procedure and Spectral Data of

1,3,3-tris(di-*tert*-butylmethyldisilyl)-2-[sodio(thf)₂](di-*tert*-butylsilyl)aminocyclotrisilene 30a

Sodium azide (7.0 mg, 0.11 mmol) was added to THF solution of cyclotrisilene **1** (80 mg, 0.11 mmol) and then stirred for 1 day. After the filtration and evaporation, the residue was recrystallized in toluene giving air- and moisture sensitive dark red crystals of title compound (20 mg, 0.022 mmol, 20% yields).; mp = 133.0-134.0 °C (dec); ^1H NMR (THF-d₈, δ) -0.09 (s, 3 H, $^1\text{Bu}_2\text{MeSi}$), 0.24 (s, 3 H, $^1\text{Bu}_2\text{MeSi}$), 0.27 (s, 6 H, $^1\text{Bu}_2\text{MeSi} \times 2$), 0.99 (s, 18 H, $^1\text{Bu}_2\text{MeSi}$), 1.07 (s, 18 H, $^1\text{Bu}_2\text{MeSi}$), 1.20 (s, 18 H, $^1\text{Bu}_2\text{MeSi}$), 1.25 (s, 18 H, $^1\text{Bu}_2\text{MeSi}$); ^{13}C NMR (THF-d₈, δ) -4.4 ($^1\text{Bu}_2\text{MeSi}$), -3.8 ($^1\text{Bu}_2\text{MeSi} \times 2$), -3.3 ($^1\text{Bu}_2\text{MeSi}$), 20.96 (CMe_3), 21.04 (CMe_3), 22.2 (CMe_3), 22.5 (CMe_3), 28.9 (CMe_3), 29.7 (CMe_3), 30.5 (CMe_3), 31.0 (CMe_3); ^{29}Si NMR (THF-d₈, δ) -179.7 (Si=Si-N), -132.3 (SiSi_4), -7.0 ($^1\text{Bu}_2\text{MeSi}$), 6.3 ($^1\text{Bu}_2\text{MeSi} \times 2$), 16.2 ($^1\text{Bu}_2\text{MeSi}$), 123.8 (Si=Si-N); ^1H NMR (C_6D_6 , δ) 0.10 (s, 3 H, $^1\text{Bu}_2\text{MeSi}$), 0.47 (s, 3 H, $^1\text{Bu}_2\text{MeSi}$), 0.54 (s, 6 H,

¹Bu₂MeSi x 2), 1.25 (s, 18 H, ¹Bu₂MeSi), 1.28 (s, 18 H, ¹Bu₂MeSi), 1.38 (s, 18 H, ¹Bu₂MeSi), 1.44 (s, 18 H, ¹Bu₂MeSi); ¹³C NMR (C₆D₆, δ) -4.3 (¹Bu₂MeSi), -3.7 (¹Bu₂MeSi x 2), -3.5 (2 x ¹Bu₂MeSi), 21.3 (2 x CMe₃), 21.4 (CMe₃), 22.3 (CMe₃), 29.1 (CMe₃), 29.8 (CMe₃) 30.7 (CMe₃) 30.9 (CMe₃); ²⁹Si NMR (C₆D₆, δ) -149.3 (Si=Si-N), -98.1 (SiSi₄), -0.9 (¹Bu₂MeSi), 3.7 (¹Bu₂MeSi x 2), 21.2 (¹Bu₂MeSi), 96.7 (Si=Si-N).

The single crystals of **30a** for X-ray diffraction analysis were grown from a pentane solution. Diffraction data were collected at 100 K on a Bruker AXS APEX II CCD X-ray diffractometer (Mo- $K\alpha$ radiation, $\lambda = 0.71073 \text{ \AA}$, 50 kV, 600 μA). The structure was solved by the direct method, using SHELXT program, and refined by the full-matrix least-squares method by SHELXL-97 program. Crystal data for **30a** at 100 K: MF = C₄₄H₁₀₀NNaO₂Si₇, MW = 894.87, orthorhombic, space group P n a 21, $a = 23.3860(12) \text{ \AA}$, $b = 12.7195(6) \text{ \AA}$, $c = 19.0584(10) \text{ \AA}$, $V = 5669.1(5) \text{ \AA}^3$, $Z = 4$, $D_{\text{calcd}} = 1.048 \text{ g/cm}^3$, the final R factor was 0.0317 ($R_w = 0.0837$ for all data) for 12580 reflections with $I > 2\sigma(I)$, GOF = 1.082.

Experimental	Procedure	and	Spectral	Data	of
1,3,3-tris(di-<i>tert</i>-butylmethylsilyl)-2-[potassio(thf)₂](di-<i>tert</i>-butylsilyl)aminocyclotrisilene 30b					

Potassium azide (22.7 mg, 0.28 mmol) was added to THF solution of cyclotrisilene **1** (200 mg, 0.28 mmol) and then stirred for 1 day. After the filtration and evaporation, the residue was recrystallized in hexane giving air- and moisture sensitive dark red crystals of title compound (40 mg, 0.052 mmol, 19% yields); mp = 110.1-111.0 °C (dec); ¹H NMR (THF-d₈, δ) -0.09 (s, 3 H, ¹Bu₂MeSi), 0.24 (s, 3 H, ¹Bu₂MeSi), 0.28 (s, 6 H, ¹Bu₂MeSi x 2), 0.99 (s, 18 H, ¹Bu₂MeSi), 1.07 (s, 18 H, ¹Bu₂MeSi), 1.20 (s, 18 H, ¹Bu₂MeSi), 1.26 (s, 18 H, ¹Bu₂MeSi); ¹³C NMR (THF-d₈, δ) -4.0 (¹Bu₂MeSi), -3.4 (¹Bu₂MeSi x 2), -2.9 (¹Bu₂MeSi), 21.3 (CMe₃), 21.4 (CMe₃), 22.5 (CMe₃), 22.9 (CMe₃), 29.3 (CMe₃), 30.1 (CMe₃), 30.8 (CMe₃) 31.4 (CMe₃); ²⁹Si NMR (THF-d₈, δ) -179.6 (Si=Si-N), -132.1 (SiSi₄), -6.9 (¹Bu₂MeSi), 6.3 (¹Bu₂MeSi x 2), 16.2 (¹Bu₂MeSi), 123.6 (Si=Si-N); ¹H NMR (C₆D₆, δ) -0.02 (s, 3 H, ¹Bu₂MeSi), 0.43 (s, 3 H, ¹Bu₂MeSi), 0.55 (s, 6 H, ¹Bu₂MeSi x 2), 1.20 (s, 18 H, ¹Bu₂MeSi), 1.22 (s, 18 H, ¹Bu₂MeSi), 1.38 (s, 18 H, ¹Bu₂MeSi), 1.45 (s, 18 H, ¹Bu₂MeSi); ¹³C NMR (C₆D₆, δ) -3.6 (¹Bu₂MeSi), -2.9 (¹Bu₂MeSi x 2), -1.4 (¹Bu₂MeSi), 21.8 (2 x CMe₃), 23.0 (CMe₃), 23.3 (CMe₃), 29.6 (CMe₃), 30.3 (CMe₃), 31.2 (CMe₃) 31.5 (CMe₃); ²⁹Si NMR (C₆D₆, δ) -153.5 (Si=Si-N), -98.9 (SiSi₄), -4.0 (¹Bu₂MeSi), 4.3 (¹Bu₂MeSi x 2), 20.5 (¹Bu₂MeSi), 101.7 (Si=Si-N).

X-ray single crystal diffraction analysis of

2-(di-*tert*-butylmethylsilyl)imino-1,3,3-tris(di-*tert*-butylmethylsilyl)-trisilacyclopropanide 33⁻·[K(222-cryptand)]⁺

The single crystals of **33⁻·[K(crypt-222)]⁺** for X-ray diffraction analysis were grown from diethyl ether solution of **30b** and 1 equivalent amount of 222-cryptand. Diffraction data were collected at 100 K on a Bruker AXS APEX II CCD X-ray diffractometer (Mo- $K\alpha$ radiation, $\lambda = 0.71073 \text{ \AA}$, 50 kV, 600 μA). The structure was solved by the direct method, using SHELXT program, and refined by the full-matrix least-squares method by SHELXL-97 program. Crystal data for **33⁻·[K(crypt-222)]⁺** at 100 K: MF = C₅₄H₁₂₀KN₃O₆Si₇, MW = 1143.26, monoclinic, space group P 1 21/n1, $a = 17.6057(14) \text{ \AA}$, $b = 20.1427(17) \text{ \AA}$, $c = 20.0982(17) \text{ \AA}$, $\beta = 98.236(1)^\circ$, $V = 7053.8(10) \text{ \AA}^3$, Z = 4, D_{calcd} = 1.077 g/cm³, The final R factor was 0.0595 ($R_w = 0.1408$ for all data) for 13367 reflections with $I > 2\sigma(I)$, GOF = 0.957.

Crystal Data

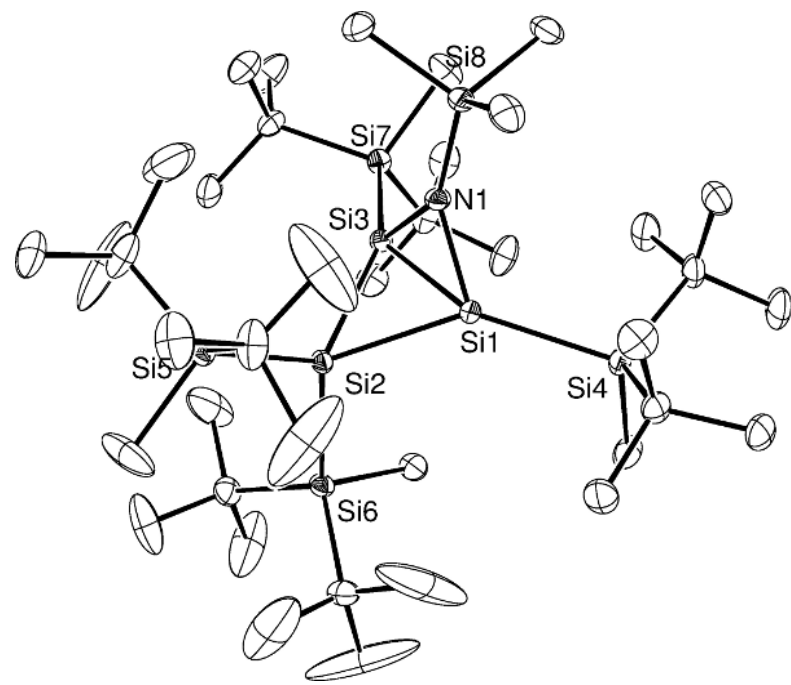


Figure 3-5-1. ORTEP drawing of **27**.

Table 3-5-1. Sample and crystal data for compound **27**.

Identification code	Si3NTMS		
Chemical formula	$C_{39}H_{93}NSi_8$		
Formula weight	800.86		
Temperature	100(1) K		
Wavelength	0.71073 Å		
Crystal size	0.140 x 0.180 x 0.220 mm		
Crystal system	monoclinic		
Space group	P 1 21/n 1		
Unit cell dimensions	$a = 11.9717(7)$ Å	$\alpha = 90^\circ$	
	$b = 19.3345(11)$ Å	$\beta = 92.3380(10)^\circ$	
	$c = 22.1927(12)$ Å	$\gamma = 90^\circ$	
Volume	$5132.6(5)$ Å ³		
Z	4		
Density (calculated)	1.036 g/cm ³		
Absorption coefficient	0.234 mm ⁻¹		
F(000)	1784		

Table 3-5-2. Data collection and structure refinement for compound **27**.

Theta range for data collection	1.40 to 27.48°
Index ranges	-15≤h≤15, -25≤k≤25, -28≤l≤28
Reflections collected	58800
Independent reflections	11755 [R(int) = 0.0239]
Max. and min. transmission	0.9675 and 0.9498
Structure solution technique	direct methods
Structure solution program	SHELXT (George Sheldrick, 2012)
Refinement method	Full-matrix least-squares on F ²
Refinement program	SHELXL-97 (George Sheldrick, 1997)
Function minimized	$\Sigma w(F_o^2 - F_c^2)^2$
Data / restraints / parameters	11755 / 0 / 434
Goodness-of-fit on F²	1.042
Δ/σ_{max}	0.002
Final R indices	10594 data; I>2σ(I) R1 = 0.0595, wR2 = 0.1361 all data R1 = 0.0654, wR2 = 0.1409
Weighting scheme	$w=1/[\sigma^2(F_o^2)+(0.0475P)^2+13.4921P]$ where P=(F _o ² +2F _c ²)/3
Extinction coefficient	0.0004(2)
Largest diff. peak and hole	1.577 and -1.624 eÅ ⁻³
R.M.S. deviation from mean	0.085 eÅ ⁻³

Table 3-5-3. Atomic coordinates and equivalent isotropic atomic displacement parameters (\AA^2) for compound **27**.U(eq) is defined as one third of the trace of the orthogonalized U_{ij} tensor.

	x/a	y/b	z/c	U(eq)
Si1	0.97643(5)	0.21219(3)	0.17129(3)	0.01349(13)
Si2	0.80945(5)	0.22600(3)	0.10868(3)	0.01308(13)
Si3	0.99025(5)	0.26411(3)	0.08140(3)	0.01338(13)
Si4	0.07477(5)	0.13212(3)	0.23629(3)	0.01658(14)
Si5	0.65880(5)	0.30527(3)	0.12967(3)	0.01671(14)
Si6	0.75800(5)	0.11570(3)	0.06317(3)	0.01608(13)
Si7	0.11520(5)	0.28467(3)	0.00155(3)	0.01625(14)
Si8	0.08509(5)	0.36898(3)	0.19102(3)	0.01761(14)
N1	0.02396(16)	0.29829(10)	0.15601(8)	0.0154(4)
C1	0.0582(2)	0.04302(13)	0.20248(12)	0.0261(5)
C2	0.2315(2)	0.15291(14)	0.23797(11)	0.0233(5)
C3	0.2638(2)	0.16992(16)	0.17343(12)	0.0303(6)
C4	0.2623(2)	0.21392(15)	0.27949(13)	0.0302(6)
C5	0.3011(2)	0.08946(16)	0.25873(13)	0.0326(6)
C6	0.0106(2)	0.13066(13)	0.31410(11)	0.0215(5)
C7	0.0001(2)	0.20261(15)	0.34251(12)	0.0302(6)
C8	0.0816(2)	0.08430(16)	0.35746(12)	0.0296(6)
C9	0.8925(2)	0.09961(15)	0.30794(12)	0.0282(6)
C10	0.5186(2)	0.26616(19)	0.1100(2)	0.0543(11)
C11	0.6592(2)	0.32519(16)	0.21431(12)	0.0303(6)
C12	0.7678(3)	0.3508(4)	0.2388(2)	0.094(2)
C13	0.6348(6)	0.2550(3)	0.2458(2)	0.104(3)
C14	0.5645(3)	0.37258(18)	0.23178(14)	0.0389(7)
C15	0.6647(3)	0.38485(15)	0.07815(13)	0.0326(6)
C16	0.5596(3)	0.43008(16)	0.08098(15)	0.0379(7)
C17	0.6783(6)	0.3613(3)	0.01419(17)	0.100(2)
C18	0.7664(3)	0.4305(2)	0.0967(3)	0.0785(17)
C19	0.8955(2)	0.06974(12)	0.05461(11)	0.0207(5)
C20	0.6715(2)	0.05925(13)	0.11645(12)	0.0222(5)
C21	0.5559(4)	0.0818(3)	0.1256(4)	0.141(4)
C22	0.7293(6)	0.0567(5)	0.1760(2)	0.177(5)
C23	0.6630(7)	0.9868(2)	0.0945(3)	0.144(4)
C24	0.6904(2)	0.12185(13)	0.98260(11)	0.0225(5)
C25	0.5682(3)	0.1435(3)	0.97996(16)	0.0559(11)
C26	0.6988(5)	0.0530(2)	0.95010(18)	0.0739(16)

	x/a	y/b	z/c	U(eq)
C27	0.7536(3)	0.1753(3)	0.94746(17)	0.0690(15)
C28	0.2385(2)	0.33067(16)	0.03799(12)	0.0296(6)
C29	0.1706(2)	0.20078(13)	0.96752(11)	0.0224(5)
C30	0.2064(3)	0.15146(15)	0.01908(12)	0.0314(6)
C31	0.0840(2)	0.16448(14)	0.92596(12)	0.0294(6)
C32	0.2754(2)	0.21620(16)	0.93142(13)	0.0320(6)
C33	0.0441(2)	0.34792(12)	0.94548(11)	0.0202(5)
C34	0.9335(3)	0.32077(15)	0.91812(15)	0.0373(7)
C35	0.1211(3)	0.36599(16)	0.89412(13)	0.0389(7)
C36	0.0196(2)	0.41479(14)	0.97952(12)	0.0280(5)
C37	0.0390(3)	0.45126(13)	0.15350(14)	0.0328(6)
C38	0.2429(2)	0.37182(14)	0.19124(12)	0.0265(5)
C39	0.0504(2)	0.37473(15)	0.27256(11)	0.0277(5)

Table 3-5-4. Bond lengths (Å) for compound **27**.

Si1-N1	1.796(2)	Si1-Si3	2.2453(8)	Si8-C37	1.868(3)	Si8-C39	1.876(3)
Si1-Si4	2.3927(8)	Si1-Si2	2.4024(8)	Si8-C38	1.890(3)	C2-C3	1.535(3)
Si2-Si3	2.3877(8)	Si2-Si5	2.4264(8)	C2-C4	1.533(4)	C6-C9	1.537(3)
Si2-Si6	2.4283(9)	Si3-N1	1.8128(19)	C2-C5	1.543(3)	C11-C12	1.473(5)
Si3-Si7	2.3983(9)	Si4-C1	1.886(3)	C6-C7	1.535(4)	C11-C13	1.559(6)
Si4-C2	1.918(3)	Si4-C6	1.918(2)	C6-C8	1.544(3)	C15-C17	1.506(5)
Si5-C10	1.877(3)	Si5-C11	1.917(3)	C11-C14	1.521(4)	C15-C18	1.545(6)
Si5-C15	1.920(3)	Si6-C19	1.887(2)	C15-C16	1.535(4)	C20-C21	1.473(5)
Si6-C24	1.936(3)	Si6-C20	1.940(3)	C20-C22	1.467(5)	C24-C26	1.519(4)
Si7-C28	1.877(3)	Si7-C33	1.919(2)	C20-C23	1.486(5)	C24-C27	1.514(4)
Si7-C29	1.919(3)	Si8-N1	1.7207(19)				

Table 3-5-5. Bond angles (°) for compound **27**.

N1-Si1-Si3	51.86(6)	N1-Si1-Si4	124.17(7)	Si1-Si3-Si7	143.26(4)	Si2-Si3-Si7	146.89(3)
Si3-Si1-Si4	140.59(4)	N1-Si1-Si2	92.88(7)	C1-Si4-C2	106.63(12)	C1-Si4-C6	107.77(12)
Si3-Si1-Si2	61.72(3)	Si4-Si1-Si2	142.94(3)	C2-Si4-C6	114.38(11)	C1-Si4-Si1	108.05(8)
Si3-Si2-Si1	55.90(2)	Si3-Si2-Si5	122.84(3)	C2-Si4-Si1	109.45(8)	C6-Si4-Si1	110.31(8)
Si1-Si2-Si5	124.52(3)	Si3-Si2-Si6	112.51(3)	C10-Si5-C11	105.99(16)	C10-Si5-C15	103.81(18)
Si1-Si2-Si6	109.51(3)	Si5-Si2-Si6	117.17(3)	C11-Si5-C15	115.07(13)	C10-Si5-Si2	111.46(10)
N1-Si3-Si1	51.19(6)	N1-Si3-Si2	92.94(7)	C11-Si5-Si2	110.04(8)	C15-Si5-Si2	110.25(9)
Si1-Si3-Si2	62.38(3)	N1-Si3-Si7	119.48(7)	C19-Si6-C24	105.62(11)	C19-Si6-C20	106.62(11)

C24-Si6-C20	112.60(11)	C19-Si6-Si2	104.35(8)	C13-C11-Si5	105.7(2)	C14-C11-Si5	113.50(19)
C24-Si6-Si2	114.81(8)	C20-Si6-Si2	111.92(8)	C17-C15-C18	108.0(4)	C17-C15-C16	109.3(3)
C28-Si7-C33	107.30(12)	C28-Si7-C29	106.96(13)	C17-C15-Si5	109.1(2)	C16-C15-C18	107.6(3)
C33-Si7-C29	115.77(11)	C28-Si7-Si3	105.26(9)	C18-C15-Si5	110.3(2)	C16-C15-Si5	112.5(2)
C33-Si7-Si3	108.14(8)	C29-Si7-Si3	112.75(8)	C22-C20-C23	106.7(5)	C22-C20-C21	107.3(5)
N1-Si8-C37	111.27(11)	N1-Si8-C39	112.08(11)	C22-C20-Si6	108.9(2)	C21-C20-C23	105.8(5)
C37-Si8-C39	107.85(14)	N1-Si8-C38	115.53(11)	C23-C20-Si6	111.2(2)	C21-C20-Si6	116.4(2)
C37-Si8-C38	104.67(13)	C39-Si8-C38	104.85(12)	C27-C24-C25	107.0(3)	C27-C24-C26	108.0(3)
Si8-N1-Si1	141.54(12)	Si8-N1-Si3	140.97(12)	C27-C24-Si6	108.60(18)	C26-C24-C25	107.8(3)
Si1-N1-Si3	76.94(8)	C4-C2-C3	109.4(2)	C25-C24-Si6	114.7(2)	C26-C24-Si6	110.58(19)
C4-C2-C5	108.6(2)	C3-C2-C5	107.2(2)	C31-C29-C32	108.7(2)	C31-C29-C30	109.0(2)
C4-C2-Si4	112.61(18)	C3-C2-Si4	108.10(17)	C31-C29-Si7	112.88(17)	C30-C29-C32	107.3(2)
C5-C2-Si4	110.83(19)	C7-C6-C9	107.5(2)	C32-C29-Si7	110.00(19)	C30-C29-Si7	108.77(17)
C7-C6-C8	108.8(2)	C9-C6-C8	108.0(2)	C34-C33-C35	108.7(2)	C34-C33-C36	107.8(2)
C7-C6-Si4	113.52(17)	C9-C6-Si4	109.04(17)	C34-C33-Si7	113.15(17)	C36-C33-C35	107.9(2)
C12-C11-C13	107.8(4)	C12-C11-C14	111.1(3)	C35-C33-Si7	111.26(18)	C36-C33-Si7	107.87(17)
C12-C11-Si5	113.3(2)	C14-C11-C13	104.8(3)				

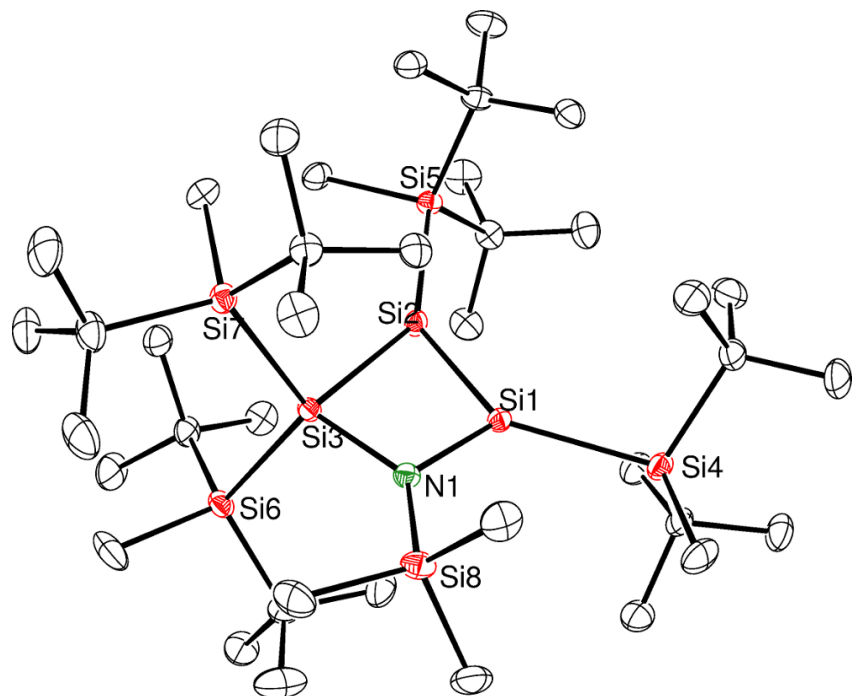


Figure 3-5-2. ORTEP drawing of **28**.

Table 3-5-6. Sample and crystal data for compound **28**.

Identification code	Si3NTMS	
Chemical formula	$C_{39}H_{93}NSi_8$	
Formula weight	800.86	
Temperature	100(1) K	
Wavelength	0.71073 Å	
Crystal size	0.070 x 0.160 x 0.300 mm	
Crystal system	monoclinic	
Space group	C 1 c 1	
Unit cell dimensions	$a = 11.3187(6)$ Å	$\alpha = 90^\circ$
	$b = 25.5654(13)$ Å	$\beta = 106.2990(10)^\circ$
	$c = 18.4956(10)$ Å	$\gamma = 90^\circ$
Volume	5136.9(5) Å ³	
Z	4	
Density (calculated)	1.036 g/cm ³	
Absorption coefficient	0.234 mm ⁻¹	
F(000)	1784	

Table 3-5-7. Data collection and structure refinement for compound **28**.

Theta range for data collection	1.59 to 27.48°
Index ranges	-14<=h<=14, -33<=k<=33, -23<=l<=23
Reflections collected	29488
Independent reflections	11657 [R(int) = 0.0227]
Max. and min. transmission	0.9838 and 0.9325
Structure solution technique	direct methods
Structure solution program	SHELXT (George Sheldrick, 2012)
Refinement method	Full-matrix least-squares on F ²
Refinement program	SHELXL-97 (George Sheldrick, 1997)
Function minimized	$\Sigma w(F_o^2 - F_c^2)^2$
Data / restraints / parameters	11657 / 2 / 434
Goodness-of-fit on F²	1.039
Δ/σ_{\max}	0.001
Final R indices	11417 data; I>2σ(I) R1 = 0.0221, wR2 = 0.0614 all data R1 = 0.0227, wR2 = 0.0618
Weighting scheme	$w=1/[\sigma^2(F_o^2)+(0.0371P)^2+0.9702P]$ where P=(F _o ² +2F _c ²)/3
Absolute structure parameter	0.0(0)
Extinction coefficient	0.0001(1)
Largest diff. peak and hole	0.258 and -0.256 eÅ ⁻³

R.M.S. deviation from mean 0.035 eÅ⁻³

Table 3. Atomic coordinates and equivalent isotropic atomic displacement parameters (Å²) for **28**.

U(eq) is defined as one third of the trace of the orthogonalized U_{ij} tensor.

	x/a	y/b	z/c	U(eq)
Si1	0.57150(3)	0.181889(13)	0.390081(19)	0.01275(7)
Si2	0.47018(3)	0.143523(13)	0.459135(19)	0.01478(7)
Si3	0.54026(3)	0.075468(13)	0.393477(19)	0.01233(7)
Si4	0.61750(3)	0.269565(14)	0.35956(2)	0.01626(7)
Si5	0.37414(3)	0.161576(14)	0.554908(19)	0.01387(7)
Si6	0.36385(3)	0.035372(14)	0.30154(2)	0.01685(7)
Si7	0.68232(3)	0.018667(14)	0.48744(2)	0.01599(7)
Si8	0.71168(3)	0.121392(15)	0.29247(2)	0.01923(8)
N1	0.61254(10)	0.12453(4)	0.34966(6)	0.0143(2)
C1	0.73024(14)	0.27599(6)	0.30252(9)	0.0270(3)
C2	0.46545(13)	0.29984(5)	0.30082(8)	0.0201(3)
C3	0.43457(14)	0.27655(6)	0.22110(8)	0.0254(3)
C4	0.47565(15)	0.35946(6)	0.29397(9)	0.0284(3)
C5	0.35816(13)	0.28773(6)	0.33385(8)	0.0237(3)
C6	0.69368(13)	0.30374(6)	0.45383(8)	0.0222(3)
C7	0.75611(17)	0.35493(6)	0.44095(10)	0.0344(4)
C8	0.59960(15)	0.31622(6)	0.49657(8)	0.0279(3)
C9	0.79396(14)	0.26763(6)	0.50245(9)	0.0274(3)
C10	0.30182(13)	0.09833(6)	0.57233(8)	0.0207(3)
C11	0.24122(12)	0.21156(5)	0.52415(8)	0.0188(3)
C12	0.16953(13)	0.20268(6)	0.44122(9)	0.0254(3)
C13	0.28532(14)	0.26853(6)	0.53237(9)	0.0260(3)
C14	0.15048(14)	0.20388(7)	0.57179(9)	0.0289(3)
C15	0.49706(12)	0.17999(6)	0.64697(7)	0.0180(3)
C16	0.57672(13)	0.22665(6)	0.63772(8)	0.0214(3)
C17	0.43638(14)	0.19256(7)	0.70959(8)	0.0277(3)
C18	0.58246(13)	0.13278(6)	0.67276(8)	0.0210(3)
C19	0.40376(16)	0.96955(6)	0.26771(10)	0.0324(4)
C20	0.30576(14)	0.07610(6)	0.21034(8)	0.0241(3)
C21	0.39605(17)	0.06730(9)	0.16304(10)	0.0410(4)
C22	0.29993(16)	0.13475(6)	0.22609(9)	0.0326(4)
C23	0.17841(15)	0.05817(7)	0.16165(9)	0.0305(3)
C24	0.23516(13)	0.02218(5)	0.34902(8)	0.0203(3)

	x/a	y/b	z/c	U(eq)
C25	0.16360(13)	0.07207(6)	0.35524(9)	0.0253(3)
C26	0.14450(16)	0.98034(7)	0.30634(10)	0.0334(4)
C27	0.29399(14)	0.00166(6)	0.42911(8)	0.0239(3)
C28	0.60281(13)	0.01219(6)	0.56403(8)	0.0221(3)
C29	0.70650(14)	0.94647(6)	0.46130(9)	0.0255(3)
C30	0.58577(15)	0.91603(6)	0.45368(10)	0.0312(3)
C31	0.80616(16)	0.91909(6)	0.52499(11)	0.0338(4)
C32	0.74199(17)	0.94035(6)	0.38754(10)	0.0345(4)
C33	0.83849(12)	0.05325(5)	0.53304(8)	0.0190(3)
C34	0.89093(14)	0.03623(6)	0.61612(9)	0.0271(3)
C35	0.93512(13)	0.04183(7)	0.49139(9)	0.0276(3)
C36	0.82140(12)	0.11284(5)	0.53380(8)	0.0202(3)
C37	0.74321(16)	0.05229(7)	0.27131(9)	0.0303(3)
C38	0.86313(13)	0.15219(7)	0.34125(9)	0.0270(3)
C39	0.64791(15)	0.15560(7)	0.19946(8)	0.0292(3)

Table 3-5-8. Bond lengths (Å) for compound **28**.

Si1-N1	1.7665(11)	Si1-Si2	2.1750(5)	C2-C5	1.536(2)	C6-C7	1.537(2)
Si1-Si4	2.4040(5)	Si1-Si3	2.7466(5)	C2-C4	1.5364(19)	C11-C13	1.533(2)
Si2-Si5	2.3693(5)	Si2-Si3	2.3815(5)	C6-C8	1.527(2)	C11-C14	1.5420(19)
Si3-N1	1.8087(11)	Si3-Si6	2.4543(5)	C6-C9	1.542(2)	C15-C16	1.5336(19)
Si3-Si7	2.4790(5)	Si4-C1	1.8771(15)	C11-C12	1.5375(19)	C15-C17	1.5371(18)
Si4-C2	1.9214(15)	Si4-C6	1.9244(15)	C15-C18	1.5362(19)	C20-C21	1.537(2)
Si5-C10	1.8806(14)	Si5-C15	1.9306(14)	C20-C22	1.532(2)	C24-C27	1.536(2)
Si5-C11	1.9338(14)	Si6-C19	1.8935(15)	C20-C23	1.540(2)	C29-C32	1.534(2)
Si6-C24	1.9300(15)	Si6-C20	1.9337(15)	C24-C25	1.533(2)	C29-C31	1.551(2)
Si7-C28	1.8867(14)	Si7-C33	1.9445(14)	C24-C26	1.5381(19)	C33-C35	1.532(2)
Si7-C29	1.9466(15)	Si8-N1	1.7466(11)	C29-C30	1.544(2)	C33-C34	1.5462(19)
Si8-C37	1.8655(16)	Si8-C38	1.8720(16)	C33-C36	1.5362(19)		
Si8-C39	1.8837(16)	C2-C3	1.537(2)				

Table 3-5-9. Bond angles (°) for compound **28**.

N1-Si1-Si2	96.82(4)	N1-Si1-Si4	125.08(4)	Si5-Si2-Si3	144.286(19)	N1-Si3-Si2	88.81(4)
Si2-Si1-Si4	137.99(2)	N1-Si1-Si3	40.37(4)	N1-Si3-Si6	111.19(4)	Si2-Si3-Si6	109.621(18)
Si2-Si1-Si3	56.452(14)	Si4-Si1-Si3	165.184(19)	N1-Si3-Si7	115.74(4)	Si2-Si3-Si7	108.288(18)
Si1-Si2-Si5	141.20(2)	Si1-Si2-Si3	73.981(16)	Si6-Si3-Si7	118.851(18)	N1-Si3-Si1	39.24(3)

Si2-Si3-Si1	49.566(13)	Si6-Si3-Si1	118.869(17)	C7-C6-C9	107.76(12)	C8-C6-Si4	111.32(10)
Si7-Si3-Si1	122.273(17)	C1-Si4-C2	106.82(7)	C7-C6-Si4	110.77(10)	C9-C6-Si4	109.02(10)
C1-Si4-C6	105.49(7)	C2-Si4-C6	115.58(6)	C13-C11-C12	107.76(12)	C13-C11-C14	108.35(12)
C1-Si4-Si1	116.09(5)	C2-Si4-Si1	106.84(4)	C12-C11-C14	107.55(11)	C13-C11-Si5	113.19(9)
C6-Si4-Si1	106.38(4)	C10-Si5-C15	107.41(6)	C12-C11-Si5	110.19(9)	C14-C11-Si5	109.62(10)
C10-Si5-C11	106.17(6)	C15-Si5-C11	114.01(6)	C16-C15-C18	107.90(11)	C16-C15-C17	108.81(12)
C10-Si5-Si2	105.88(5)	C15-Si5-Si2	109.79(4)	C18-C15-C17	107.80(11)	C16-C15-Si5	113.08(9)
C11-Si5-Si2	113.02(4)	C19-Si6-C24	106.00(7)	C18-C15-Si5	108.49(9)	C17-C15-Si5	110.59(10)
C19-Si6-C20	104.15(7)	C24-Si6-C20	112.07(6)	C22-C20-C21	108.81(14)	C22-C20-C23	108.62(13)
C19-Si6-Si3	112.15(5)	C24-Si6-Si3	109.20(4)	C21-C20-C23	106.64(13)	C22-C20-Si6	112.54(10)
C20-Si6-Si3	113.01(5)	C28-Si7-C33	106.34(6)	C21-C20-Si6	107.46(11)	C23-C20-Si6	112.54(10)
C28-Si7-C29	103.48(7)	C33-Si7-C29	111.39(6)	C25-C24-C27	107.88(12)	C25-C24-C26	109.08(13)
C28-Si7-Si3	103.04(5)	C33-Si7-Si3	111.69(4)	C27-C24-C26	107.68(12)	C25-C24-Si6	111.78(10)
C29-Si7-Si3	119.34(5)	N1-Si8-C37	111.33(6)	C27-C24-Si6	108.68(10)	C26-C24-Si6	111.59(11)
N1-Si8-C38	110.24(6)	C37-Si8-C38	107.23(8)	C32-C29-C30	108.25(14)	C32-C29-C31	108.26(13)
N1-Si8-C39	112.65(6)	C37-Si8-C39	107.15(7)	C30-C29-C31	106.16(13)	C32-C29-Si7	114.06(11)
C38-Si8-C39	108.01(7)	Si8-N1-Si1	125.76(6)	C30-C29-Si7	108.54(10)	C31-C29-Si7	111.25(11)
Si8-N1-Si3	133.46(6)	Si1-N1-Si3	100.39(5)	C35-C33-C36	107.65(12)	C35-C33-C34	108.48(12)
C5-C2-C3	108.13(12)	C5-C2-C4	108.59(12)	C36-C33-C34	106.50(11)	C35-C33-Si7	112.68(10)
C3-C2-C4	107.90(12)	C5-C2-Si4	112.12(9)	C36-C33-Si7	110.69(9)	C34-C33-Si7	110.60(10)
C3-C2-Si4	108.23(10)	C4-C2-Si4	111.72(10)				
C8-C6-C7	108.66(13)	C8-C6-C9	109.23(12)				

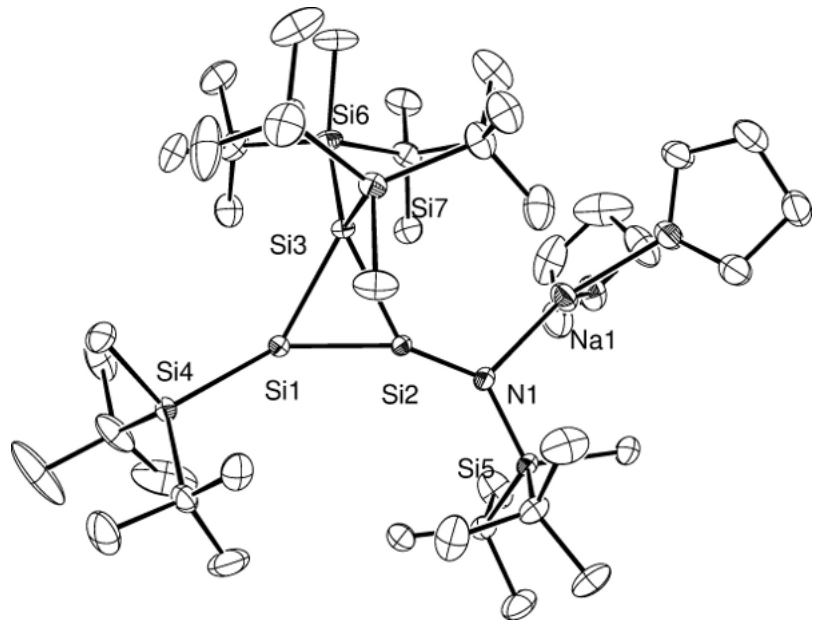


Figure 5-3-3. ORTEP drawing of **30a**.

Table 3-5-11. Sample and crystal data for **30a**.

Identification code	Si3NNa		
Chemical formula	C ₄₄ H ₁₀₀ NNaO ₂ Si ₇		
Formula weight	894.87		
Temperature	100(1) K		
Wavelength	0.71073 Å		
Crystal size	0.120 x 0.190 x 0.290 mm		
Crystal system	orthorhombic		
Space group	P n a 21		
Unit cell dimensions	a = 23.3860(12) Å	α = 90°	
	b = 12.7195(6) Å	β = 90°	
	c = 19.0584(10) Å	γ = 90°	
Volume	5669.1(5) Å ³		
Z	4		
Density (calculated)	1.048 g/cm ³		
Absorption coefficient	0.207 mm ⁻¹		
F(000)	1984		

Table 3-5-12. Data collection and structure refinement for compound **30a**.

Theta range for data collection	1.74 to 27.48°
Index ranges	-30<=h<=30, -16<=k<=16, -24<=l<=24
Reflections collected	63607
Independent reflections	12978 [R(int) = 0.0289]
Max. and min. transmission	0.9749 and 0.9429
Structure solution technique	direct methods
Structure solution program	SHELXT (George Sheldrick, 2012)
Refinement method	Full-matrix least-squares on F ²
Refinement program	SHELXL-97 (George Sheldrick, 1997)
Function minimized	Σ w(F _o ² - F _c ²) ²
Data / restraints / parameters	12978 / 1 / 496
Goodness-of-fit on F²	1.082
Δ/σ_{max}	0.001
Final R indices	12580 data; I>2σ(I) R1 = 0.0317, wR2 = 0.0828 all data R1 = 0.0331, wR2 = 0.0837
Weighting scheme	w=1/[σ ² (F _o ²)+(0.0432P) ² +2.0180P] where P=(F _o ² +2F _c ²)/3
Absolute structure parameter	0.1(1)
Largest diff. peak and hole	0.896 and -0.256 eÅ ⁻³
R.M.S. deviation from mean	0.045 eÅ ⁻³

Table 3-5-13. Atomic coordinates and equivalent isotropic atomic displacement parameters (\AA^2) for compound **30a**.
 U(eq) is defined as one third of the trace of the orthogonalized U_{ij} tensor.

	x/a	y/b	z/c	U(eq)
Si1	0.87725(2)	0.27924(4)	0.70278(2)	0.01748(9)
Si2	0.888448(19)	0.13196(3)	0.75782(2)	0.01405(9)
Si3	0.911329(18)	0.28280(3)	0.82057(2)	0.01400(9)
Si4	0.81431(2)	0.38126(4)	0.63411(2)	0.01635(9)
Si5	0.86342(2)	0.89746(3)	0.72734(3)	0.01777(9)
Si6	0.007172(19)	0.34213(4)	0.83404(3)	0.01982(10)
Si7	0.84420(2)	0.30040(4)	0.91462(3)	0.01937(10)
Na1	0.97047(3)	0.94289(6)	0.83268(4)	0.02767(16)
O1	0.05645(7)	0.86989(13)	0.79894(9)	0.0365(3)
O2	0.96886(7)	0.87234(12)	0.94325(8)	0.0312(3)
N1	0.89629(6)	0.00423(11)	0.76335(8)	0.0186(3)
C1	0.80028(10)	0.50912(16)	0.68043(13)	0.0348(5)
C2	0.85640(10)	0.4141(2)	0.55040(11)	0.0420(6)
C3	0.87704(13)	0.3149(3)	0.51315(15)	0.0738(11)
C4	0.82164(12)	0.4836(4)	0.49978(17)	0.0926(16)
C5	0.90943(10)	0.4765(2)	0.57399(14)	0.0476(7)
C6	0.74188(8)	0.31498(15)	0.61909(10)	0.0253(4)
C7	0.71655(8)	0.28432(16)	0.69058(12)	0.0308(4)
C8	0.74713(13)	0.2158(2)	0.57513(13)	0.0460(6)
C9	0.69943(10)	0.3921(2)	0.58452(17)	0.0492(7)
C10	0.89287(10)	0.77551(14)	0.77135(12)	0.0300(4)
C11	0.88239(8)	0.88447(14)	0.62940(10)	0.0221(3)
C12	0.85280(12)	0.78963(18)	0.59414(13)	0.0407(5)
C13	0.86740(9)	0.98305(16)	0.58764(10)	0.0289(4)
C14	0.94715(9)	0.8691(2)	0.62434(13)	0.0406(5)
C15	0.78303(8)	0.89691(14)	0.74766(10)	0.0249(4)
C16	0.77518(11)	0.9200(2)	0.82587(14)	0.0467(6)
C17	0.75415(9)	0.79097(17)	0.73287(14)	0.0375(5)
C18	0.75133(9)	0.98235(19)	0.70609(16)	0.0430(6)
C19	0.01832(9)	0.4059(2)	0.92260(12)	0.0363(5)
C20	0.02789(8)	0.44957(15)	0.76724(11)	0.0274(4)
C21	0.04016(9)	0.40467(17)	0.69386(11)	0.0321(4)
C22	0.97767(10)	0.52696(16)	0.76140(14)	0.0365(5)
C23	0.08105(10)	0.51183(19)	0.79127(15)	0.0418(5)
C24	0.05666(7)	0.22070(15)	0.83251(10)	0.0244(4)

	x/a	y/b	z/c	U(eq)
C25	0.11983(8)	0.2494(2)	0.84452(12)	0.0338(5)
C26	0.03847(9)	0.14722(18)	0.89244(12)	0.0329(5)
C27	0.05207(8)	0.15865(15)	0.76397(11)	0.0270(4)
C28	0.77540(8)	0.24818(19)	0.87587(11)	0.0331(5)
C29	0.82785(10)	0.44419(16)	0.94044(12)	0.0325(5)
C30	0.83237(16)	0.5130(2)	0.87573(17)	0.0665(10)
C31	0.76739(10)	0.45557(18)	0.97072(13)	0.0376(5)
C32	0.86986(11)	0.4869(2)	0.99664(17)	0.0527(7)
C33	0.86057(9)	0.20922(17)	0.99296(11)	0.0286(4)
C34	0.81552(9)	0.21885(19)	0.05108(11)	0.0350(5)
C35	0.85942(11)	0.09466(18)	0.96528(13)	0.0393(5)
C36	0.91951(9)	0.2272(2)	0.02529(12)	0.0418(6)
C37	0.08796(12)	0.8741(2)	0.73456(14)	0.0463(6)
C38	0.14709(11)	0.9105(2)	0.7545(2)	0.0578(8)
C39	0.15103(12)	0.8863(3)	0.8323(2)	0.0752(12)
C40	0.09657(12)	0.8286(2)	0.84817(14)	0.0538(7)
C41	0.99740(10)	0.91514(19)	0.00391(11)	0.0337(5)
C42	0.97374(10)	0.8586(2)	0.06720(11)	0.0372(5)
C43	0.95536(10)	0.7539(2)	0.03725(12)	0.0393(5)
C44	0.93535(11)	0.7837(2)	0.96420(12)	0.0415(6)

Table 3-5-14. Bond lengths (Å) for compound **33a**.

Si1-Si2	2.1629(6)	Si1-Si4	2.3587(6)	C2-C3	1.526(4)	C6-C7	1.536(3)
Si1-Si3	2.3827(6)	Si2-N1	1.6384(14)	C2-C4	1.540(4)	C11-C13	1.526(3)
Si2-Si3	2.3232(6)	Si2-Na1	3.3910(9)	C6-C8	1.520(3)	C11-C12	1.545(3)
Si3-Si6	2.3789(6)	Si3-Si7	2.3931(6)	C6-C9	1.543(3)	C15-C16	1.530(3)
Si4-C1	1.879(2)	Si4-C6	1.9135(19)	C11-C14	1.530(3)	C15-C18	1.536(3)
Si4-C2	1.921(2)	Si5-N1	1.7046(15)	C15-C17	1.534(3)	C20-C22	1.537(3)
Si5-C10	1.8932(19)	Si5-C15	1.9195(19)	C20-C21	1.538(3)	C24-C26	1.536(3)
Si5-C11	1.926(2)	Si5-Na1	3.2606(9)	C20-C23	1.544(3)	C29-C30	1.516(3)
Si6-C19	1.891(2)	Si6-C20	1.929(2)	C24-C27	1.530(3)	C29-C32	1.551(4)
Si6-C24	1.9302(19)	Si7-C28	1.891(2)	C24-C25	1.539(2)	C33-C36	1.527(3)
Si7-C33	1.929(2)	Si7-C29	1.932(2)	C29-C31	1.534(3)	C33-C35	1.550(3)
Na1-O2	2.2907(16)	Na1-O1	2.3062(17)	C33-C34	1.534(3)	C37-C38	1.507(4)
Na1-N1	2.3161(16)	O1-C40	1.427(3)	C38-C39	1.517(5)	C39-C40	1.501(5)
O1-C37	1.432(3)	O2-C44	1.430(3)	C41-C42	1.510(3)	C42-C43	1.511(4)
O2-C41	1.442(3)	C2-C5	1.539(4)	C43-C44	1.517(3)		

Table 3-5-15. Bond angles ($^{\circ}$) for compound **30a**.

Si2-Si1-Si4	145.20(3)	Si2-Si1-Si3	61.249(19)	Si2-N1-Na1	117.04(8)	Si5-N1-Na1	107.40(7)
Si4-Si1-Si3	136.14(3)	N1-Si2-Si1	154.63(6)	C3-C2-C5	107.9(2)	C3-C2-C4	110.5(3)
N1-Si2-Si3	139.47(6)	Si1-Si2-Si3	64.05(2)	C5-C2-C4	108.2(2)	C3-C2-Si4	111.6(2)
N1-Si2-Na1	37.47(5)	Si1-Si2-Na1	152.47(3)	C5-C2-Si4	106.41(16)	C4-C2-Si4	112.00(18)
Si3-Si2-Na1	103.82(2)	Si2-Si3-Si6	122.31(2)	C8-C6-C7	108.02(17)	C8-C6-C9	110.1(2)
Si2-Si3-Si1	54.705(18)	Si6-Si3-Si1	115.01(2)	C7-C6-C9	106.97(18)	C8-C6-Si4	112.13(15)
Si2-Si3-Si7	108.16(2)	Si6-Si3-Si7	120.50(2)	C7-C6-Si4	108.70(13)	C9-C6-Si4	110.70(14)
Si1-Si3-Si7	119.21(2)	C1-Si4-C6	107.28(10)	C13-C11-C14	107.43(17)	C13-C11-C12	108.17(17)
C1-Si4-C2	106.93(12)	C6-Si4-C2	115.17(10)	C14-C11-C12	108.42(18)	C13-C11-Si5	112.47(13)
C1-Si4-Si1	108.93(7)	C6-Si4-Si1	113.14(6)	C14-C11-Si5	107.47(14)	C12-C11-Si5	112.69(14)
C2-Si4-Si1	105.12(7)	N1-Si5-C10	108.08(8)	C16-C15-C17	107.16(18)	C16-C15-C18	108.0(2)
N1-Si5-C15	111.30(8)	C10-Si5-C15	105.30(9)	C17-C15-C18	108.32(18)	C16-C15-Si5	108.26(15)
N1-Si5-C11	110.78(8)	C10-Si5-C11	105.98(9)	C17-C15-Si5	113.43(14)	C18-C15-Si5	111.48(14)
C15-Si5-C11	114.89(8)	N1-Si5-Na1	42.68(5)	C21-C20-C22	108.34(19)	C21-C20-C23	108.07(17)
C10-Si5-Na1	65.99(6)	C15-Si5-Na1	128.94(6)	C22-C20-C23	107.97(18)	C21-C20-Si6	112.57(13)
C11-Si5-Na1	115.79(6)	C19-Si6-C20	104.50(10)	C22-C20-Si6	108.03(13)	C23-C20-Si6	111.71(16)
C19-Si6-C24	105.91(10)	C20-Si6-C24	113.97(9)	C27-C24-C26	107.55(17)	C27-C24-C25	108.45(16)
C19-Si6-Si3	111.24(7)	C20-Si6-Si3	112.96(7)	C26-C24-C25	107.42(17)	C27-C24-Si6	112.56(13)
C24-Si6-Si3	108.03(6)	C28-Si7-C33	105.06(10)	C26-C24-Si6	108.04(13)	C25-C24-Si6	112.58(14)
C28-Si7-C29	105.28(10)	C33-Si7-C29	114.28(10)	C30-C29-C31	108.4(2)	C30-C29-C32	108.4(2)
C28-Si7-Si3	103.47(7)	C33-Si7-Si3	113.16(6)	C31-C29-C32	106.91(19)	C30-C29-Si7	108.98(16)
C29-Si7-Si3	114.15(7)	O2-Na1-O1	96.49(6)	C31-C29-Si7	111.57(15)	C32-C29-Si7	112.44(17)
O2-Na1-N1	130.13(6)	O1-Na1-N1	129.02(7)	C36-C33-C34	108.47(18)	C36-C33-C35	107.06(19)
O2-Na1-Si5	118.97(5)	O1-Na1-Si5	115.24(5)	C34-C33-C35	108.01(18)	C36-C33-Si7	113.67(15)
N1-Na1-Si5	29.93(4)	O2-Na1-Si2	130.96(5)	C34-C33-Si7	112.01(14)	C35-C33-Si7	107.35(15)
O1-Na1-Si2	131.41(5)	N1-Na1-Si2	25.49(4)	O1-C37-C38	105.5(2)	O2-C41-C42	106.92(17)
Si5-Na1-Si2	55.411(16)	C40-O1-C37	103.81(19)	C37-C38-C39	103.9(2)	C41-C42-C43	102.85(18)
C40-O1-Na1	122.55(15)	C37-O1-Na1	132.25(14)	C40-C39-C38	104.2(2)	C42-C43-C44	102.40(19)
C44-O2-C41	109.12(16)	C44-O2-Na1	125.08(13)	O1-C40-C39	104.2(2)	O2-C44-C43	106.50(18)
C41-O2-Na1	125.60(12)	Si2-N1-Si5	135.53(10)				

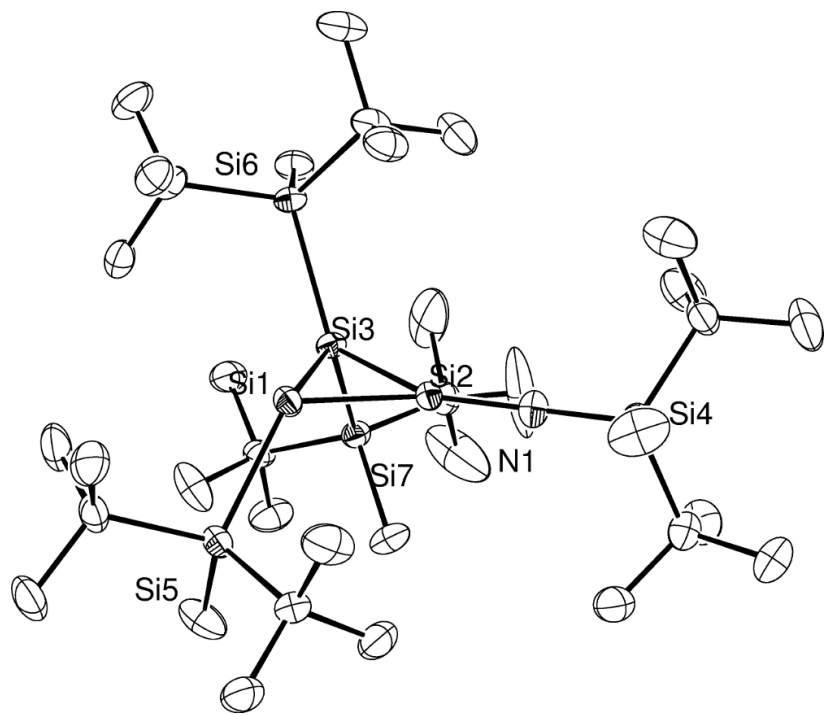


Figure 3-5-4. ORTEP drawing of $\mathbf{33}^- \cdot [\mathbf{K}^+(222\text{-cryptand})]$.

Table 3-5-16. Sample and crystal data for compound **33⁻·[K⁺(222-cryptand)]**.

Identification code	Si3NKcryptfix	
Chemical formula	C ₅₄ H ₁₂₀ KN ₃ O ₆ Si ₇	
Formula weight	1143.26	
Temperature	100(1) K	
Wavelength	0.71073 Å	
Crystal size	0.150 x 0.190 x 0.300 mm	
Crystal system	monoclinic	
Space group	P 1 21/n 1	
Unit cell dimensions	a = 17.6057(14) Å	α = 90°
	b = 20.1427(17) Å	β = 98.2360(10)°
	c = 20.0982(17) Å	γ = 90°
Volume	7053.8(10) Å ³	
Z	4	
Density (calculated)	1.077 g/cm ³	
Absorption coefficient	0.236 mm ⁻¹	
F(000)	2520	

Table 3-5-17. Data collection and structure refinement for **33⁻·[K⁺(222-cryptand)]**.

Theta range for data collection	1.44 to 27.48°
Index ranges	-22<=h<=22, -26<=k<=26, -26<=l<=25
Reflections collected	81012
Independent reflections	16149 [R(int) = 0.0382]
Max. and min. transmission	0.9658 and 0.9324
Structure solution technique	direct methods
Structure solution program	SHELXT (George Sheldrick, 2012)
Refinement method	Full-matrix least-squares on F ²
Refinement program	SHELXL-97 (George Sheldrick, 1997)
Function minimized	Σ w(F _o ² - F _c ²) ²
Data / restraints / parameters	16149 / 0 / 640
Goodness-of-fit on F²	0.957
Δ/σ_{max}	0.001
Final R indices	13367 data; I>2σ(I) R1 = 0.0595, wR2 = 0.1331 all data R1 = 0.0718, wR2 = 0.1408
Weighting scheme	w=1/[σ ² (F _o ²)+(0.0396P) ² +18.4351P] where P=(F _o ² +2F _c ²)/3
Largest diff. peak and hole	2.563 and -1.089 eÅ ⁻³
R.M.S. deviation from mean	0.071 eÅ ⁻³

Table 3-5-17. Atomic coordinates and equivalent isotropic atomic displacement parameters (\AA^2) for **33⁻·K⁺(222-cryptand)**.

U(eq) is defined as one third of the trace of the orthogonalized U_{ij} tensor.

	x/a	y/b	z/c	U(eq)
K1	0.09956(3)	0.27621(3)	0.25117(3)	0.02302(11)
Si1	0.19287(4)	0.28679(3)	0.89849(3)	0.02137(14)
Si2	0.16032(4)	0.18495(3)	0.92421(3)	0.02202(14)
Si3	0.07711(4)	0.25054(3)	0.84102(3)	0.02045(14)
Si4	0.31070(4)	0.40695(4)	0.93343(4)	0.02763(16)
Si5	0.23953(4)	0.09340(3)	0.90679(3)	0.02250(14)
Si6	0.95689(4)	0.26882(3)	0.87883(3)	0.02167(14)
Si7	0.09651(4)	0.25700(3)	0.72675(3)	0.02239(14)
O1	0.11763(10)	0.17484(10)	0.34931(9)	0.0307(4)
O2	0.13247(11)	0.30968(11)	0.38863(9)	0.0328(4)
O3	0.97702(10)	0.21664(9)	0.16745(9)	0.0302(4)
O4	0.95743(10)	0.34068(10)	0.22860(9)	0.0306(4)
O5	0.21413(11)	0.24065(10)	0.17685(9)	0.0297(4)
O6	0.18743(11)	0.37693(10)	0.19651(10)	0.0337(4)
N1	0.24501(14)	0.35167(12)	0.90203(14)	0.0364(6)
N2	0.11324(13)	0.13359(11)	0.21024(11)	0.0300(5)
N3	0.09022(14)	0.41873(12)	0.29399(13)	0.0362(6)
C1	0.3653(2)	0.3807(2)	0.01720(16)	0.0513(9)
C2	0.25824(16)	0.48766(13)	0.94853(14)	0.0315(6)
C3	0.2184(2)	0.47566(19)	0.01096(18)	0.0523(9)
C4	0.1954(2)	0.50376(17)	0.89048(17)	0.0468(8)
C5	0.3104(2)	0.54855(17)	0.9615(2)	0.0596(10)
C6	0.38696(16)	0.41465(14)	0.87497(14)	0.0308(6)
C7	0.3538(2)	0.44856(16)	0.80886(15)	0.0414(7)
C8	0.45866(17)	0.45289(17)	0.90829(17)	0.0428(7)
C9	0.41153(18)	0.34385(15)	0.85891(17)	0.0400(7)
C10	0.2479(2)	0.06817(16)	0.81791(15)	0.0432(8)
C11	0.34187(15)	0.11467(14)	0.94865(15)	0.0318(6)
C12	0.37447(18)	0.16554(17)	0.9029(2)	0.0539(10)
C13	0.39480(16)	0.05375(15)	0.95610(16)	0.0373(7)
C14	0.34313(17)	0.14663(19)	0.01806(18)	0.0493(9)
C15	0.19382(15)	0.01760(12)	0.94478(14)	0.0285(5)
C16	0.22820(19)	0.95076(14)	0.92670(18)	0.0419(7)
C17	0.19983(18)	0.02331(15)	0.02137(15)	0.0392(7)

	x/a	y/b	z/c	U(eq)
C18	0.10802(17)	0.01703(14)	0.91579(19)	0.0442(8)
C19	0.87898(15)	0.29978(15)	0.81083(14)	0.0310(6)
C20	0.96791(16)	0.33771(14)	0.94660(14)	0.0316(6)
C21	0.9857(2)	0.40269(15)	0.91206(18)	0.0466(8)
C22	0.03295(17)	0.32502(16)	0.00516(15)	0.0378(7)
C23	0.89278(18)	0.34724(18)	0.97659(16)	0.0428(7)
C24	0.91711(14)	0.18566(14)	0.90888(14)	0.0285(5)
C25	0.95629(17)	0.16509(15)	0.97884(14)	0.0347(6)
C26	0.82949(16)	0.18896(17)	0.91059(17)	0.0421(7)
C27	0.93049(15)	0.13109(14)	0.85908(14)	0.0316(6)
C28	0.20275(15)	0.24152(16)	0.72637(16)	0.0367(7)
C29	0.04324(15)	0.18759(13)	0.67394(13)	0.0264(5)
C30	0.0670(2)	0.12170(15)	0.70760(17)	0.0496(9)
C31	0.95624(16)	0.19486(17)	0.67041(16)	0.0401(7)
C32	0.06298(18)	0.18378(19)	0.60146(15)	0.0433(8)
C33	0.07799(17)	0.34466(13)	0.68924(14)	0.0310(6)
C34	0.9955(2)	0.3660(2)	0.6875(3)	0.0933(19)
C35	0.0925(5)	0.3484(2)	0.6159(3)	0.132(3)
C36	0.1279(3)	0.39312(19)	0.7307(3)	0.105(2)
C37	0.10468(18)	0.08897(14)	0.26619(15)	0.0357(6)
C38	0.14688(17)	0.11195(15)	0.33327(15)	0.0362(6)
C39	0.14784(18)	0.19486(17)	0.41587(14)	0.0398(7)
C40	0.11302(18)	0.25896(18)	0.43234(14)	0.0417(7)
C41	0.11243(19)	0.37351(18)	0.41085(16)	0.0448(8)
C42	0.13131(18)	0.42544(16)	0.36252(17)	0.0447(8)
C43	0.05329(18)	0.12080(15)	0.15250(15)	0.0368(6)
C44	0.97536(17)	0.14588(14)	0.16274(14)	0.0346(6)
C45	0.90332(16)	0.24302(15)	0.17453(16)	0.0362(6)
C46	0.90641(16)	0.31701(15)	0.17227(14)	0.0337(6)
C47	0.95756(18)	0.41110(16)	0.23080(18)	0.0428(7)
C48	0.00796(18)	0.43385(18)	0.29300(19)	0.0482(8)
C49	0.19001(18)	0.12496(15)	0.19054(15)	0.0375(7)
C50	0.21307(18)	0.17781(16)	0.14423(15)	0.0389(7)
C51	0.23900(16)	0.29124(16)	0.13515(14)	0.0355(6)
C52	0.25615(16)	0.35268(16)	0.17632(15)	0.0361(6)
C53	0.19983(19)	0.43849(16)	0.23072(19)	0.0460(8)
C54	0.1238(2)	0.46317(16)	0.2485(2)	0.0487(8)

Table 3-5-18. Bond lengths (Å) for **33⁻·[K⁺(222-cryptand)]..**

K1-O5	2.7707(18)	K1-O4	2.7979(19)	N2-C37	1.464(4)	N2-C49	1.472(4)
K1-O3	2.8083(19)	K1-O2	2.8219(19)	N2-C43	1.475(4)	N3-C42	1.467(4)
K1-O1	2.8250(19)	K1-O6	2.864(2)	N3-C54	1.463(4)	N3-C48	1.477(4)
K1-N2	3.007(2)	K1-N3	3.008(2)	C2-C5	1.532(4)	C2-C4	1.523(4)
Si1-N1	1.593(2)	Si1-Si2	2.2109(9)	C6-C7	1.533(4)	C2-C3	1.542(4)
Si1-Si3	2.3123(9)	Si2-Si5	2.3681(9)	C11-C14	1.534(4)	C6-C9	1.538(4)
Si2-Si3	2.4465(9)	Si3-Si7	2.3734(9)	C11-C12	1.541(4)	C6-C8	1.547(4)
Si3-Si6	2.3778(9)	Si4-N1	1.663(2)	C15-C17	1.532(4)	C11-C13	1.535(4)
Si4-C1	1.891(3)	Si4-C6	1.913(3)	C15-C16	1.541(4)	C15-C18	1.539(4)
Si4-C2	1.915(3)	Si5-C10	1.883(3)	C20-C22	1.541(4)	C20-C21	1.535(4)
Si5-C11	1.924(3)	Si5-C15	1.933(3)	C24-C25	1.532(4)	C20-C23	1.542(4)
Si6-C19	1.898(3)	Si6-C20	1.935(3)	C29-C30	1.521(4)	C24-C27	1.527(4)
Si6-C24	1.945(3)	Si7-C28	1.897(3)	C29-C32	1.547(4)	C24-C26	1.549(4)
Si7-C29	1.917(3)	Si7-C33	1.929(3)	C33-C36	1.487(5)	C29-C31	1.530(4)
O1-C38	1.422(4)	O1-C39	1.425(3)	C33-C35	1.534(5)	C33-C34	1.511(5)
O2-C40	1.421(4)	O2-C41	1.422(4)	C37-C38	1.516(4)	C39-C40	1.487(5)
O3-C44	1.428(3)	O3-C45	1.428(3)	C41-C42	1.497(5)	C43-C44	1.504(4)
O4-C47	1.419(4)	O4-C46	1.423(3)	C45-C46	1.492(4)	C47-C48	1.497(5)
O5-C50	1.424(3)	O5-C51	1.427(3)	C49-C50	1.508(4)	C51-C52	1.495(4)
O6-C52	1.417(3)	O6-C53	1.420(4)	C53-C54	1.518(5)		

Table 3-5-19. Bond angles (°) for **33⁻·[K⁺(222-cryptand)]..**

O5-K1-O4	137.38(6)	O5-K1-O3	97.04(6)	Si2-Si1-Si3	65.44(3)	Si1-Si2-Si5	120.67(4)
O4-K1-O3	60.57(6)	O5-K1-O2	121.76(6)	Si1-Si2-Si3	59.28(3)	Si5-Si2-Si3	128.84(4)
O4-K1-O2	95.81(6)	O3-K1-O2	136.14(6)	Si1-Si3-Si7	103.14(3)	Si1-Si3-Si6	123.55(4)
O5-K1-O1	99.88(6)	O4-K1-O1	117.21(6)	Si7-Si3-Si6	123.98(4)	Si1-Si3-Si2	55.28(3)
O3-K1-O1	96.29(6)	O2-K1-O1	60.16(6)	Si7-Si3-Si2	122.40(4)	Si6-Si3-Si2	109.79(3)
O5-K1-O6	60.09(6)	O4-K1-O6	97.40(6)	N1-Si4-C1	112.83(16)	N1-Si4-C6	109.41(13)
O3-K1-O6	118.92(6)	O2-K1-O6	99.20(6)	C1-Si4-C6	104.91(14)	N1-Si4-C2	107.67(13)
O1-K1-O6	140.07(6)	O5-K1-N2	60.82(6)	C1-Si4-C2	106.95(15)	C6-Si4-C2	115.18(13)
O4-K1-N2	120.25(6)	O3-K1-N2	60.83(6)	C10-Si5-C11	106.21(15)	C10-Si5-C15	104.79(14)
O2-K1-N2	118.86(6)	O1-K1-N2	59.68(6)	C11-Si5-C15	114.82(12)	C10-Si5-Si2	118.57(10)
O6-K1-N2	120.19(6)	O5-K1-N3	118.35(7)	C11-Si5-Si2	107.23(9)	C15-Si5-Si2	105.62(9)
O4-K1-N3	61.27(6)	O3-K1-N3	120.69(6)	C19-Si6-C20	105.11(12)	C19-Si6-C24	104.56(12)
O2-K1-N3	60.26(7)	O1-K1-N3	119.69(7)	C20-Si6-C24	113.79(13)	C19-Si6-Si3	113.92(9)
O6-K1-N3	59.23(6)	N2-K1-N3	178.47(7)	C20-Si6-Si3	109.39(9)	C24-Si6-Si3	110.02(8)
N1-Si1-Si2	156.61(11)	N1-Si1-Si3	137.95(11)	C28-Si7-C29	106.40(13)	C28-Si7-C33	105.10(13)

C29-Si7-C33	114.15(12)	C28-Si7-Si3	105.87(10)	C36-C33-C35	109.9(4)	C34-C33-C35	104.8(4)
C29-Si7-Si3	111.65(8)	C33-Si7-Si3	112.86(9)	C36-C33-Si7	109.2(2)	C34-C33-Si7	112.2(2)
C38-O1-C39	111.5(2)	C38-O1-K1	119.60(15)	C35-C33-Si7	112.3(2)	N2-C37-C38	113.8(2)
C39-O1-K1	116.13(17)	C40-O2-C41	111.3(2)	O1-C38-C37	109.1(2)	O4-C47-C48	109.3(3)
C40-O2-K1	113.56(16)	C41-O2-K1	119.87(18)	O1-C39-C40	110.1(2)	N3-C48-C47	114.3(3)
C44-O3-C45	111.6(2)	C44-O3-K1	118.21(15)	O2-C40-C39	110.1(2)	N2-C49-C50	114.9(2)
C45-O3-K1	114.35(16)	C47-O4-C46	111.0(2)	O2-C41-C42	109.9(2)	O5-C50-C49	109.3(2)
C47-O4-K1	117.47(16)	C46-O4-K1	114.93(15)	N3-C42-C41	114.8(3)	O5-C51-C52	108.7(2)
C50-O5-C51	110.4(2)	C50-O5-K1	121.02(16)	N2-C43-C44	113.4(2)	O6-C52-C51	109.3(2)
C51-O5-K1	116.11(16)	C52-O6-C53	111.2(2)	O3-C44-C43	109.5(2)	O6-C53-C54	108.7(3)
C52-O6-K1	113.33(17)	C53-O6-K1	119.14(17)	O3-C45-C46	109.3(2)	N3-C54-C53	113.3(3)
Si1-N1-Si4	158.62(19)	C37-N2-C49	109.5(2)	O4-C46-C45	109.4(2)		
C37-N2-C43	110.9(2)	C49-N2-C43	110.4(2)				
C37-N2-K1	110.81(16)	C49-N2-K1	107.39(17)				
C43-N2-K1	107.80(16)	C42-N3-C54	110.0(3)				
C42-N3-C48	110.1(2)	C54-N3-C48	110.4(3)				
C42-N3-K1	108.46(18)	C54-N3-K1	111.19(18)				
C48-N3-K1	106.65(18)	C4-C2-C5	108.2(3)				
C4-C2-C3	107.0(3)	C5-C2-C3	108.6(3)				
C4-C2-Si4	111.9(2)	C5-C2-Si4	114.5(2)				
C3-C2-Si4	106.4(2)	C9-C6-C7	108.4(2)				
C9-C6-C8	108.4(3)	C7-C6-C8	109.8(2)				
C9-C6-Si4	107.28(19)	C7-C6-Si4	110.8(2)				
C8-C6-Si4	112.1(2)	C14-C11-C13	108.5(3)				
C14-C11-C12	107.8(3)	C13-C11-C12	108.5(2)				
C14-C11-Si5	112.44(19)	C13-C11-Si5	112.4(2)				
C12-C11-Si5	107.0(2)	C17-C15-C18	107.7(3)				
C17-C15-C16	109.2(2)	C18-C15-C16	107.6(2)				
C17-C15-Si5	111.40(19)	C18-C15-Si5	107.33(19)				
C16-C15-Si5	113.4(2)	C21-C20-C22	108.0(3)				
C21-C20-C23	108.3(3)	C22-C20-C23	107.9(2)				
C21-C20-Si6	107.42(19)	C22-C20-Si6	114.03(19)				
C23-C20-Si6	111.1(2)	C27-C24-C25	108.4(2)				
C27-C24-C26	107.0(2)	C25-C24-C26	108.1(2)				
C27-C24-Si6	108.67(17)	C25-C24-Si6	112.54(19)				
C26-C24-Si6	111.96(19)	C30-C29-C31	108.3(3)				
C30-C29-C32	106.9(2)	C31-C29-C32	108.6(2)				
C30-C29-Si7	107.98(19)	C31-C29-Si7	111.28(18)				
C32-C29-Si7	113.5(2)	C36-C33-C34	108.4(4)				

References

- 1) R. West, M. J. Fink, and J. Michl, *Science* **1981**, *214*, 1343.
- 2) A. G. Brook, F. Abdesaken, B. Gutekunst, G. Gutekunst, and R. K. Kallury, *J. Chem. Soc., Chem. Commun.* **1981**, 191.
- 3) Reviews on disilenes: (a) G. Raabe, J. Michl, *Chem. Rev.* **1985**, *85*, 419; (b) R. West, *Angew. Chem., Int. Ed.* **1987**, *26*, 1201; (c) J. Barrau, J. Escudie, J. Satge, *Chem. Rev.* **1990**, *90*, 283; (d) T. Tsumuraya, S. A. Batcheller, S. Masamune, *Angew. Chem., Int. Ed.* **1991**, *30*, 902; (e) R. Okazaki, R. West, *Adv. Organomet. Chem.* **1996**, *39*, 231; (f) M. Kira, T. Iwamoto, *Adv. Organomet. Chem.* **2006**, *54*, 73; (g) T. L. Morking, T. R. Owens, W. J. Leigh, in *The Chemistry of Organic Silicon Compounds Vol. 3*, (Ed. by Z. Rappoport, Y. Apeloig) John Wiley & Sons, Ltd, Chichester, 2001, chap 17.
- 4) Reviews on Bicyclo[1.1.0]tetrasilane: (a) M. Karni, J. Kapp, P. v. R. Schleyer, Y. Apeloig in *The Chemistry of Organic Silicon Compounds Vol. 3*, (Ed. by Z. Rappoport, Y. Apeloig) John Wiley & Sons, Ltd, Chichester, 2001 chap. 1; (b) M. Rohmer, M. Bénard, *Chem. Soc. Rev.* **2001**, *30*, 340; (c) M. Kira, *Organometallics* **2014**, *33*, 644; (d) T. Müller in *Organosilicon Chemistry IV From Molecules to Materials*, (Ed. by N. Auner and J. Weis) Wiley-VCH Ltd, 2000, 110.
- 5) V. Ya. Lee, H. Yasuda, A. Sekiguchi, *J. Am. Chem. Soc.* **2007**, *129*, 2436.
- 6) (a) V. Ya. Lee, S. Miyazaki, H. Yasuda, and A. Sekiguchi, *J. Am. Chem. Soc.* **2008**, *130*, 2758; (b) V. Ya. Lee, O. A. Gapurenko, S. Miyazaki, A. Sekiguchi, R. M. Minyaev, V. I. Minkin, and H. Gornitzka, *Angew. Chem., Int. Ed.* **2015**, *127*, 14324.
- 7) M. Ichinohe, T. Matsuno, A. Sekiguchi, *Angew. Chem., Int. Ed.* **1999**, *38*, 2194.
- 8) A. Sekiguchi, R. Kinjo, M. Ichinohe, *Science* **2004**, *305*, 1755.
- 9) K. Takeuchi, M. Ichinohe, A. Sekiguchi, *J. Am. Chem. Soc.* **2011**, *133*, 12478.
- 10) K. Ueba-Ohshima, T. Iwamoto, M. Kira, *Organometallics* **2008**, *27*, 320.
- 11) T. Honda, M. Mori, *J. Org. Chem.* **1996**, *61*, 1196.
- 12) M. Nakamoto, T. Fukawa, V. Ya. Lee, A. Sekiguchi, *J. Am. Chem. Soc.* **2002**, *124*, 15160.
- 13) J. R. DamewoodJr., C. M. Hadad, *J. Phys. Chem.* **1988**, *92*, 33.
- 14) H. V. R. Dias, M. M. Olmstead, K. Ruhlandt-Senge, P. P. Power, *J. Organomet. Chem.* **1993**, *462*, 1.
- 15) (a) N. Wiberg, K. churz, G. Reber, G. Müller, *J. Chem. Soc., Chem. Commun.* **1986**, 591. (b) N. Wiberg, K. Schurz, G. Müller, J. Riede, *Angew. Chem., Int. Ed.* **1988**, *27*, 935.

List of Publication

1. "Functionalized Cyclic Disilenes via Ring-Expansion of Cyclotrisilenes with Isonitriles."
Ohmori, Y.; Ichinohe, M.; Sekiguchi, A.; Cowley, M. J.; Huch, V.; Scheschkewitz, D. *Organometallics* **2013**, *32*, 1591-1594.
2. "Carbonylation of Cyclotrisilenes"
Cowley, M.J.; Ohmori, Y.; Huch, V.; Ichinohe, M.; Sekiguchi, A.; Scheschkewitz, D. *Angew. Chem., Int. Ed.* **2013**, *52*, 13247-13250.

Acknowledgement

The studies described in this dissertation have been carried out under the direction of Professor Dr. Akira Sekiguchi at the Department of Chemistry, Graduated School of Pure and Applied Sciences, University of Tsukuba. These works were supported by JSPS Research Fellowship for Young Scientist.

The author sincerely wishes to express great thanks to Professor Dr. Akira Sekiguchi for his continuing guidance, valuable discussions and encouragement throughout the course of studies. Grateful acknowledgement is made to Associate Professor Dr. Masaaki Ichinohe for helpful discussions, suggestions, and supports in X-ray crystallographic analysis. The author also expresses deep gratitude to Dr. Masaaki Nakamoto for helpful discussions and suggestions. The author would express his sincerest gratitude to Dr. Vladimir Ya. Lee for kindly discussion, helps with English, and making of helpful suggestions.

The author also specially thanks to Prof. Dr. David Scheschkewitz and Dr. Michael Cowley (Saarland University) for helpful discussions and suggestions in their joint works since ASIS-IV.

The author appreciates very much to all seniors in Professor Sekiguchi research group: Dr. Torahiko Yamaguchi, Dr. Kiera McNeice, Dr. Matt Asay, Dr. Katsuhiko Takeuchi, Dr. Hiroaki Tanaka, Dr. Yusuke Inagaki, Dr. Takeshi Nozawa, Dr. Yuki Ito, Mr. Masahisa Endo, Ms. Marina Kachi, Mr. Takahiro Yamaguchi, Ms. Kanako Taira, Mr. Shinji Aoki, Mr. Tatsumi Ochiai, Mr. Masashi Miyano for their helpful discussions, helpful suggestions, and kindness. The author is especially grateful to Mr. Yuzuru Kobayashi, Mr. Satoru Horiguchi, Mr. Takumi, Furuya, Mr. Toshihiro Takeuchi and junior members of Sekiguchi laboratory: Mr. Taichi Kitagawa, Mr. Kenshiro Haga, Ms. Yuri Ikeda, Ms. Nozomi Tamura, Mr. Toshiharu Ohfuchi, Mr. Ryo Sakai, Mr. Kazuhisa Kaminaga, Mr. Seiichiro Nakazawa, Mr. Hitoshi Maruyama, Ms. Hiroko Yotsuyanagi, Mr. Akira Mori, Mr. Takahiko Meguro, Mr. Ryo Uchihashi, Mr. Kazuho Urayama, Ms. Yukako Shoji, Mr. Yuta Takahara, Mr. Masahiro Nishituka, Ms. Mako Iwasaki, Mr. Kento Okaniwa, Ms. Haruka Sugawsawa, Mr. Futa Hattori, Mr. Takayuki Suzuki, Mr. Junichi Usuda and Ms. Yui Kikuchi for helpful discussions, encouragement and friendships.

Finally, the author would like to express his deep appreciation to his parents Mr. Shigeru Ohmori and Mrs. Kayo Ohmori as well as his big brother Mr. Yo Ohmori for their long assistance, continuous encouragement, and understanding.

February 2016

Yu Ohmori